

# Inelastic X-Ray Scattering & Lattice Dynamics

Esen **Ercan** Alp  
Advanced Photon Source, Argonne National Laboratory

[alp@anl.gov](mailto:alp@anl.gov)

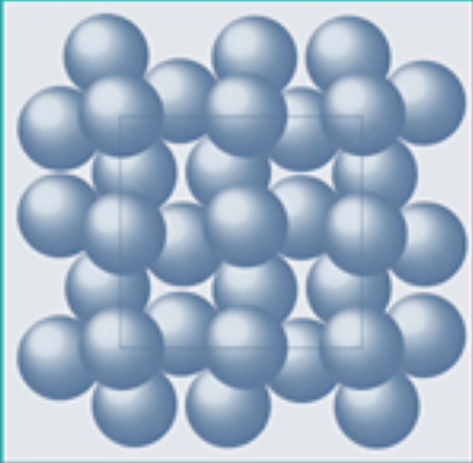
NX School 2017  
August 7, 2017, Argonne National Laboratory, Argonne, IL

Thanks : T. S. Toellner, J. Zhao, M. Y. Hu, A. Alatas, W. Bi, A. Said, T. Gog

# Lattice dynamics for beginners

4 Cambridge topics in  
MINERAL PHYSICS AND CHEMISTRY

## Introduction to Lattice Dynamics



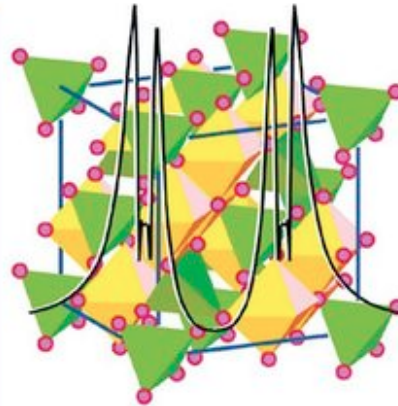
MARTIN T. DOVE

Yi-Long Chen, De-Ping Yang

WILEY-VCH

## Mössbauer Effect in Lattice Dynamics

Experimental Techniques and Applications



## THE PHYSICS OF PHONONS



G. P. SRIVASTAVA



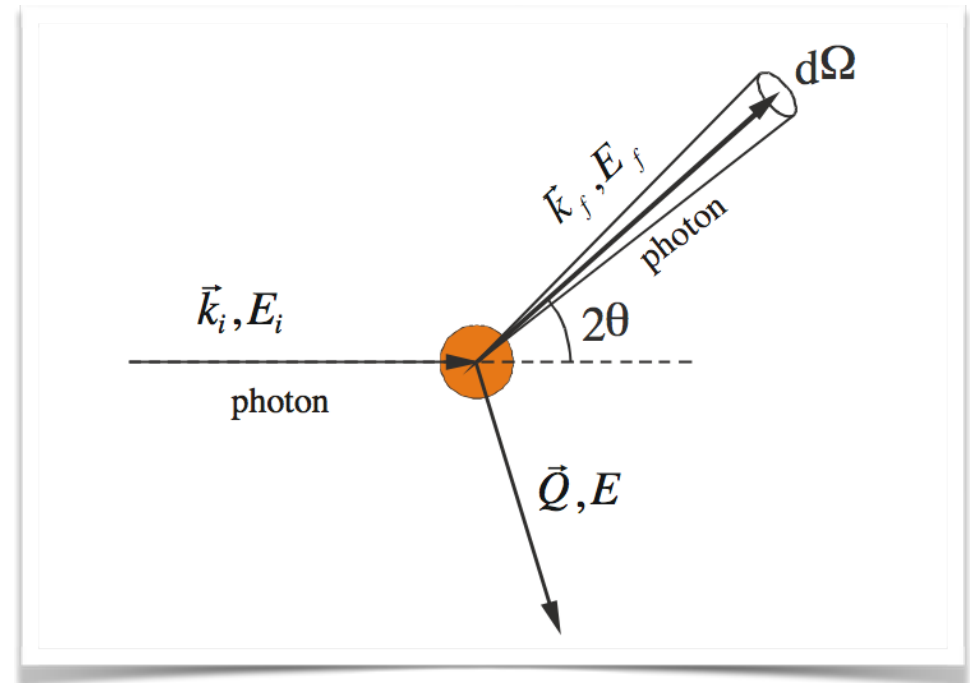
# Inelastic X-Ray Scattering & Spectroscopy @ APS

**IXS**

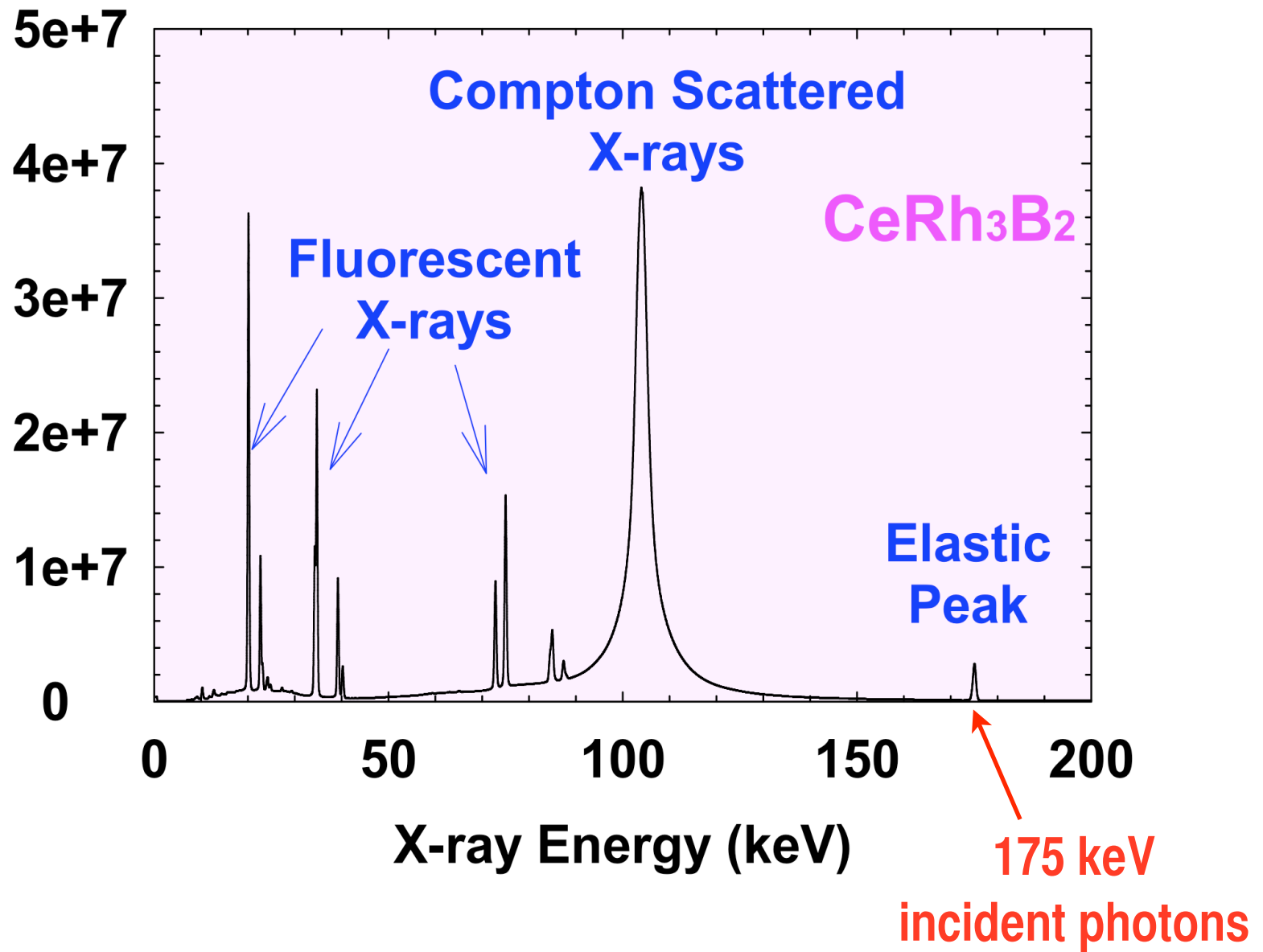
**NRIXS**      **RIXS**      **MCS**

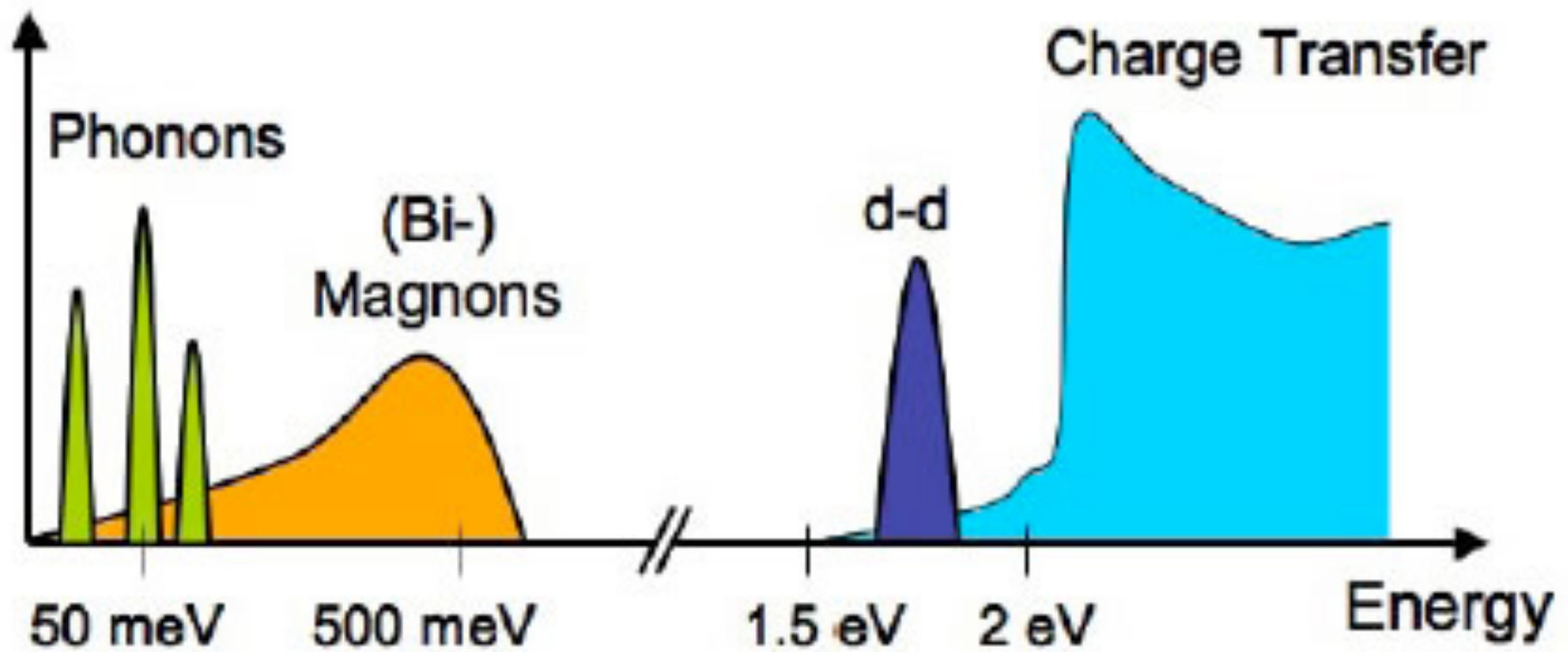
**NRIS**      **XES**      **XRS**

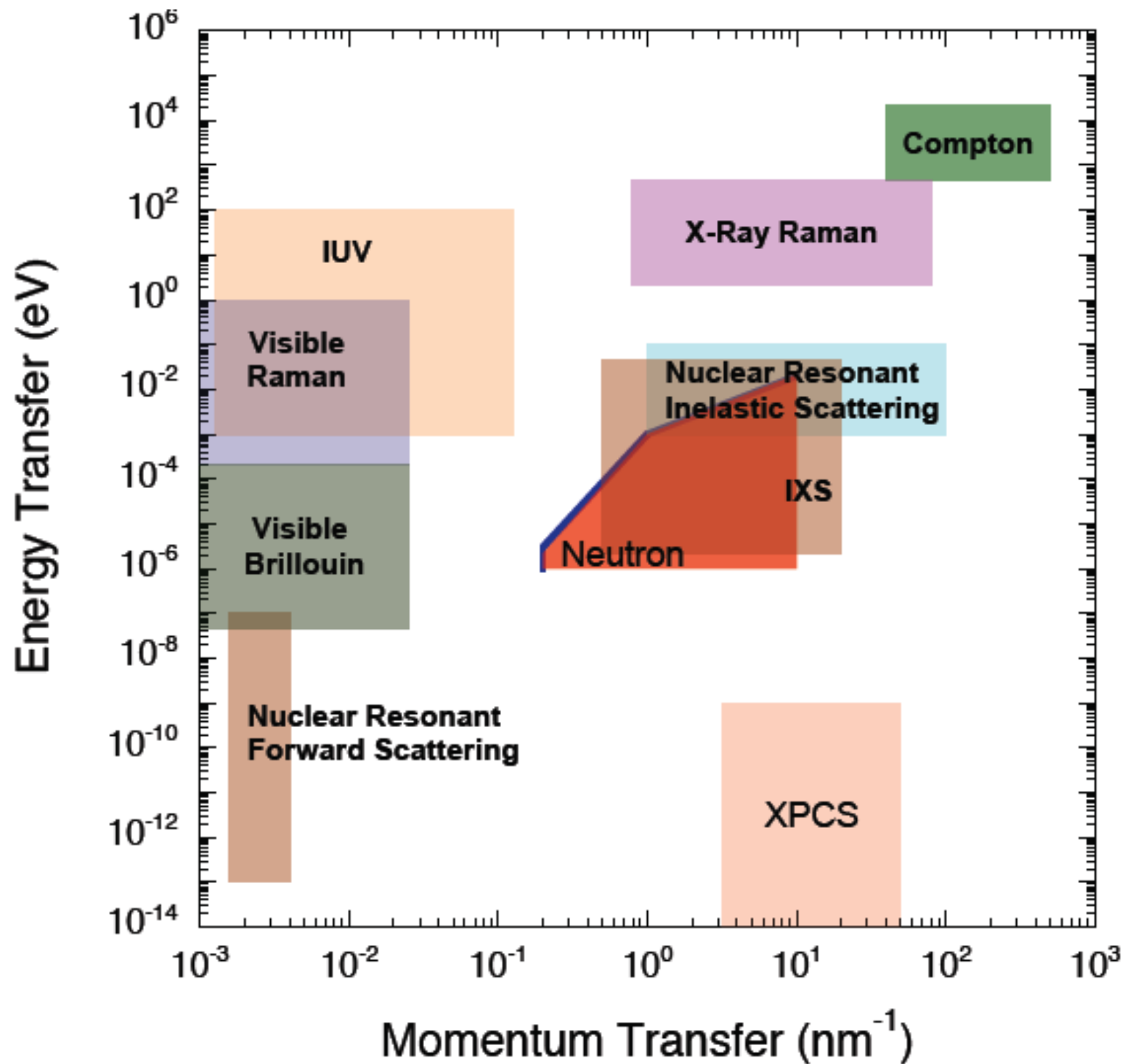
**Compton**



- Nuclear Resonant Inelastic X-Ray scattering, NRIXS: **Sectors 3, 16, 30**
- Momentum Resolved High Energy Resolution IXS (**HERIX**) **Sectors 3, 30**
- Resonant Inelastic X-Ray Scattering, RIXS : **Sector 27**
- X-Ray Raman Scattering, XRS : **Sectors 13, 16, 20**
- X-Ray Emission Spectroscopy, XES: **Sectors 6, 13, 16, 17**







# Lattice dynamics for beginners

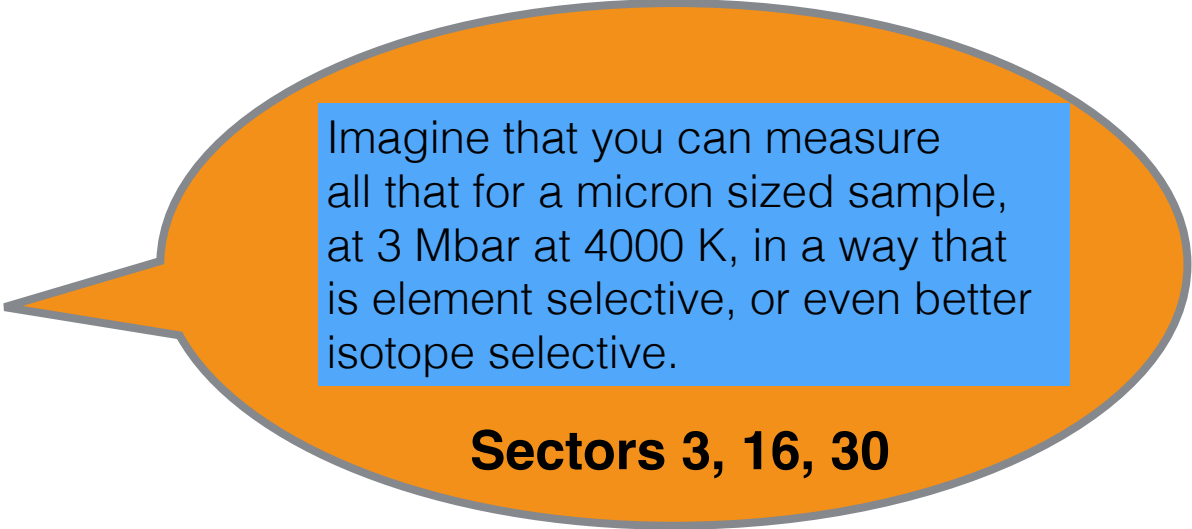
**Lattice dynamics describes vibrations of atoms in condensed matter:**

- crystalline solids
- glasses, and
- liquids

However, some of the convenience gained by symmetry or periodic lattice is lost for glasses and liquids. Also, effect of surfaces and defects are glowing short-comings of the classical model.

**Lattice dynamics is a reflection of forces acting upon atoms and leads to**

- sound velocity
- vibrational entropy
- specific heat
- force constant
- compression tensor
- Young's modulus
- stiffness and resilience
- Gruneisen constant
- viscosity



Imagine that you can measure all that for a micron sized sample, at 3 Mbar at 4000 K, in a way that is element selective, or even better isotope selective.

**Sectors 3, 16, 30**

**Many experimental techniques exist to study lattice dynamics**

- sound velocity, deformation, thermal expansion, heat capacity....
- spectroscopic methods using light, x-rays and neutrons, and electrons
- point contact spectroscopy

## Atomic motions are described as harmonic traveling waves, characterized by

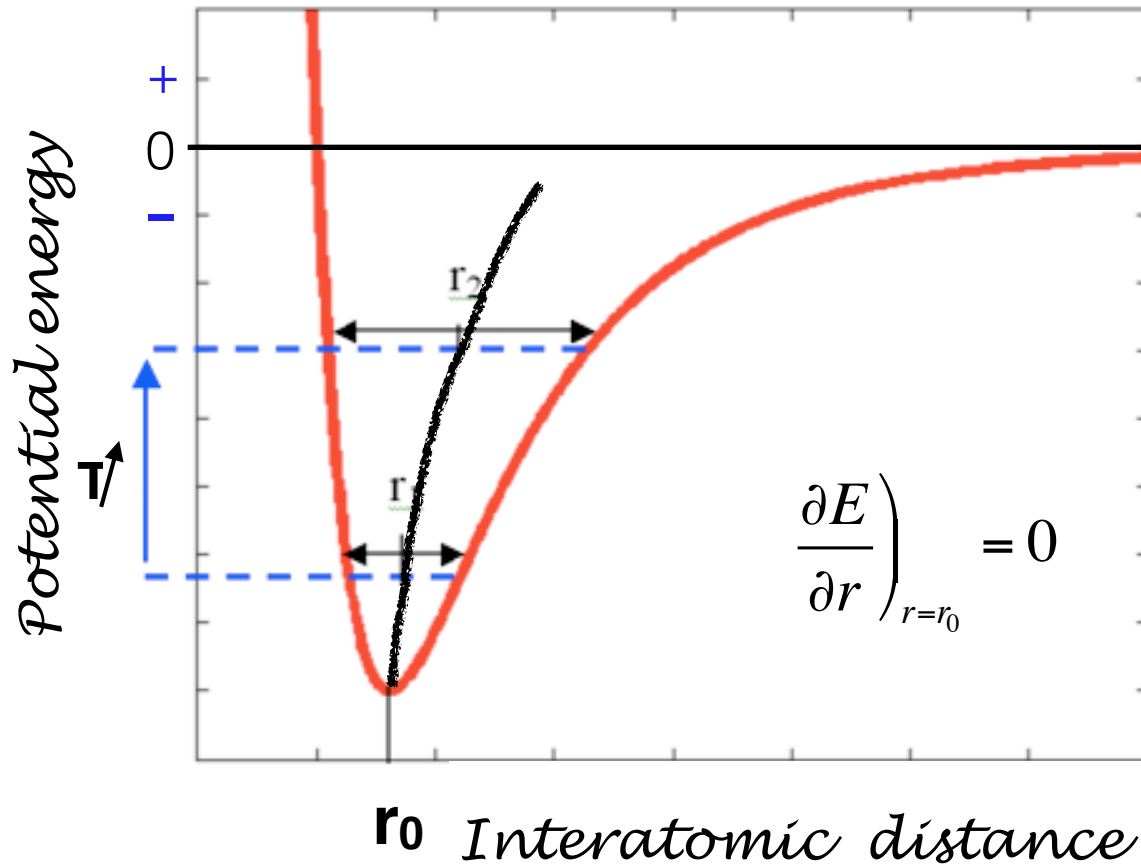
- wavelength,  $\lambda$
- angular frequency,  $\omega$
- momentum vector along the direction of propagation,  $\vec{k} = \frac{\lambda}{2\pi}$

## Two main approximations should be noticed:

- **Born-Oppenheimer (adiabatic) approximation**
  - Motion of atoms are independent and decoupled from the electrons.
  - All electrons follow the nuclei. This can be justified by considering the time scales involved:  $10^{-15}$  s (femto) for electrons,  $10^{-12}$  s (pico) for nuclei
- **Harmonic approximation**
  - At equilibrium, attractive and repulsive forces are balanced.
  - When atoms move away from the equilibrium positions, they are forced to come back by restoring forces.
  - Magnitude of atomic displacements are small compared to interatomic distance.
  - All atoms in equivalent positions in every unit cell move together.



Lennard-Jones 12:6 Potential



There should be no thermal expansion in the harmonic model.

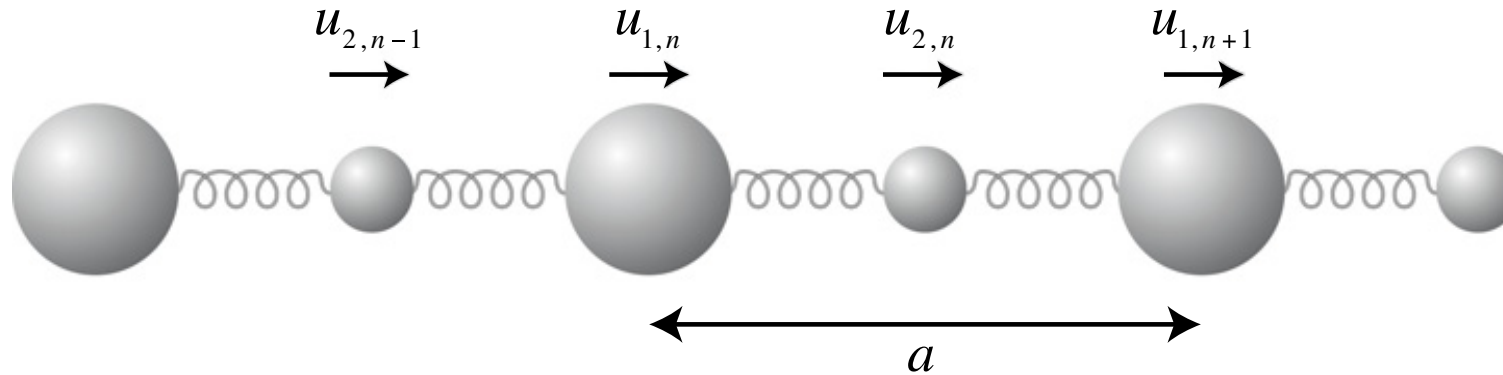
The fact that there is thermal expansion is an indication that the potential under which the atoms move is not harmonic.

However, harmonic model has so many convenient features that we adopt it to explain many features of atomic vibrations.

$$E(r) = E_0 + \frac{1}{2} \left. \frac{\partial^2 E}{\partial r^2} \right|_{r_0} (r - r_0)^2 + \frac{1}{3!} \left. \frac{\partial^3 E}{\partial r^3} \right|_{r_0} (r - r_0)^3 + \frac{1}{4!} \left. \frac{\partial^4 E}{\partial r^4} \right|_{r_0} (r - r_0)^4 + \dots$$

*ignoring these terms is the harmonic approximation*

## Diatomic infinite 1-D chain



$$E = \frac{1}{2} J \sum_n (u_{1,n} - u_{2,n})^2 + \frac{1}{2} J \sum_n (u_{2,n} - u_{1,n+1})^2$$

$$J = \frac{\partial^2 E}{\partial u_{1,n} \partial u_{2,n}}$$

**Force constant (spring constant)**

$$u_{1,n}(t) = \tilde{u}_1 \exp(i(kna - \omega t))$$

$$u_{2,n}(t) = \tilde{u}_2 \exp(i(kna - \omega t))$$

**Time dependent displacement of two atoms  
in terms of relative displacement of each atom**

$$E_{1,n} = \frac{1}{2} J(u_{1,n} - u_{2,n})^2 + \frac{1}{2} J(u_{1,n} - u_{2,n-1})^2$$

$$E_{2,n} = \frac{1}{2} J(u_{2,n} - u_{1,n})^2 + \frac{1}{2} J(u_{2,n} - u_{1,n+1})^2$$

**Energy**

$$f_{1,n} = -\frac{\partial E_{1,n}}{\partial u_{1,n}} = -J(u_{1,n} - u_{2,n}) - J(u_{1,n} - u_{2,n-1})$$

$$f_{2,n} = -\frac{\partial E_{2,n}}{\partial u_{2,n}} = -J(u_{2,n} - u_{1,n}) - J(u_{2,n} - u_{1,n+1})$$

**Force as derivative of energy**

$$\ddot{u}_{1,n}(t) = -\omega^2 \tilde{u}_1 \exp i(kna - \omega t) = -\omega^2 u_{1,n}(t)$$

$$\ddot{u}_{2,n}(t) = -\omega^2 \tilde{u}_2 \exp i(kna - \omega t) = -\omega^2 u_{2,n}(t)$$

**Acceleration**

$$m_1 \ddot{u}_{1,n}(t) = -m_1 \omega^2 u_{1,n}(t) = -J(2u_{1,n}(t) - u_{2,n}(t) - u_{2,n-1}(t))$$

$$m_2 \ddot{u}_{2,n}(t) = -m_2 \omega^2 u_{2,n}(t) = -J(2u_{2,n}(t) - u_{1,n}(t) - u_{1,n+1}(t))$$

**Newton's eq<sup>n</sup> of motion**

$$e_1 = m_1^{1/2} \tilde{u}_1; \quad e_2 = m_2^{1/2} \tilde{u}_2$$

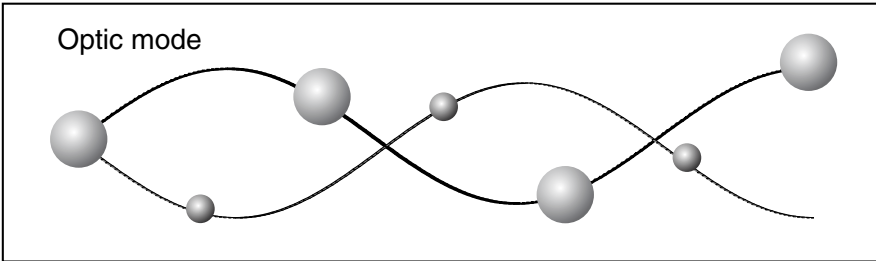
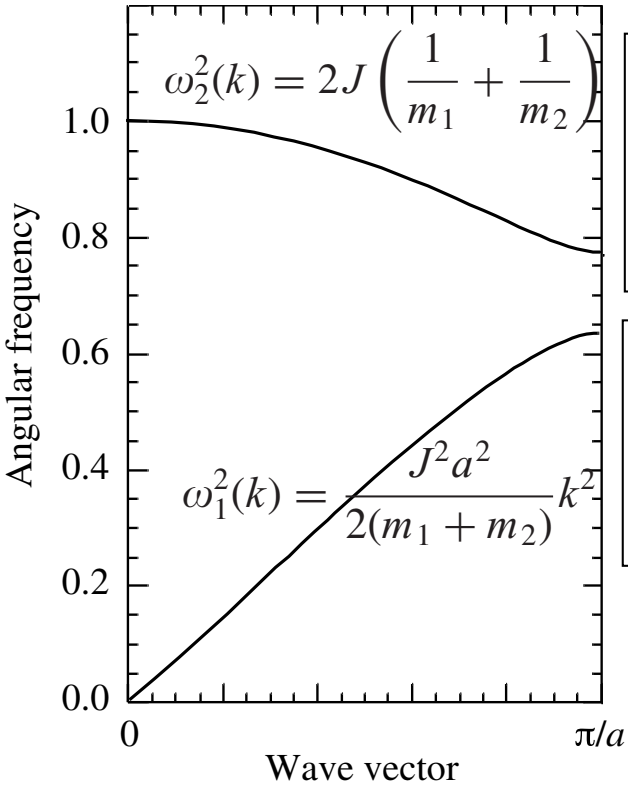
**Mass normalized displacements (real)**

$$\omega^2 \begin{pmatrix} e_1 \\ e_2 \end{pmatrix} = \mathbf{D}(k) \cdot \begin{pmatrix} e_1 \\ e_2 \end{pmatrix}$$

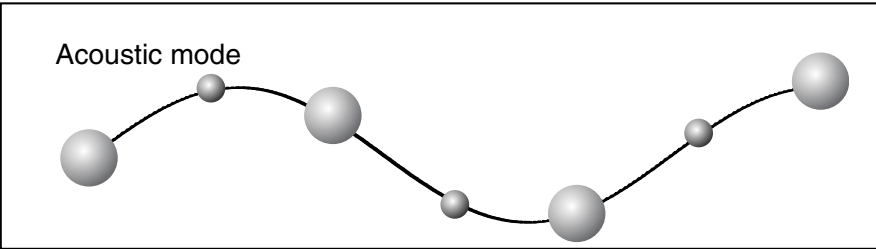
**Matrix form of Newton's eq<sup>n</sup> of motion**

$$\mathbf{D}(k) = \begin{pmatrix} 2J/m_1 & -J(1 + \exp(-ika)) / \sqrt{m_1 m_2} \\ -J(1 + \exp(+ika)) / \sqrt{m_1 m_2} & 2J/m_2 \end{pmatrix}$$

**Eigen solutions**

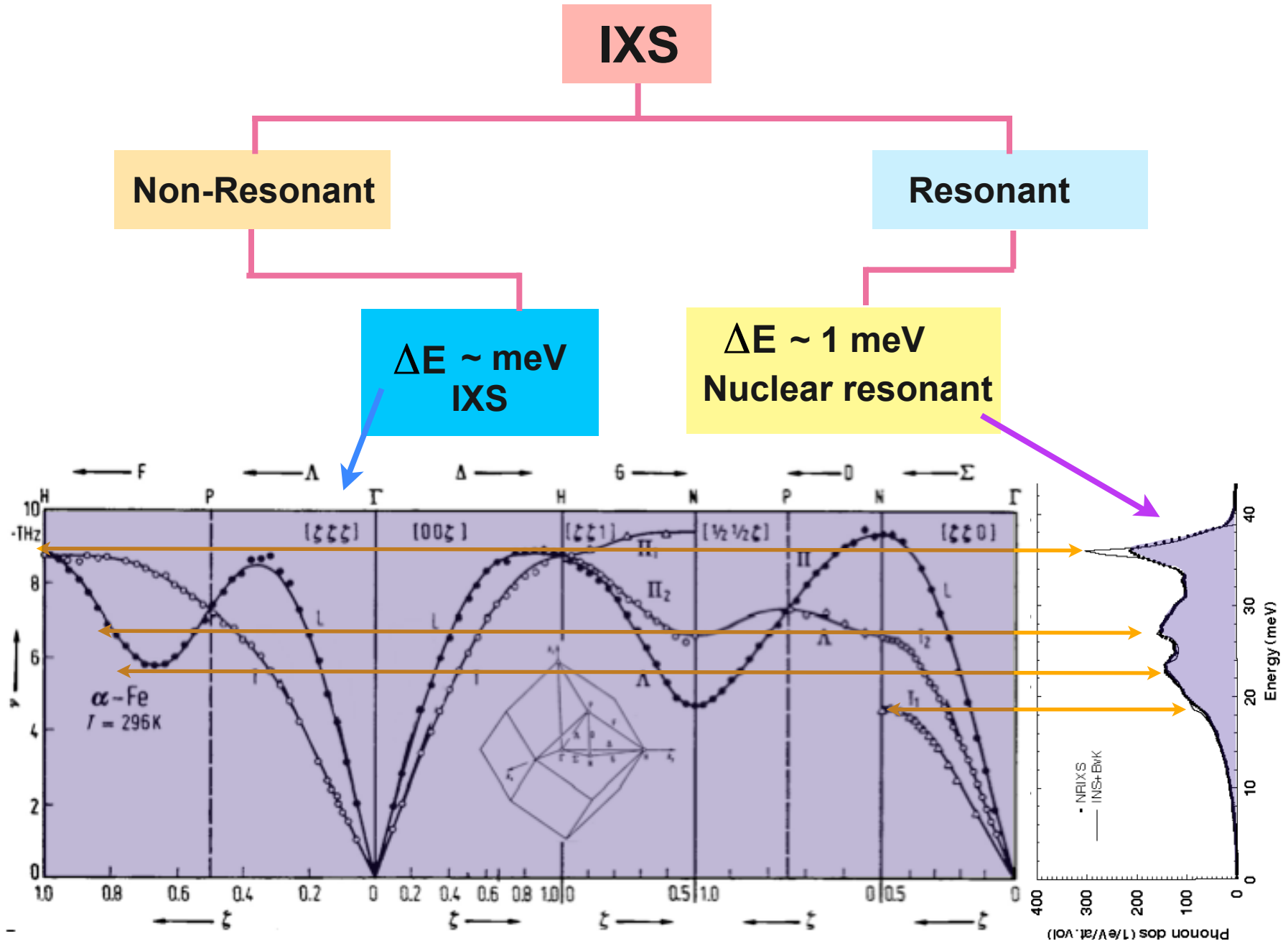


**out-of-phase**  
 $m_1^{1/2} e_1 = -m_2^{1/2} e_2$

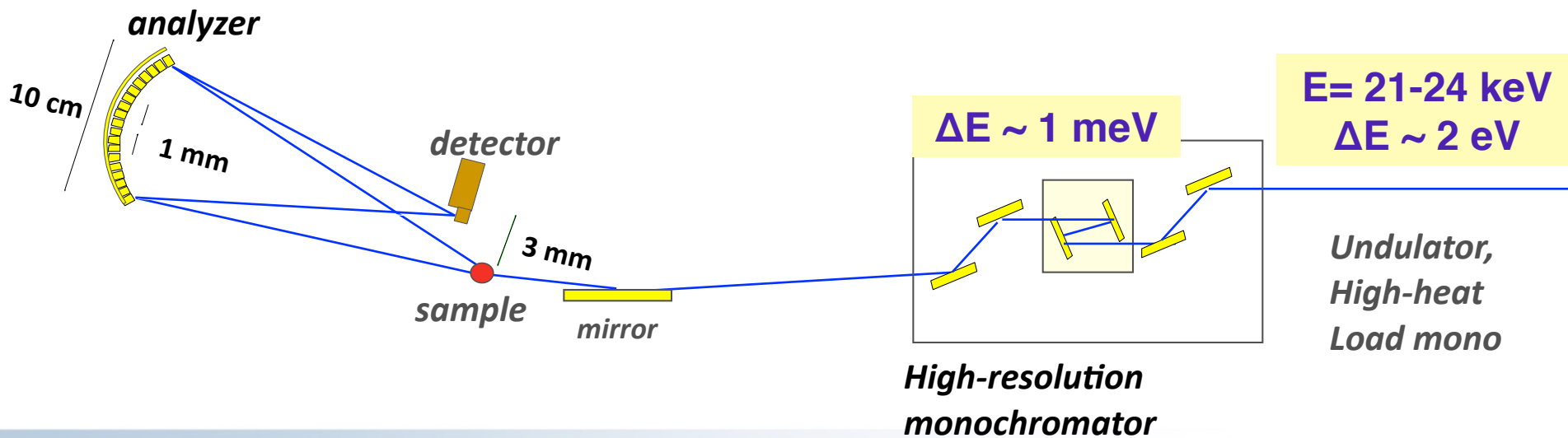
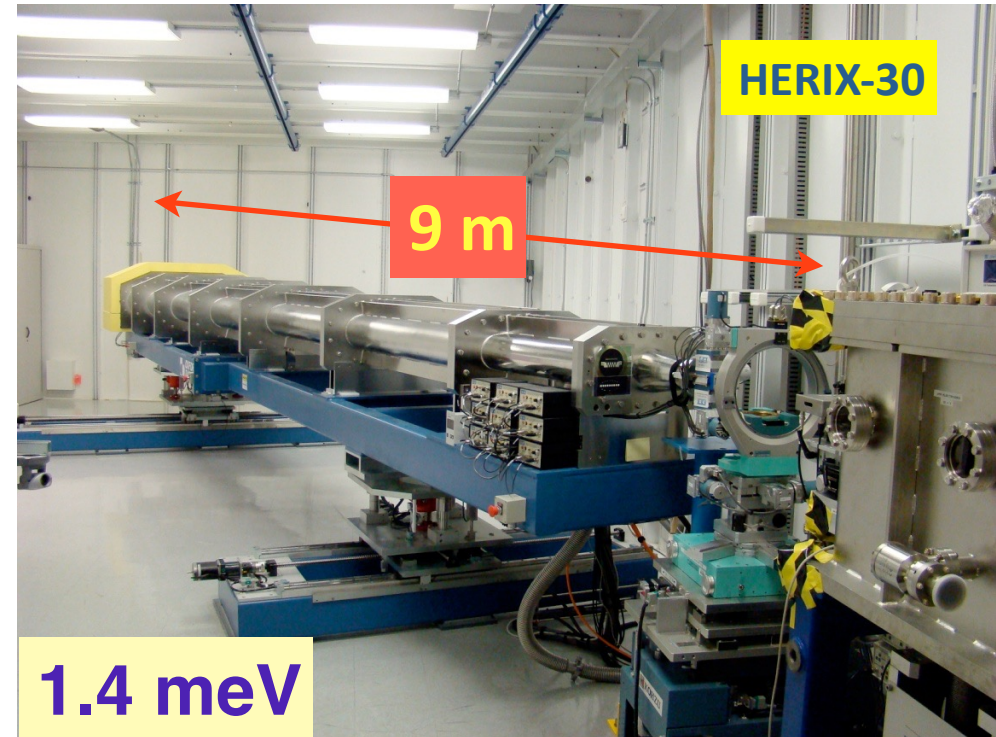
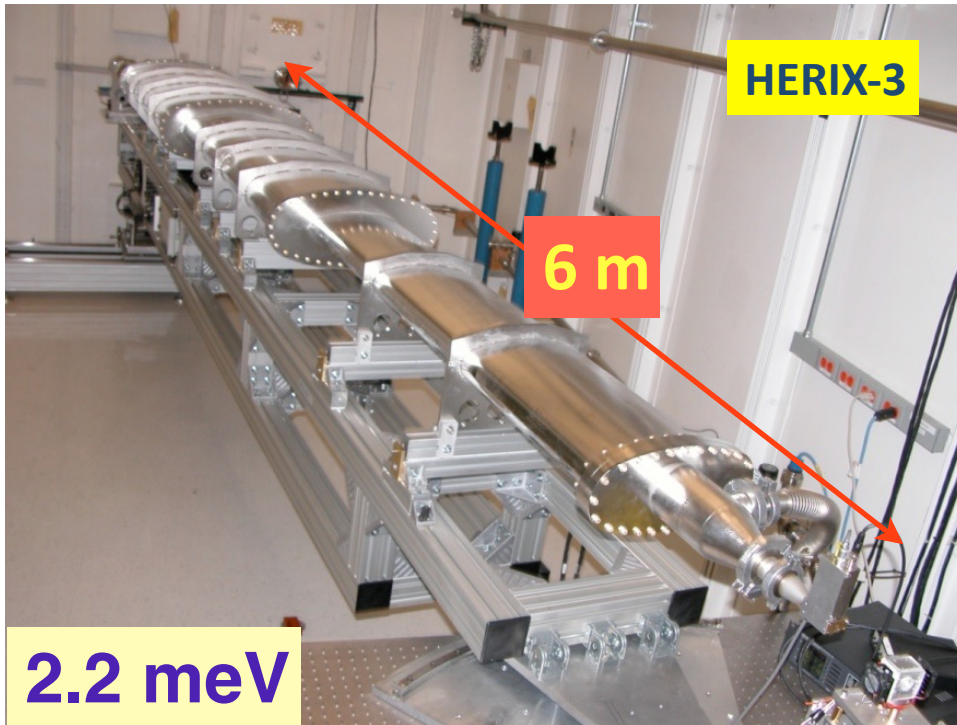


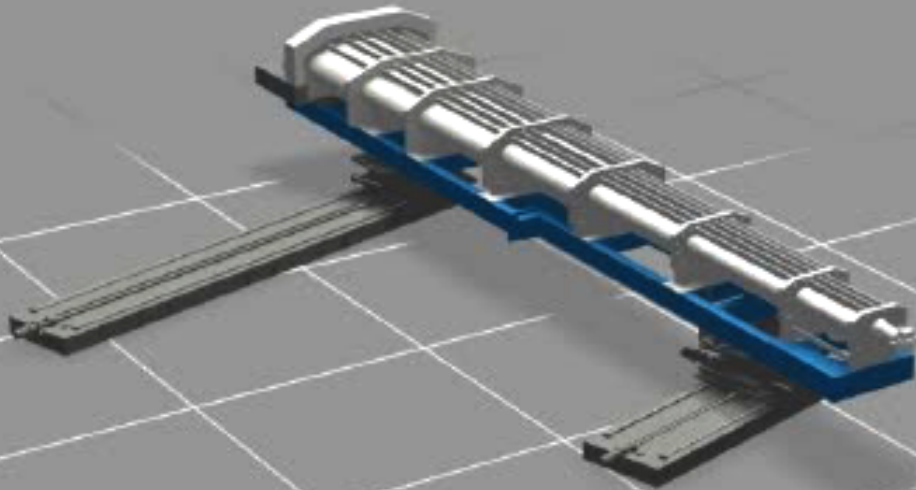
$m_1^{-1/2} e_1 = m_2^{-1/2} e_2$   
**in-phase**

# Inelastic X-Ray Scattering: A plethora of different techniques



# HERIX-3 and HERIX-30





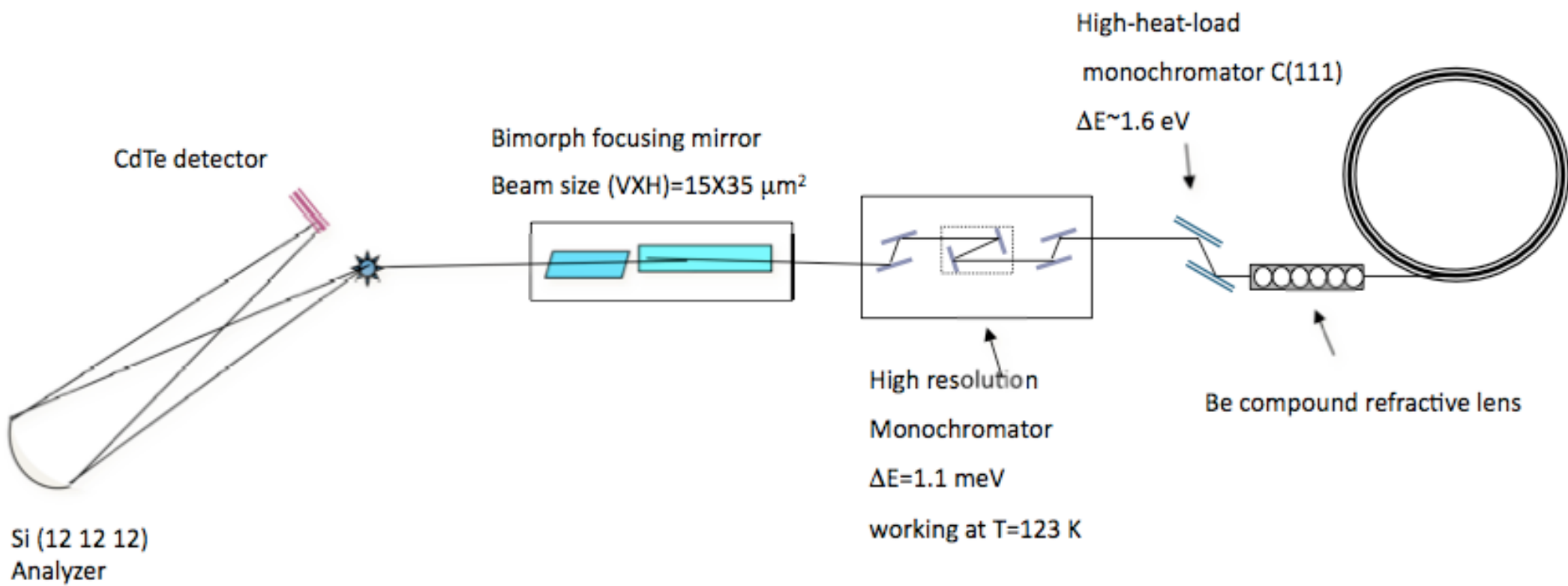




**Table 1.** Crystal contributions for different silicon reflections. The reflections are higher orders of the (1, 1, 1) and the (3, 1, 0) reflections, currently used at the existing spectrometers.

Reflection	$E$ (keV)	$\tau_{\text{ext}}$ ( $\mu\text{m}$ )	$\tau_{\text{abs}}$ ( $\mu\text{m}$ )	$\delta E_{\text{crystal}}$ (meV)	Reflectivity (%)
(7, 7, 7)	13.839	40	300	5.13	81
(12, 4, 0)	14.438	30	380	6.21	87
(8, 8, 8)	15.816	50	500	4.42	85
(9, 9, 9)	17.793	100	700	1.99	76
(18, 6, 0)	21.657	200	1220	1.23	78
(11, 11, 11)	21.747	280	1240	0.85	70
(12, 12, 12)	23.724	270	1590	0.79	75
(13, 13, 13)	25.701	600	1990	0.37	61
(24, 8, 0)	28.876	840	2730	0.255	61
(15, 15, 15)	29.655	1400	2930	0.153	46

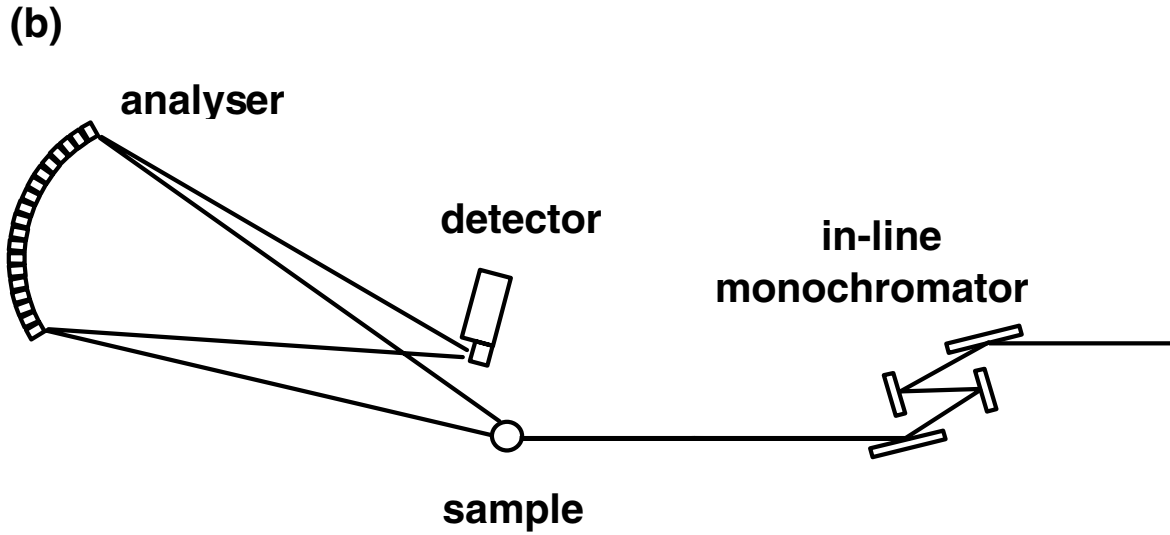


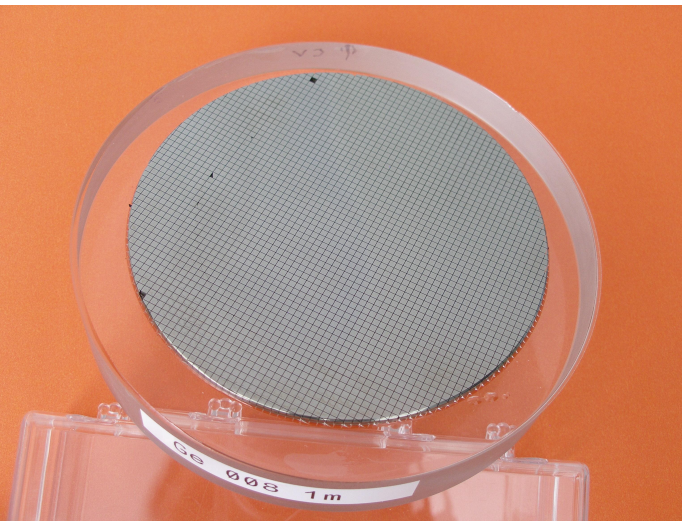
**Table 2.** Settings for the analyser for different energy resolutions. The total energy resolution is here twice the value of the geometrical contribution of the analyser.

$\delta E_{\text{total}}$ (meV)	$\delta E_{\text{geom}}$ (meV)	Reflection	$E$ (keV)	$\theta_{\text{Bragg}}$ (deg)	$L$ (m)
12.42	6.21	(12, 4, 0)	14.438	89.95	2.22
10.26	5.13	(7, 7, 7)	13.839	89.96	2.39
8.84	4.42	(8, 8, 8)	15.816	89.97	2.76
3.98	1.99	(9, 9, 9)	17.793	89.976	4.35
2.46	1.23	(18, 6, 0)	21.657	89.983	6.11
1.70	0.85	(11, 11, 11)	21.747	89.986	7.36
1.58	0.79	(12, 12, 12)	23.724	89.989	7.98
0.74	0.37	(13, 13, 13)	25.701	89.991	12.1
0.51	0.255	(24, 8, 0)	28.876	89.993	15.5 <sub>18</sub>
0.30	0.153	(15, 15, 15)	29.655	89.995	20.2

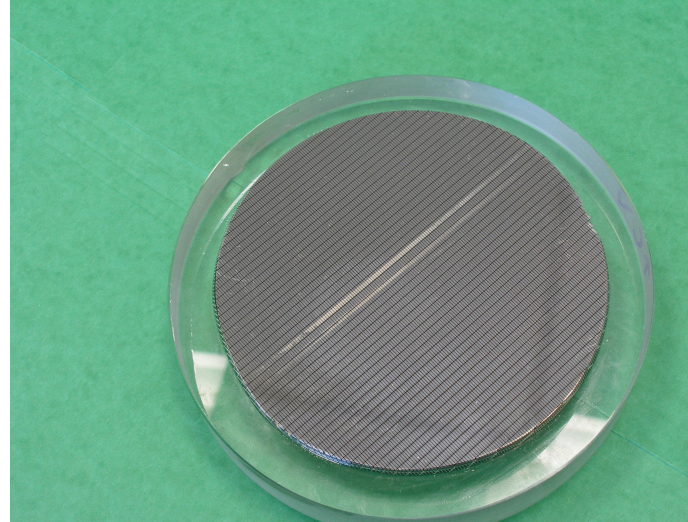
# Choice of energy

<b>Si Reflection at 90 °</b>	<b>Energy (keV)</b>	<b>Resolution (meV)</b>	<b>Reflectivity (%)</b>
<b>18 6 0</b>	<b>21.657</b>	<b>1.23</b>	<b>78</b>
<b>11 11 11</b>	<b>21.747</b>	<b>0.83</b>	<b>70</b>
<b>13 11 9</b>	<b>21.985</b>	<b>0.81</b>	<b>69</b>
<b>15 11 7</b>	<b>22.685</b>	<b>0.70</b>	<b>68</b>
<b>20 4 0</b>	<b>23.280</b>	<b>0.87</b>	<b>76</b>
<b>12 12 12</b>	<b>23.724</b>	<b>0.80</b>	<b>75</b>
<b>14 14 8</b>	<b>24.374</b>	<b>0.69</b>	<b>74</b>
<b>22 2 0</b>	<b>25.215</b>	<b>0.576</b>	<b>71</b>
<b>13 13 13</b>	<b>25.701</b>	<b>0.37</b>	<b>60</b>

# Bent-diced IXS analyzers



Si



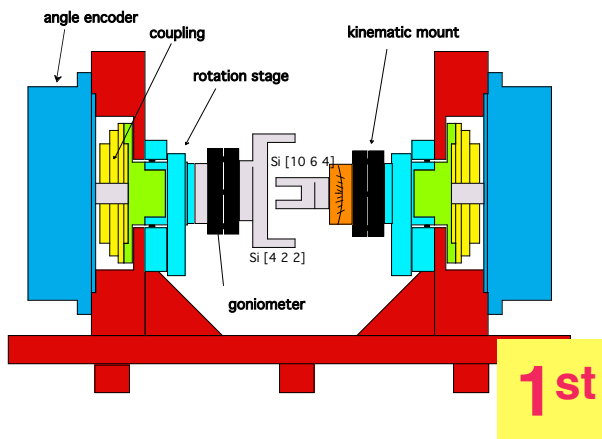
Ge



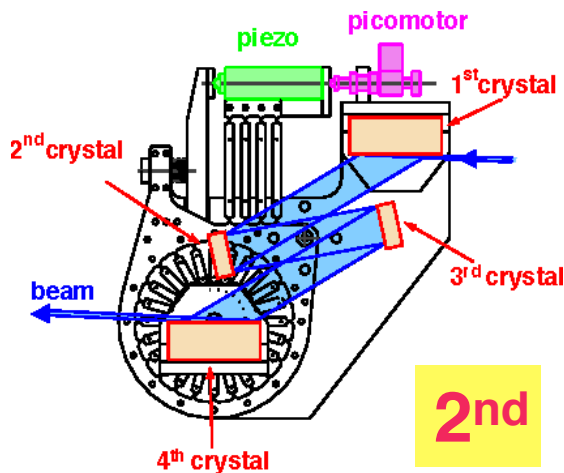
LiNbO<sub>3</sub>

# Generations of high-resolution monochromators

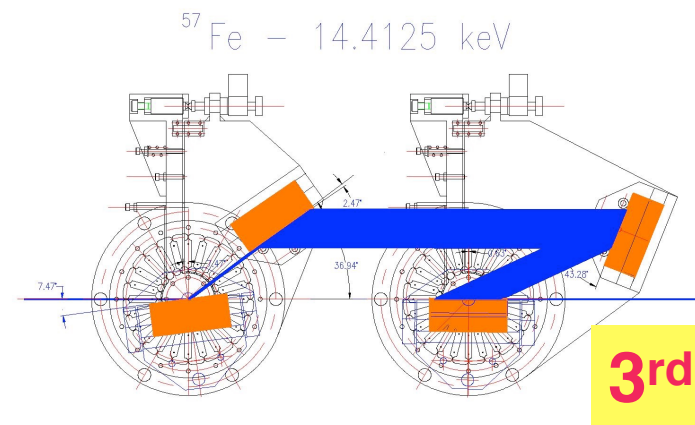
1992



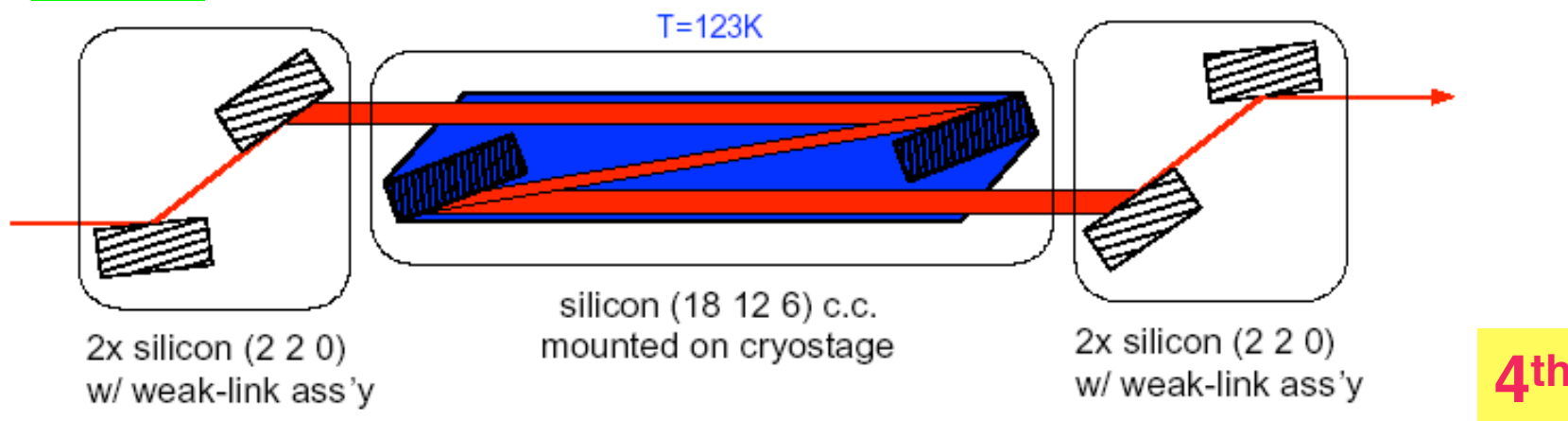
1999



2002



2004



# What is being measured ?

$$\frac{d^2\sigma}{d\Omega d\omega} = r_0^2 \frac{\omega_f}{\omega_i} |\mathbf{e}_i \cdot \mathbf{e}_f| N \sum_{i,f} \left| \langle i | \sum e^{i\mathbf{Q}\cdot\mathbf{r}_j} | f \rangle \right|^2 \delta(E_f - E_i - \hbar\omega)$$

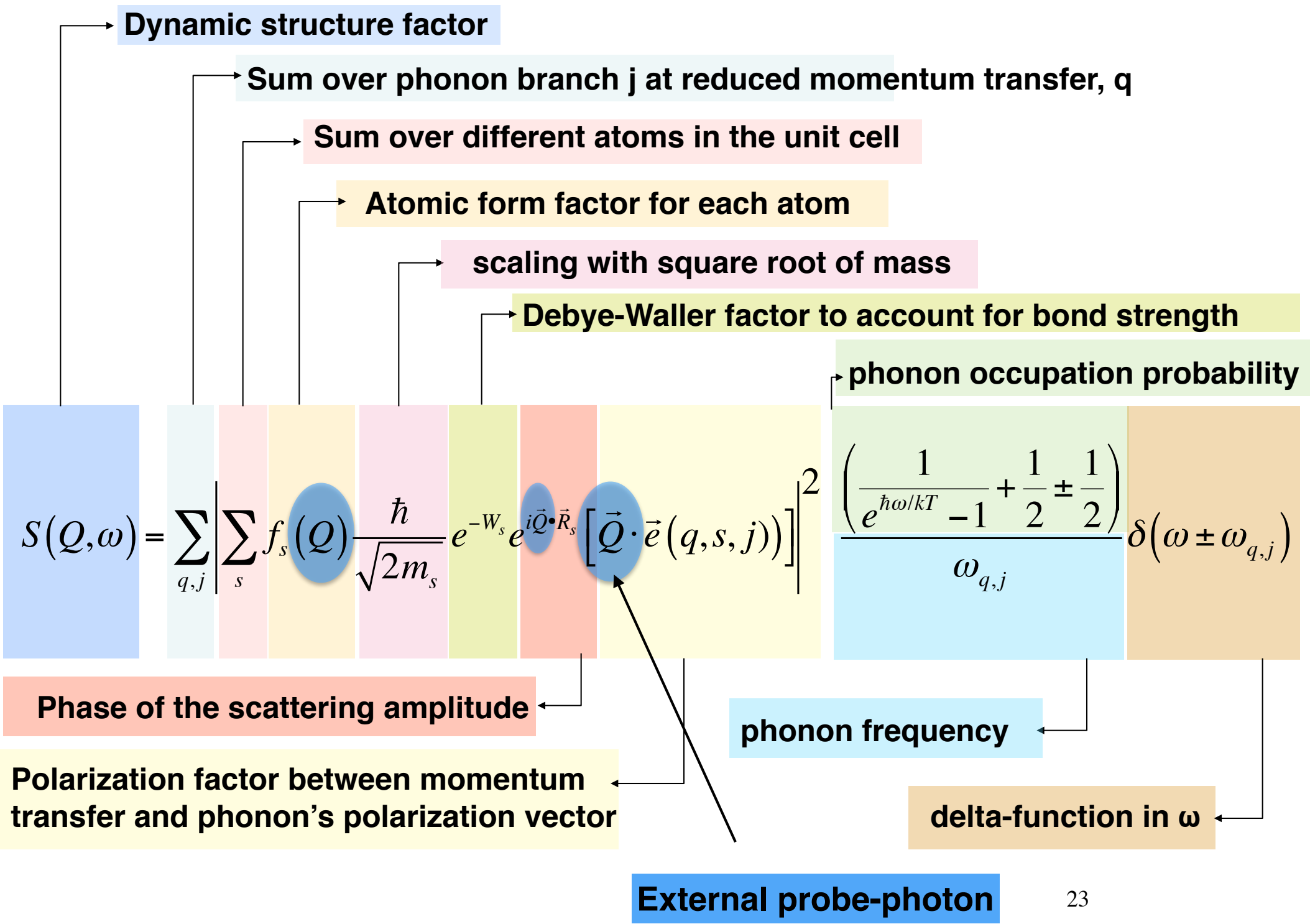
Thomson cross section

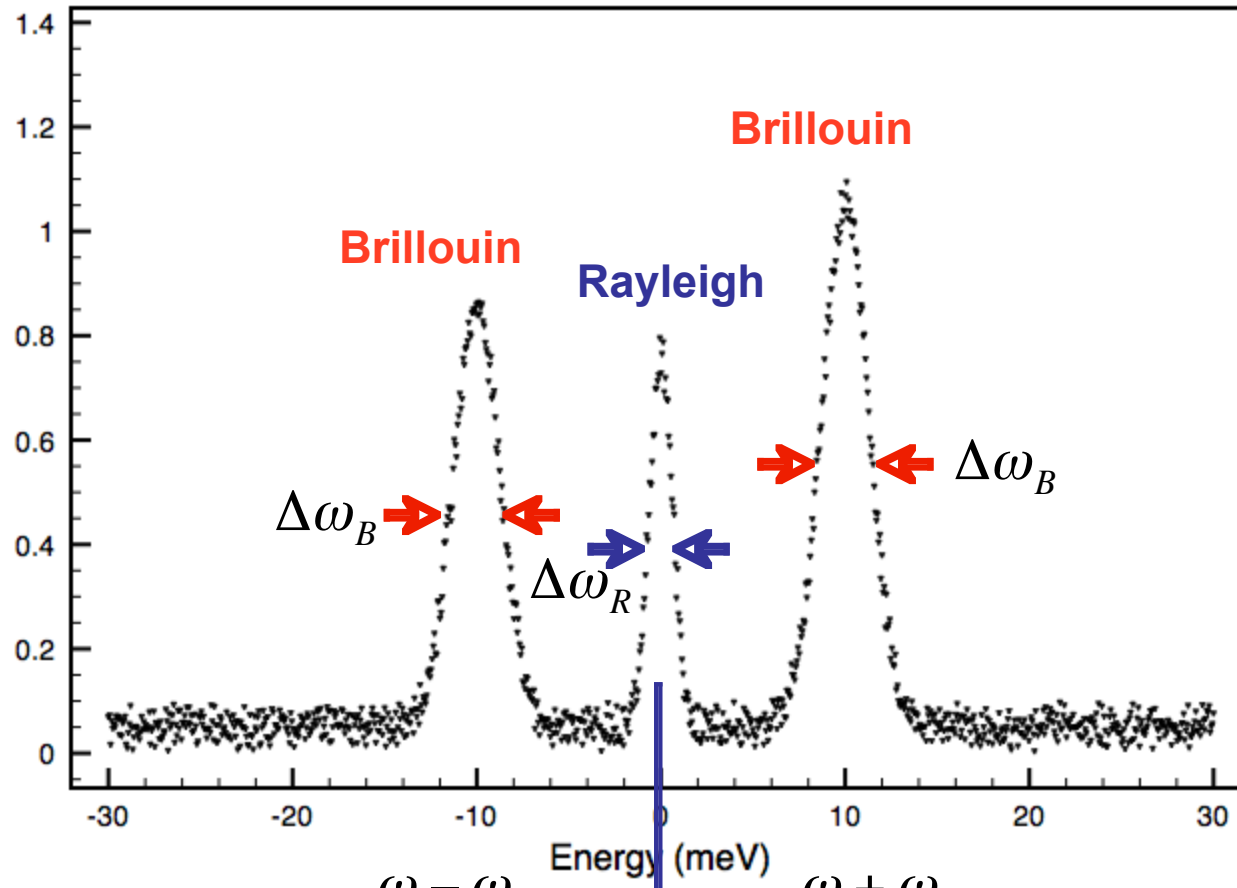
Dynamical structure factor  $S(\mathbf{Q},\omega)$

$$S(\mathbf{Q},\omega) = \frac{1}{2\pi} \int dt e^{-i\omega t} \langle \phi_i | \sum_{ll'} f_l(\mathbf{Q}) e^{-i\mathbf{Q}\cdot\mathbf{r}_l(t)} f_{l'}(\mathbf{Q}) e^{i\mathbf{Q}\cdot\mathbf{r}_{l'}(0)} | \phi_i \rangle$$

Density-density correlations

$$f(\mathbf{Q}) = f_{ion}(\mathbf{Q}) + f_{valence}(\mathbf{Q}) \quad \text{Atomic form factor}$$





Entropy fluctuations,

$$\Delta\omega_R \sim \alpha q^2$$

Concentration fluctuations

$$\Delta\omega_R \sim Dq^2$$

Pressure fluctuations

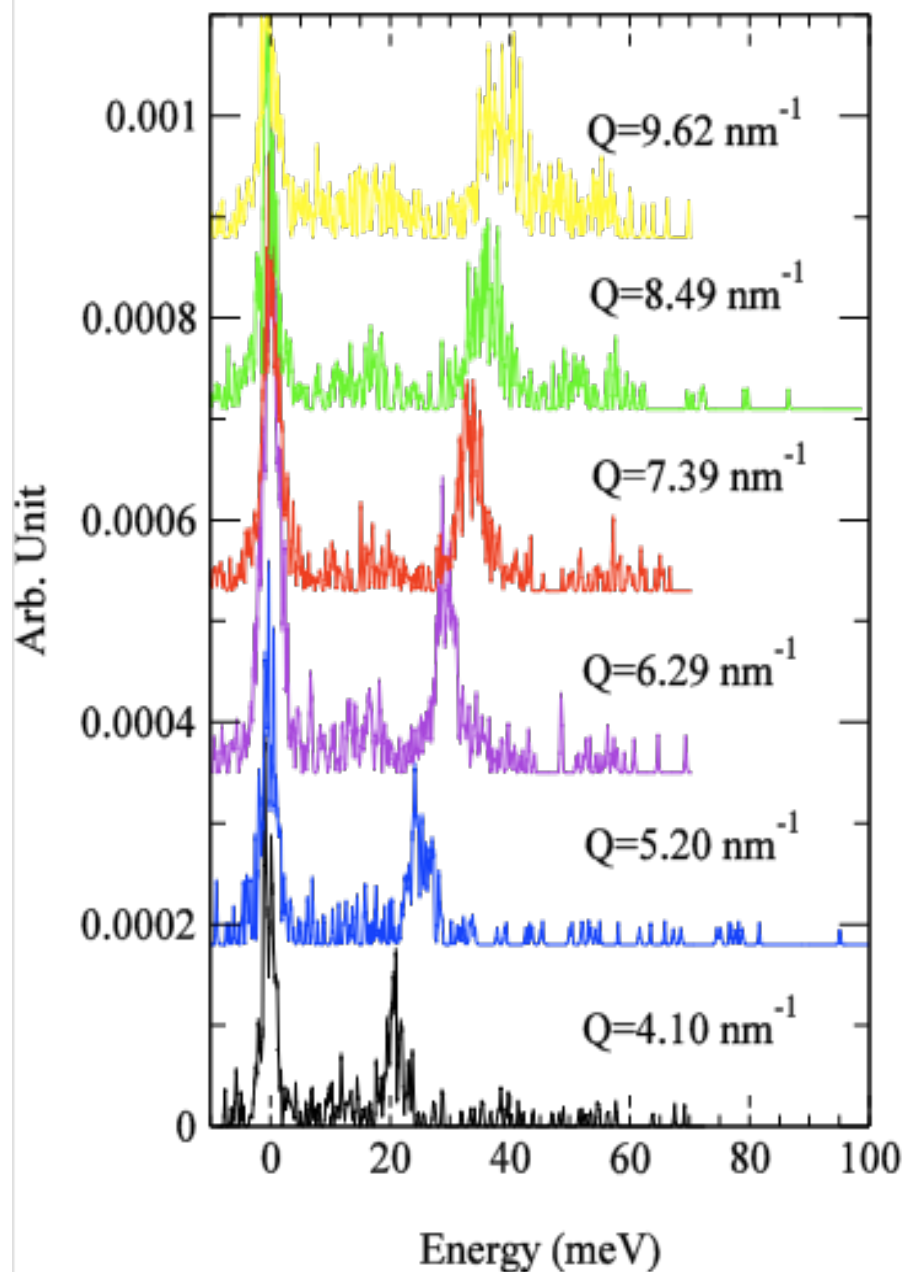
$$\omega_B(q) = V \cdot q$$

$$\Delta\omega_B \sim Vq^2$$



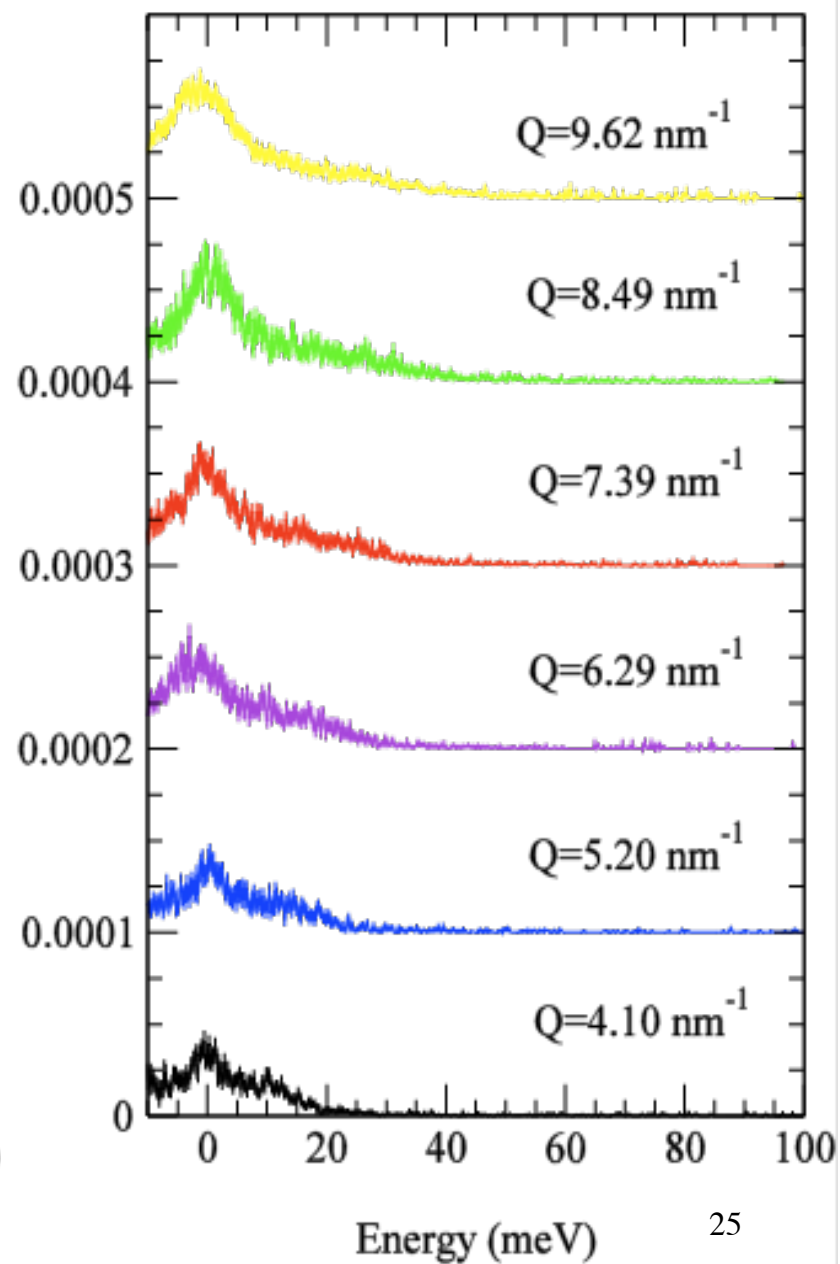
### Hot Solid Silicon

$T=1300\text{ C}^\circ$



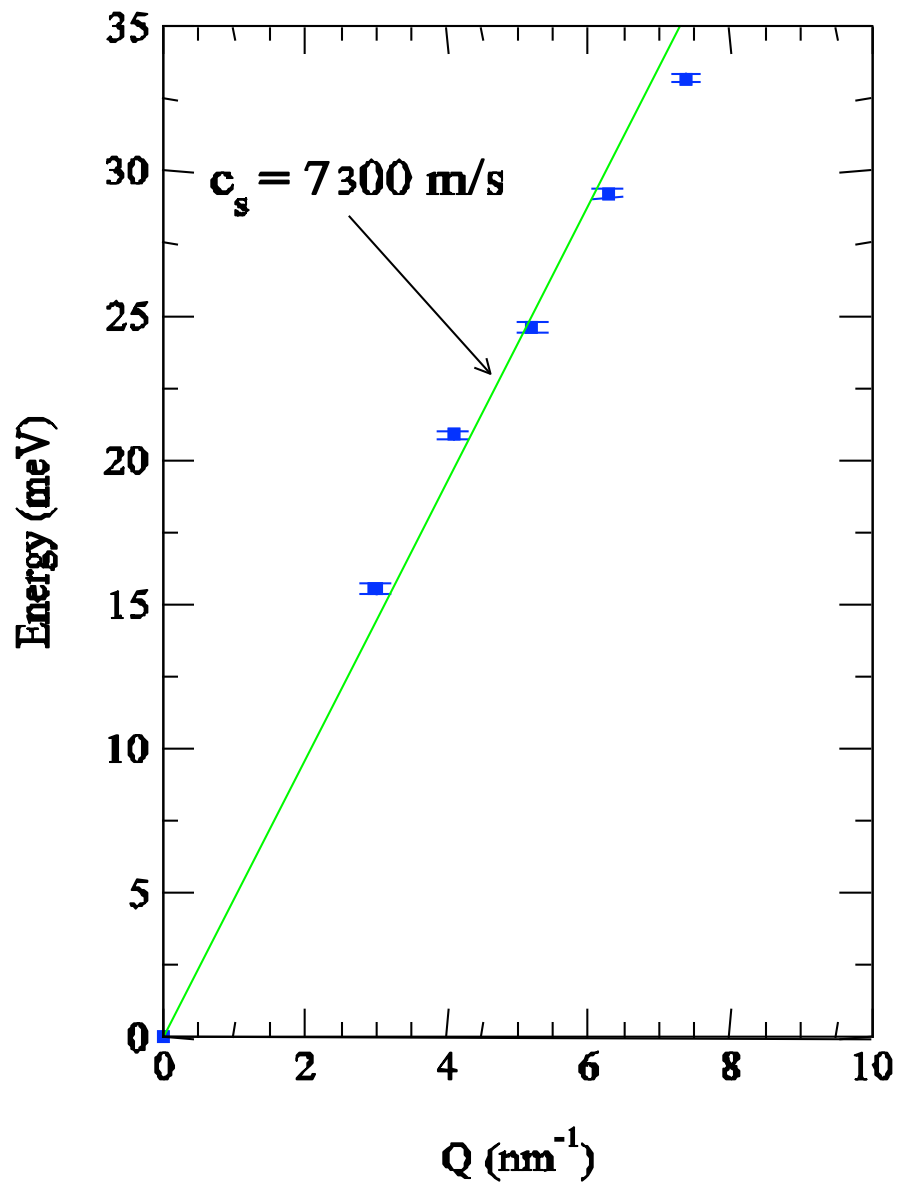
### Supercooled Silicon

$T=1300\text{ C}^\circ$



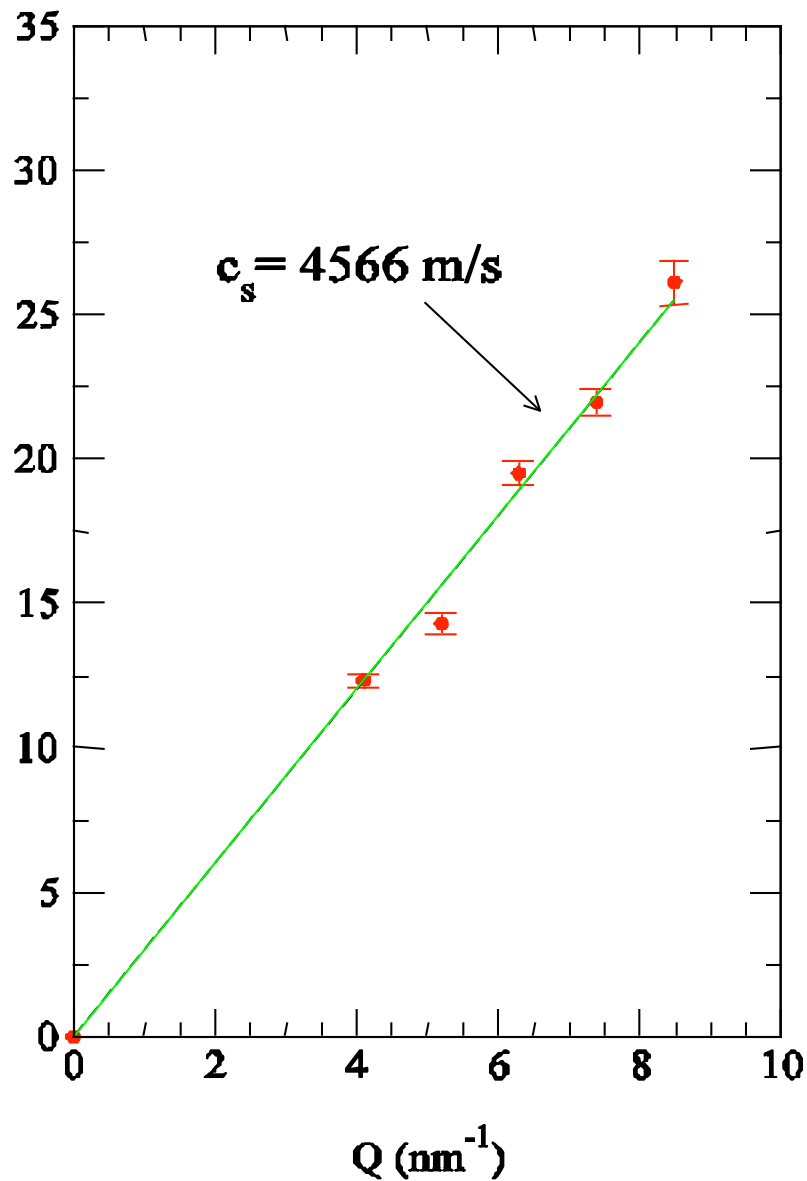
### Hot Solid Si

$T=1300\text{ C}^\circ$



### Supercooled Si

$T=1300\text{ C}^\circ$



# Where is quantum mechanics in all of this?

$$E_{1,n} = \frac{1}{2} J(u_{1,n} - u_{2,n})^2 + \frac{1}{2} J(u_{1,n} - u_{2,n-1})^2$$

$$E_{2,n} = \frac{1}{2} J(u_{2,n} - u_{1,n})^2 + \frac{1}{2} J(u_{2,n} - u_{1,n+1})^2$$

**Diatomic model**

$$E = \frac{1}{4} \sum_{n,n'} \sum_{j,j'} \phi_{n,n'}^{j,j'} (u_{j,n} - u_{j',n'})^2 = \frac{1}{2} \sum_{n,n'} \sum_{j,j'} u_{j,n} \Phi_{n,n'}^{j,j'} u_{j',n'}$$

**Generalized model**

$j, j'$ : atoms in the unit cell

$n, n'$ : unit cells in the crystal

$\phi_{j,j'}^{n,n'}$ : differential of individual bond energy with respect to displacement

$\Phi_{j,j'}^{n,n'}$ : differential of overall bond energy of all lattice

# PHONON's: $\phi\omega\nu\acute{\eta}$ (phonē), *sound*

- Phonons are periodic oscillations in condensed systems.
- They are inherently involved in thermal and electrical conductivity.
- They can show anomalous (non-linear) behavior near a phase transition.
- They can carry sound (acoustic modes) or couple to electromagnetic radiation or neutrons (acoustical and optical).
- Have energy of  $\hbar\omega$  as quanta of excitation of the lattice vibration mode of angular frequency  $\omega$ . Since momentum,  $\hbar k$ , is exact, they are delocalized, collective excitations.
- Phonons are bosons, and they are not conserved. They can be created or annihilated during interactions with neutrons or photons.
- They can be detected by Brillouin scattering (acoustic), Raman scattering, FTIR (optical).
- Their dispersion throughout the BZ can ONLY be monitored with x-rays (IXS), or neutrons (INS).
- Accurate prediction of phonon dispersion require correct knowledge about the force constants:  
COMPUTATIONAL TECHNIQUES ARE ESSENTIAL.

$$u_{j\ell}(t) = \frac{1}{\sqrt{Nm_j}} \sum_{\mathbf{k}, \lambda} \mathbf{e}_{\mathbf{k}, \lambda} \exp(i\mathbf{k} \cdot \mathbf{r}_{j\ell}) Q(\mathbf{k}, \lambda, t)$$

Fourier relationship between real space and time and reciprocal space and time

$\mathbf{e}_{\mathbf{k}, \lambda}$  : mode eigenvector

$Q(\mathbf{k}, \lambda, t)$  : normal mode coordinate

$$\dot{u}_{j\ell}(t) = \frac{-i}{\sqrt{Nm_j}} \sum_{\mathbf{k}, \lambda} \omega_{\mathbf{k}, \lambda} \mathbf{e}_{\mathbf{k}, \lambda} \exp(i\mathbf{k} \cdot \mathbf{r}_{j\ell}) Q(\mathbf{k}, \lambda, t)$$

Velocity

$$\frac{1}{2} \sum_{j, \ell} m_j |\dot{\mathbf{u}}_{j\ell}|^2 = \frac{1}{2} \sum_{\mathbf{k}, \lambda} \omega_{\mathbf{k}, \lambda}^2 |Q(\mathbf{k}, \lambda)|^2$$

Kinetic energy

$$\frac{1}{2} \sum_{\substack{j, j' \\ \ell, \ell'}} \mathbf{u}_{j\ell}^T \cdot \Phi_{\ell, \ell'}^{j, j'} \cdot \mathbf{u}_{j'\ell'} = \frac{1}{2} \sum_{\mathbf{k}, \lambda} \omega_{\mathbf{k}, \lambda}^2 |Q(\mathbf{k}, \lambda)|^2$$

Potential energy (via Virial theorem)

$$\frac{1}{2} \sum_{j, \ell} m_j |\dot{\mathbf{u}}_{j\ell}|^2 + \frac{1}{2} \sum_{\substack{j, j' \\ \ell, \ell'}} \mathbf{u}_{j\ell}^T \cdot \Phi_{\ell, \ell'}^{j, j'} \cdot \mathbf{u}_{j'\ell'} = \sum_{\mathbf{k}, \lambda} \omega_{\mathbf{k}, \lambda}^2 |Q(\mathbf{k}, \lambda)|^2$$

Total energy, in terms of normal mode coordinates

$$\omega^2 \mathbf{e} = \mathbf{D}(\mathbf{k}) \cdot \mathbf{e} \quad \Rightarrow \quad \omega^2 = \mathbf{e}^T \cdot \mathbf{D}(\mathbf{k}) \cdot \mathbf{e}$$

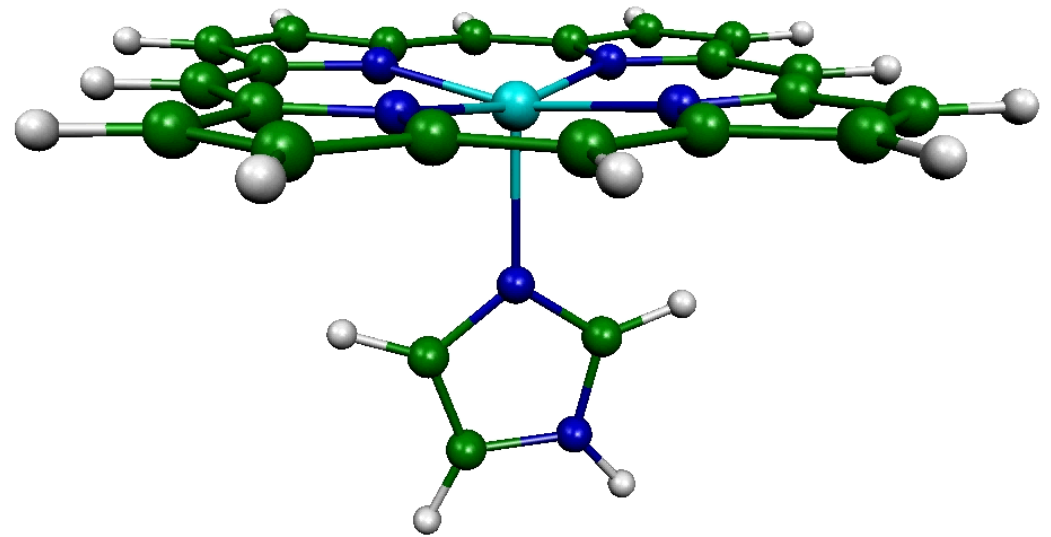
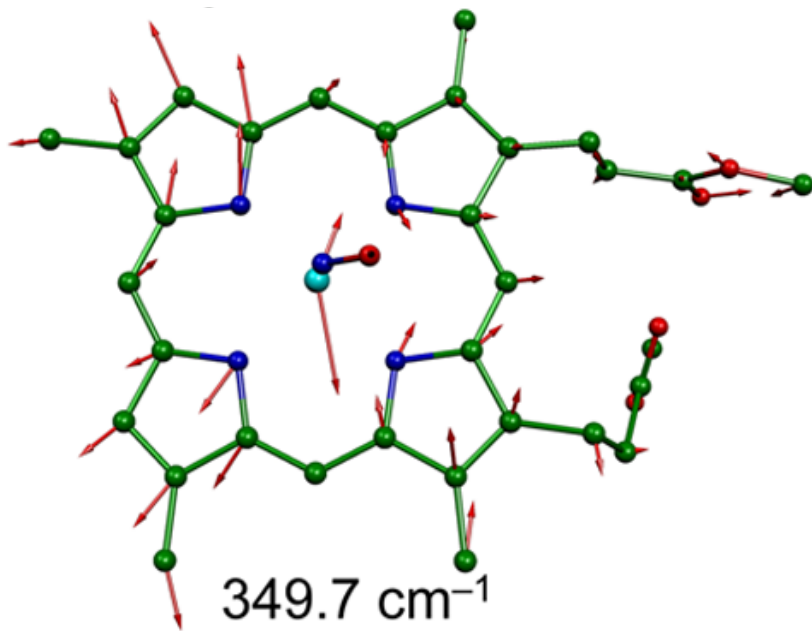
**Eigenvalue eq<sup>n</sup>.**

$$D_{j,j'}(\mathbf{k}) = \frac{1}{\sqrt{m_j m_{j'}}} \sum_{n'} \Phi_{0,n'}^{j,j'} \exp(i\mathbf{k} \cdot (\mathbf{r}_{j,0} - \mathbf{r}_{j',n'}))$$

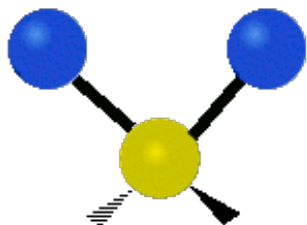
**Dynamical matrix**

$$\mathbf{e}_\lambda^T \cdot \mathbf{e}_\lambda = 1; \quad \mathbf{e}_{\lambda'}^T \cdot \mathbf{e}_\lambda = \delta_{\lambda',\lambda}$$

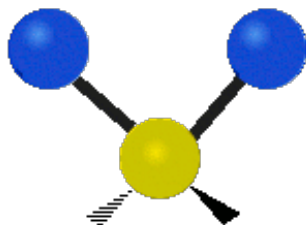
**Eigenvalues are orthonormal..**



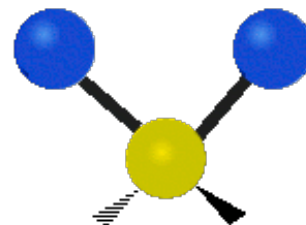
symmetrical  
stretching



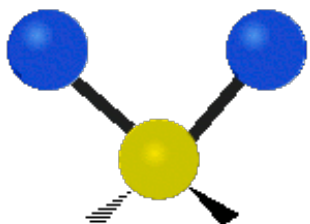
asymmetrical  
stretching



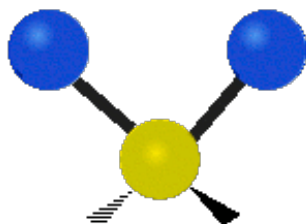
scissoring



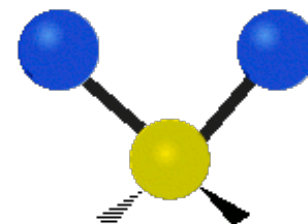
rocking

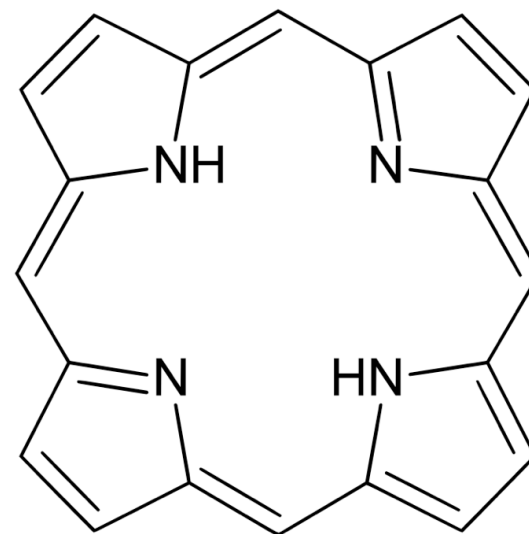
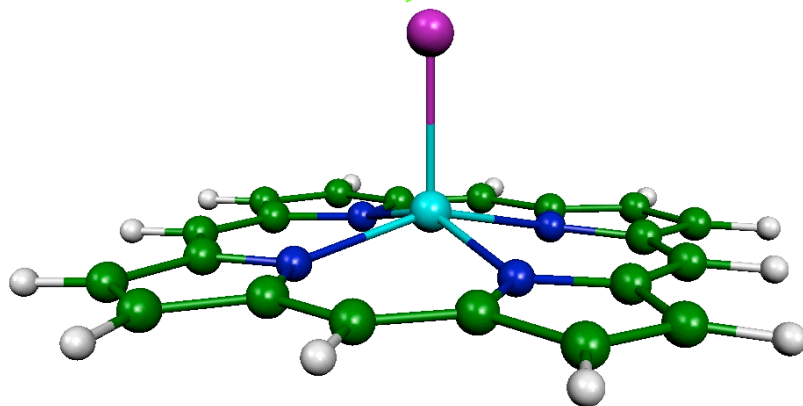
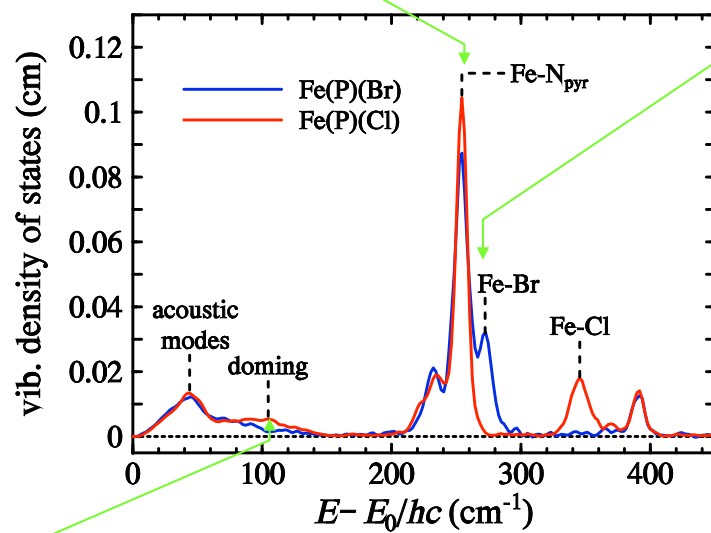
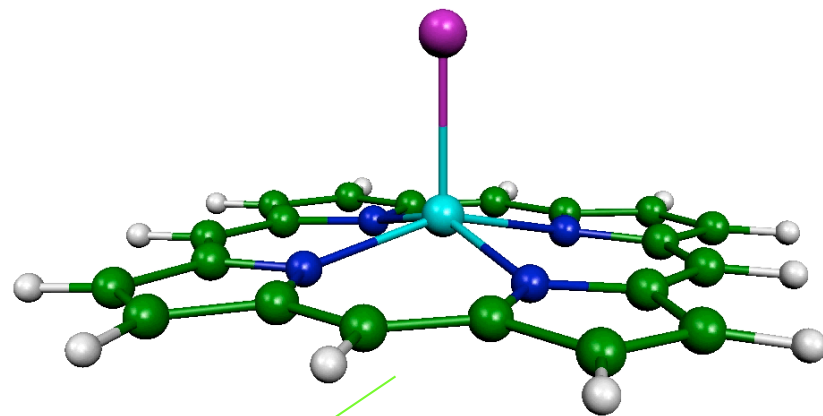
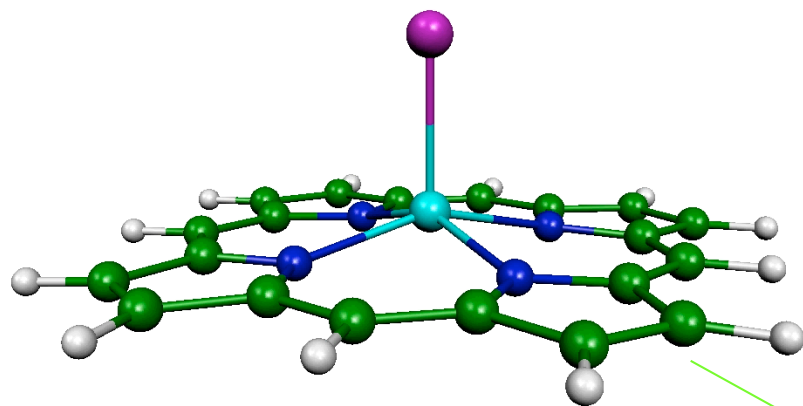


wagging



twisting







# PHONONS (cont'd)

$$E_n = \left( n + \frac{1}{2} \right) \hbar \omega$$

Energy of a single oscillation as a function of number of phonons. The second term +1/2 is the “zero-point” energy.

$$E = \sum_{\mathbf{k}, \lambda} \omega_{\mathbf{k}, \lambda}^2 |Q(\mathbf{k}, \lambda)|^2 = \sum_{\mathbf{k}, \lambda} \left( n_{\mathbf{k}, \lambda} + \frac{1}{2} \right) \hbar \omega_{\mathbf{k}, \lambda}$$

Total energy, in terms of normal mode coordinates

$$\langle n(\omega_{\mathbf{k}, \lambda}) \rangle = \frac{1}{\exp(\hbar \omega_{\mathbf{k}, \lambda} / k_B T) - 1}$$

Bose-Einstein statistics for average number of modes at a given temperature

$$\mathcal{H} = \frac{1}{2} \sum_{j, \ell} m_j |\dot{\mathbf{u}}_{j\ell}|^2 + \frac{1}{2} \sum_{\substack{j, j' \\ \ell, \ell'}} \mathbf{u}_{j\ell}^T \cdot \Phi_{\ell, \ell'}^{j, j'} \cdot \mathbf{u}_{j'\ell'}$$

Hamiltonian of the system:

$\mathcal{H} = \text{Kin. En.} + \text{Pot. En}$

## ***Phonon density of states***

Many thermodynamic functions like free energy, specific heat, and entropy are additive functions of phonon density of states.

This stems from the notion that the normal modes do not interact in the harmonic approximation.

Phonon density of states is the number of modes in a unit energy interval.

$$c_v(T) = 3Nk \int \frac{\hbar^2 \omega^2 e^{\hbar\omega/kT}}{(kT)^2 (1 - e^{\hbar\omega/kT})^2} \cdot g(\omega) \cdot d\omega$$

Vibrational specific heat

Phonon density of states is a key ingredient for many thermodynamic properties

If we choose to write in terms of energy,  $E = \hbar\omega$ ,  $\beta = 1/k_B T$

$$c_v(T) = 3k_B \int (\beta E / 2)^2 \operatorname{csc} h(\beta E) \cdot g(E) \cdot dE$$

Vibrational specific heat

$$S_v(T) = 3k_B \int_0^{\infty} \{ \beta E / 2 \cdot \cot h(\beta E) - \ln [2 \sin h(\beta E)] \} \cdot g(E) \cdot dE$$

Vibrational entropy

$$f_{LM} = e^{-E_R} \int \{ g(E) / 2 \} \cdot \operatorname{coth}(\beta E / 2) dE$$

Lamb-Mössbauer factor

$$g(E) = \frac{3m}{2\pi^2 \hbar^3 \rho v_D^3} E^2$$

Debye Sound velocity

$$\langle F \rangle = \frac{M}{\hbar^2} \int_0^{\infty} E^2 g(E) dE$$

Average restoring force constant

# And, some thermodynamics

$$\mathcal{Z} = \frac{1}{1 - \exp(-\beta\hbar\omega)}$$

Partition function

$$F = -k_B T \ln \mathcal{Z}$$

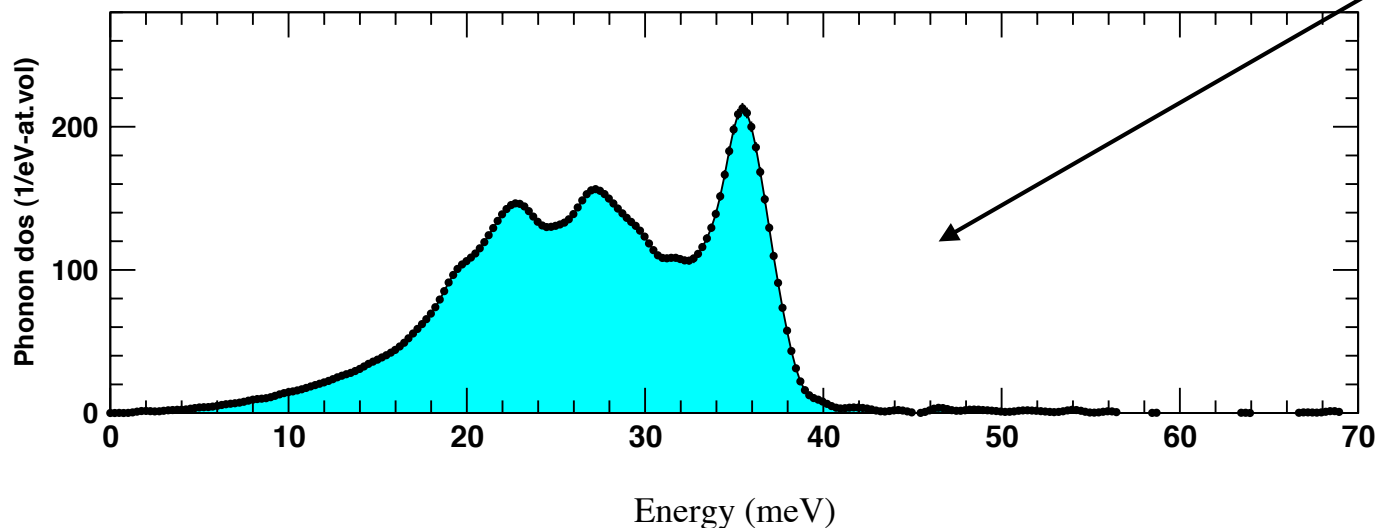
Free energy

$$C = -T \frac{\partial^2 F}{\partial T^2}$$

Heat capacity

$$E = \sum_{\mathbf{k}, \lambda} \left( \langle n(\omega_{\mathbf{k}, \lambda}) \rangle + \frac{1}{2} \right) \hbar \omega_{\mathbf{k}, \lambda} \equiv \int \left( \langle n(\omega) \rangle + \frac{1}{2} \right) \hbar \omega g(\omega) d\omega.$$

Energy in terms of  
***phonon density of states***

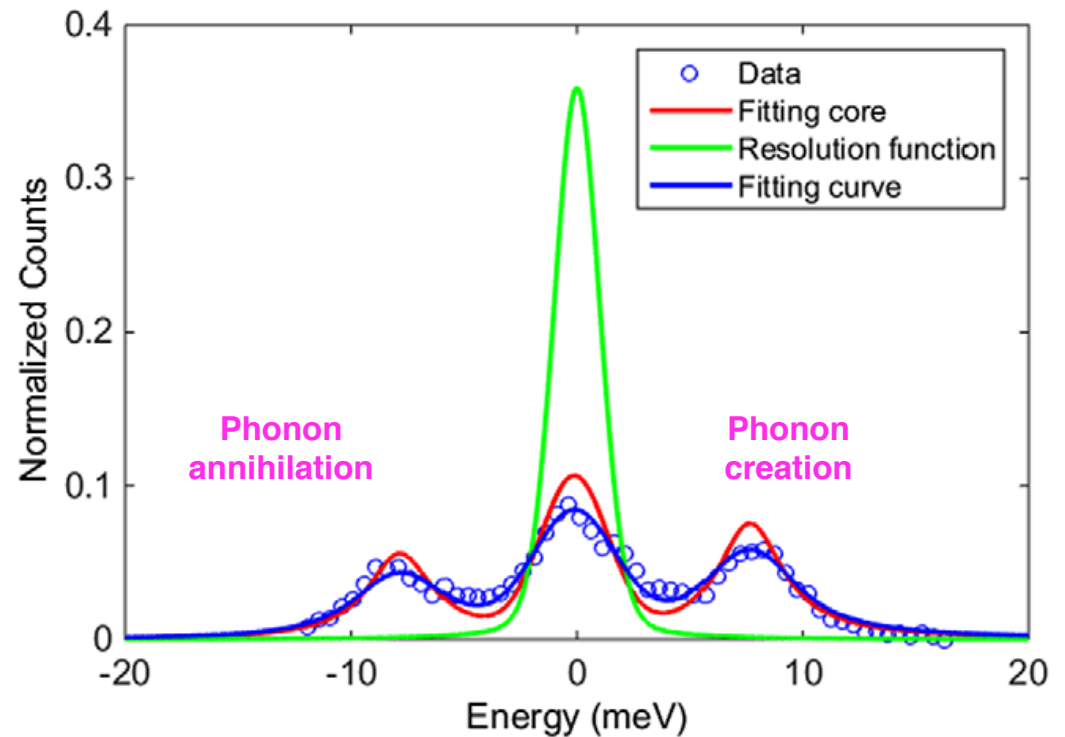
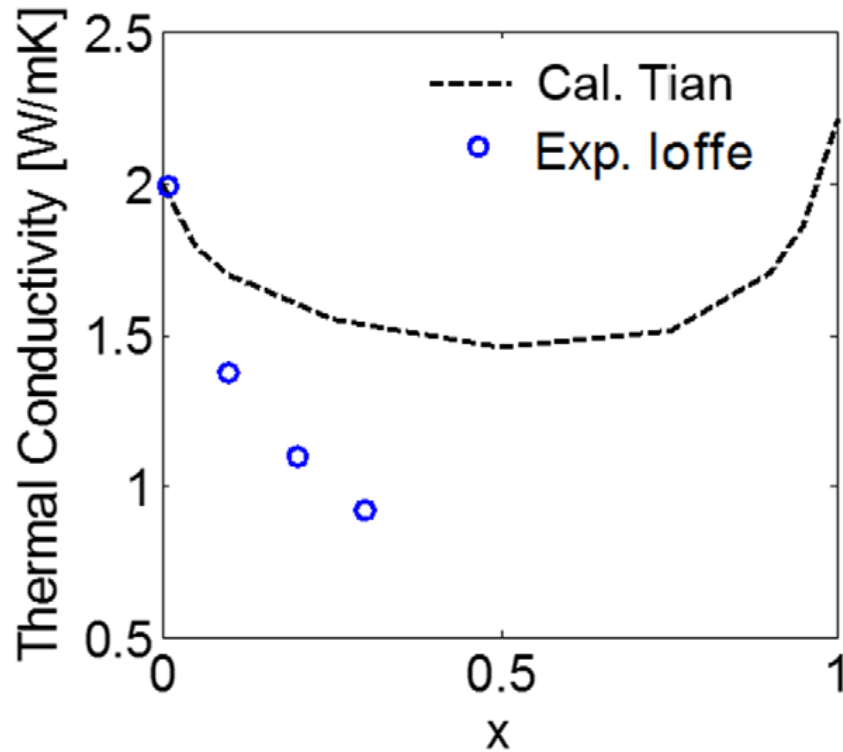


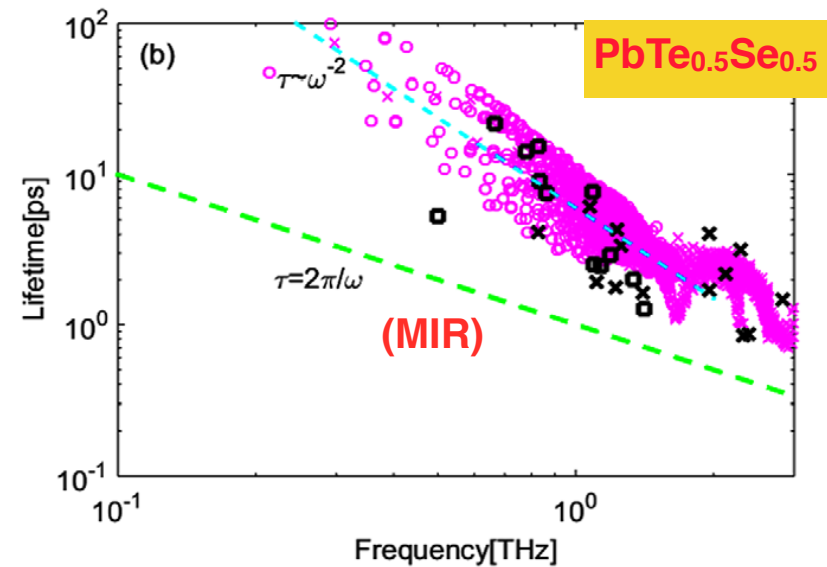
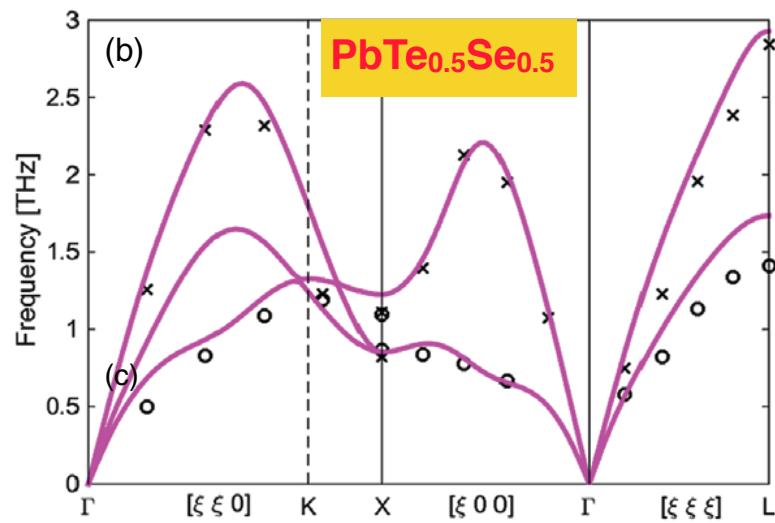
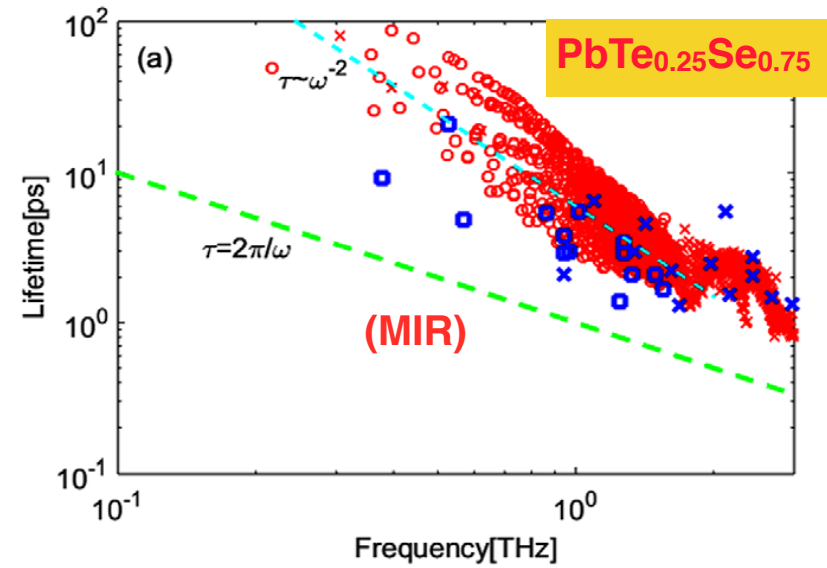
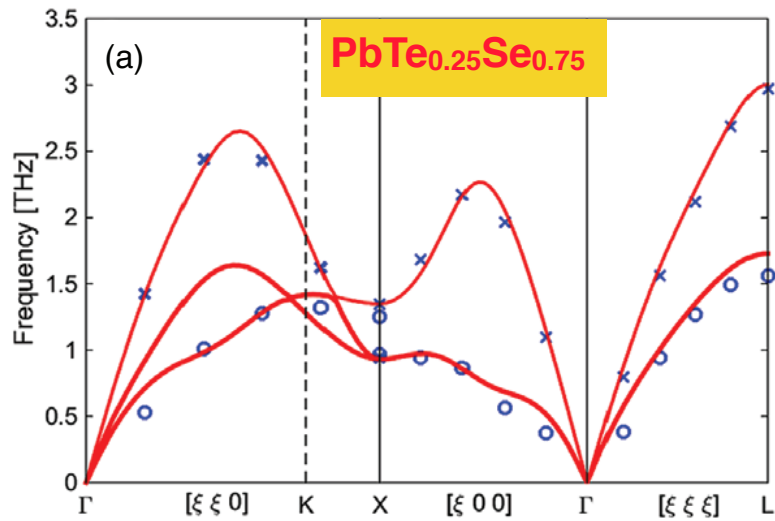
## Inelastic x-ray scattering measurements of phonon dispersion and lifetimes in $\text{PbTe}_{1-x}\text{Se}_x$ alloys:

Do phonons remain a good representation of the vibrational modes in  $\text{PbTe}_{1-x}\text{Se}_x$  alloys when alloying seems to decrease thermal conductivity?

$ZT = S^2\sigma T / \kappa$  where  $S$ ,  $\sigma$ ,  $\kappa$ ,  $T$  represent the Seebeck coefficient, electrical conductivity, thermal conductivity and absolute temperature. For thermoelectric materials, higher  $ZT$  is desirable, hence lowering  $\kappa$  while keeping  $\sigma$  is required.

Phonon lifetime measurements is one way to learn why thermal conductivity is lowered upon alloying.

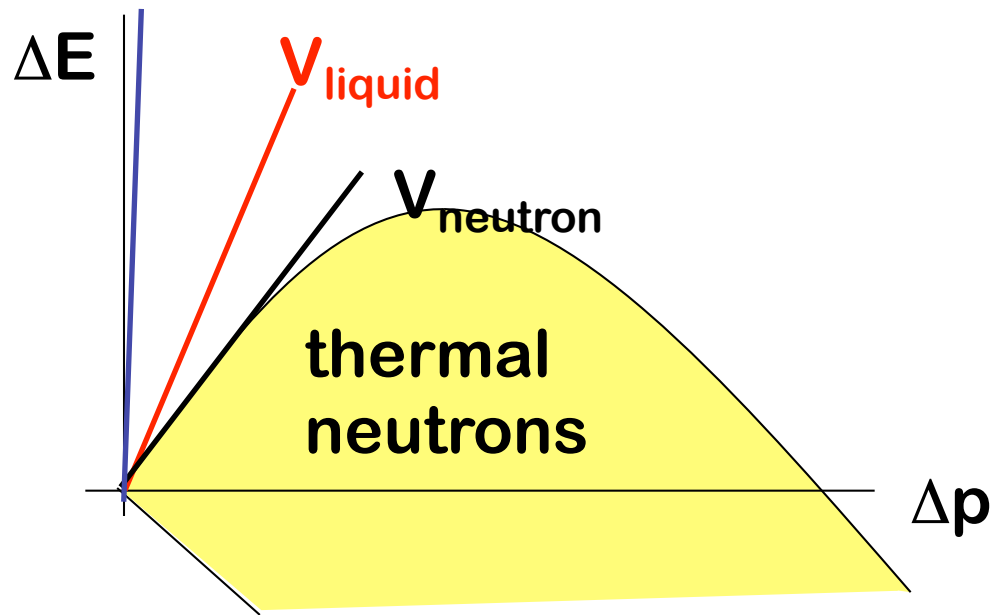




**Mott-Ioffe-Regel limit (MIR)** : When electron scattering rate is comparable to Fermi energy,  $E_F/h$ , thermal resistivity reaches its maximum. The discrepancy between virtual crystal approximation and measured thermal conductivity can be attributed to mass disorder as well as force constant variations.

The experimental data on phonon lifetimes provide a bench mark for theoretical work to directly compare lifetimes and advance our understanding of the thermal transport in alloys.

# Why x-rays instead of neutrons or visible light ?

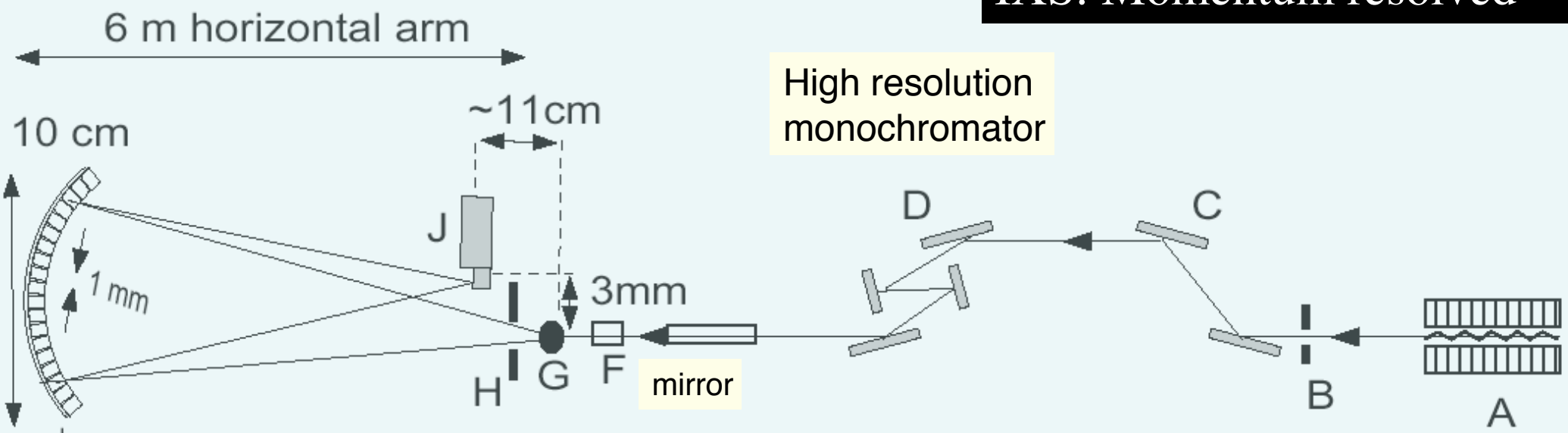


Limited momentum transfer capability of neutrons at low energies favor x-rays to study collective excitations with large dispersion, like sound modes.

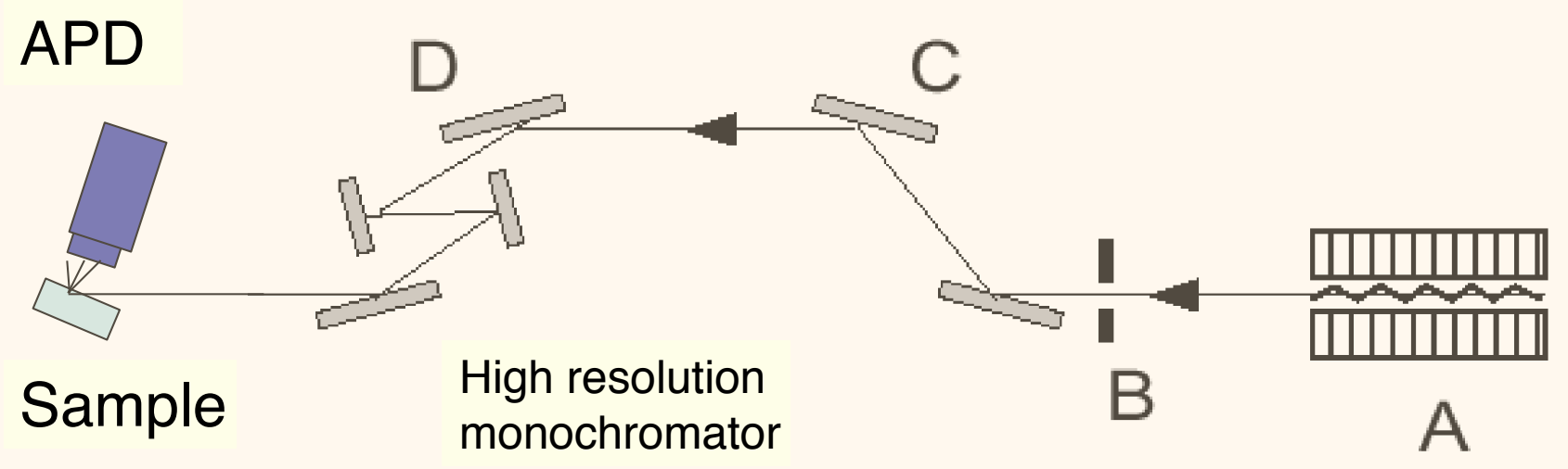
When the sound velocity exceeds that of neutrons in the liquid, x-rays become unique. The low-momentum/high-energy transfer region is only accessible by x-rays.

# Inelastic X-Ray Scattering: two approaches

**IXS: Momentum resolved**



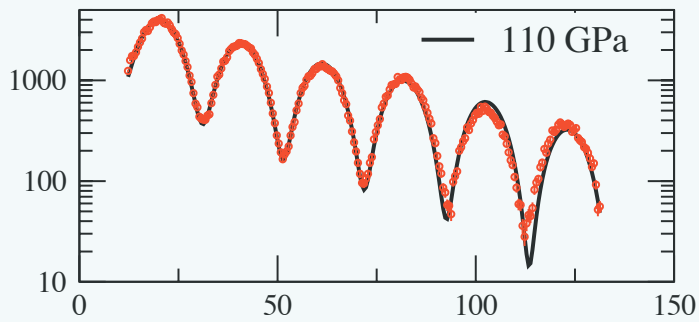
**NRIXS: Momentum integrated**





# **Nuclear Resonant Scattering**

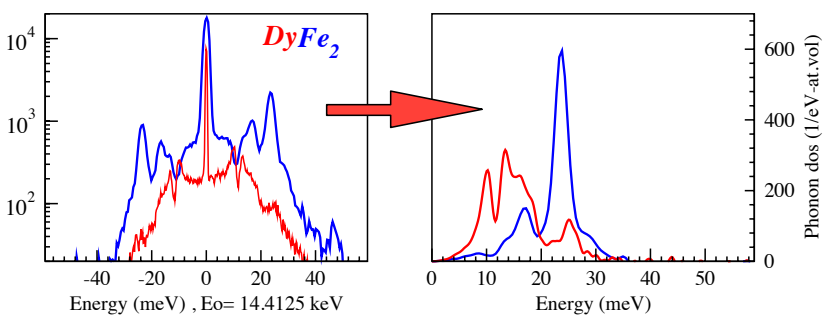
# SMS: Synchrotron Mössbauer Spectroscopy NFS : Nuclear Forward Scattering



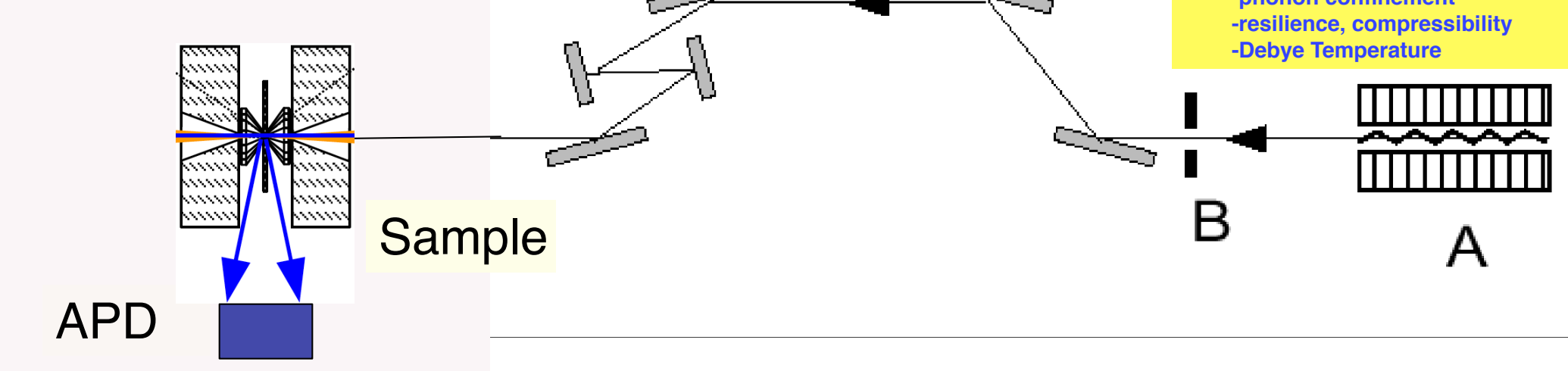
- Isomer shift
- Quadrupole splitting
- Magnetic hyperfine field
  - valence state
  - local crystallographic symmetry
  - magnetic ordering
  - relaxation



# NRIXS: Nuclear Resonant Inelastic X-ray Scattering NRVS: Nuclear Resonant Vibrational Spectroscopy



- Partial phonon density of states
- Recoil-free fraction
  - speed of sound
  - vibrational modes
  - entropy and specific heat
  - phonon confinement
  - resilience, compressibility
  - Debye Temperature



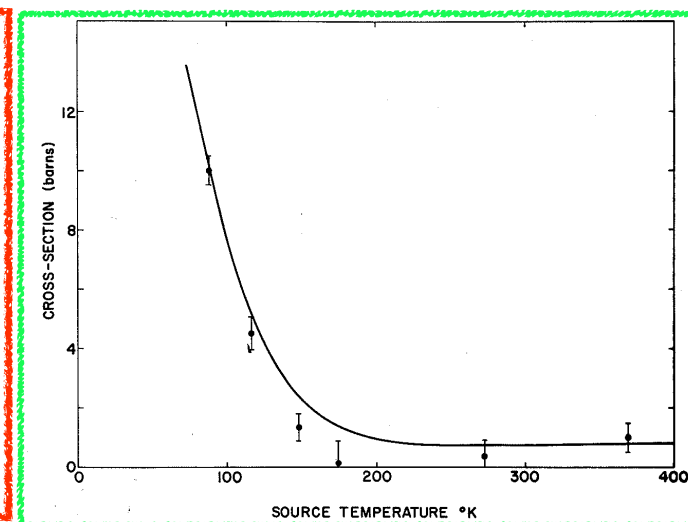
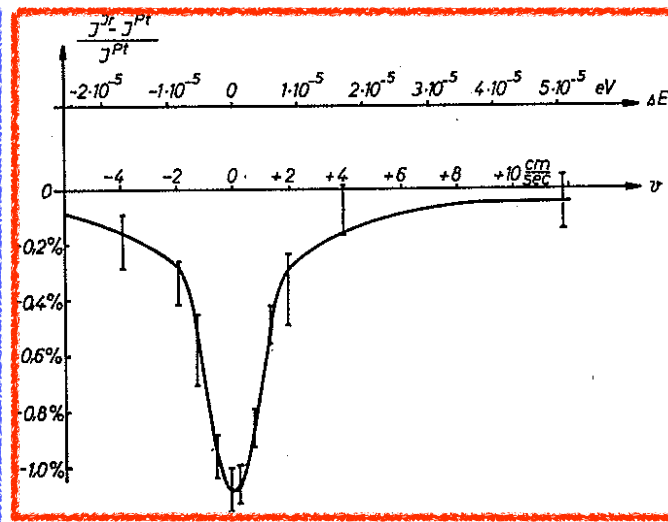
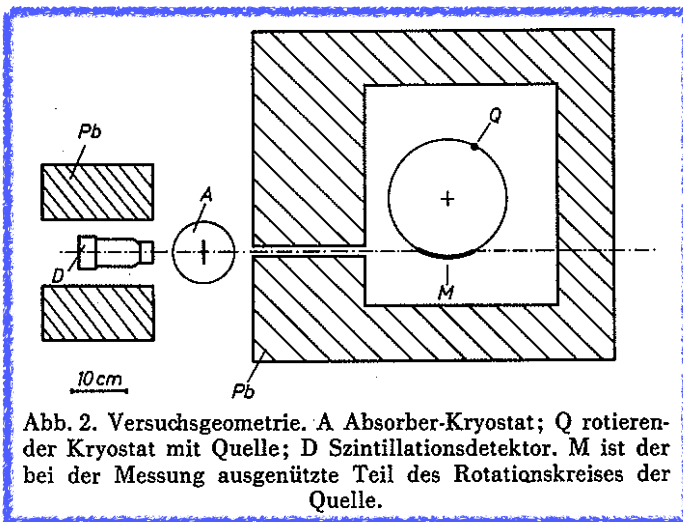
# Kernresonanzabsorption von $\gamma$ -Strahlung in $\text{Ir}^{191}$

VON RUDOLF L. MÖSSBAUER

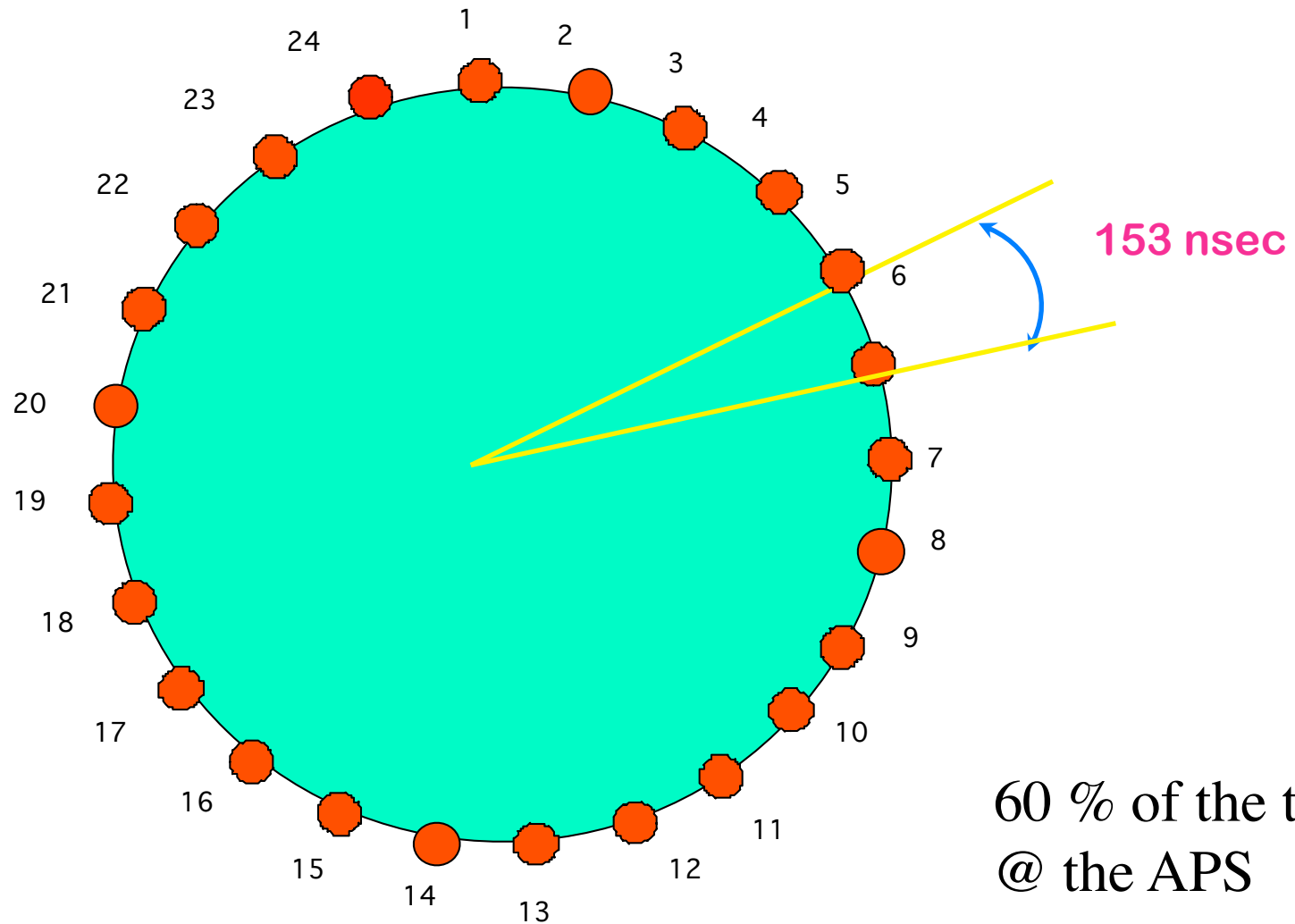
Aus dem Laboratorium für technische Physik der Technischen Hochschule in München  
und dem Institut für Physik im Max-Planck-Institut für medizinische Forschung in Heidelberg

(Z. Naturforschg. 14 a, 211—216 [1959]; eingegangen am 5. November 1958)

Bei der Emission und Selbstabsorption von weicher  $\gamma$ -Strahlung in Kernen treten bei tiefen Temperaturen in Festkörpern sehr starke Linien mit der natürlichen Linienbreite auf. Diese Linien erscheinen als Folge davon, daß bei tiefen Temperaturen bei einem Teil der Quantenübergänge der  $\gamma$ -Rückstoßimpuls nicht mehr vom einzelnen Kern aufgenommen wird, sondern von dem Kristall als Ganzes. Da die scharfen Emissions- und Absorptionslinien energetisch an der gleichen Stelle liegen, tritt ein sehr starker **Resonanzfluoreszenzeffekt** auf. Durch eine „Zentrifugen“-Methode, bei der die Emissions- und Absorptionslinien gegeneinander verschoben werden, läßt sich der Fluoreszenzeffekt unterdrücken und so eine unmittelbare Bestimmung der natürlichen Linienbreite von Resonanzlinien vornehmen. Erste Messungen nach dieser Methode ergeben für die Lebenszeit  $\tau$  des 129 keV-Niveaus in  $\text{Ir}^{191}$ :  $\tau = \left(1,4 \begin{smallmatrix} +0,2 \\ -0,1 \end{smallmatrix}\right) \cdot 10^{-10}$  sec.

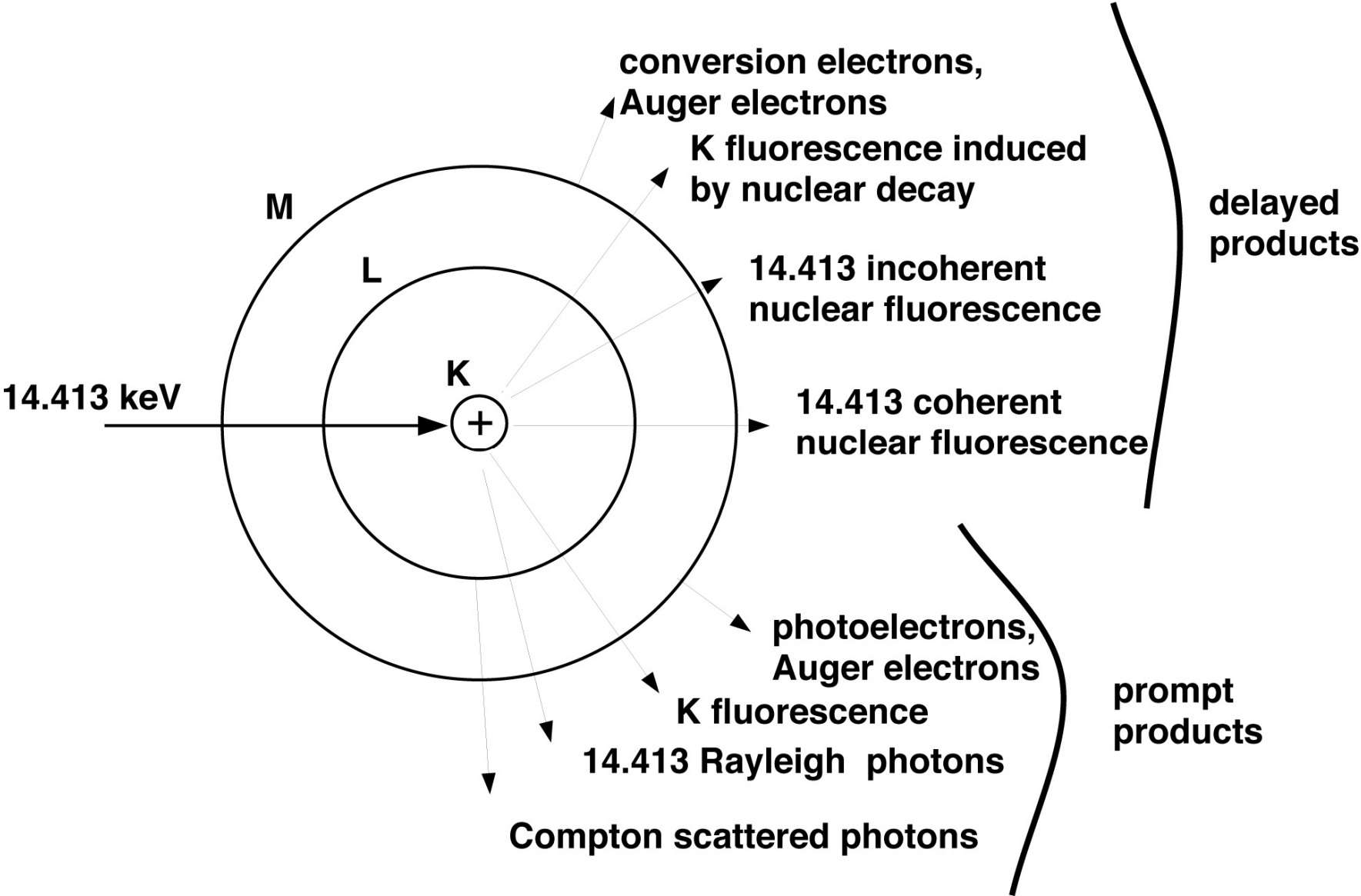


# Standard Time structure @ APS



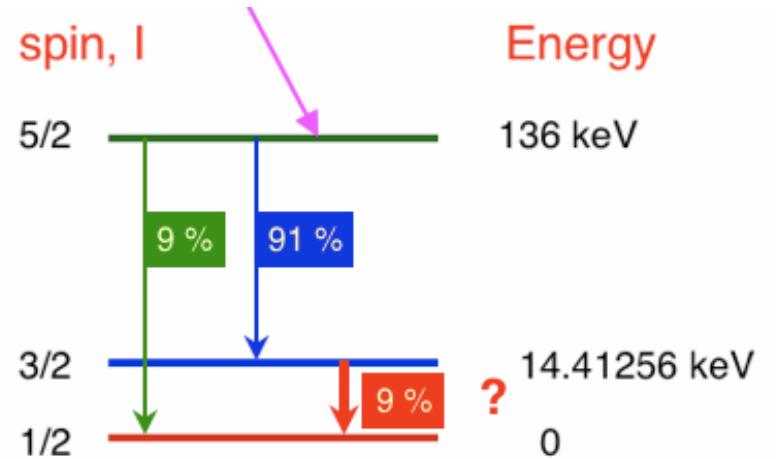
**1 revolution = 3.68  $\mu$ sec  $\Rightarrow$  1296 buckets**

# Nuclear Resonance and Fallout in $^{57}\text{Fe}$ -decay



# Detection of nuclear decay

$^{57}\text{Fe}$



prompt photons

log I

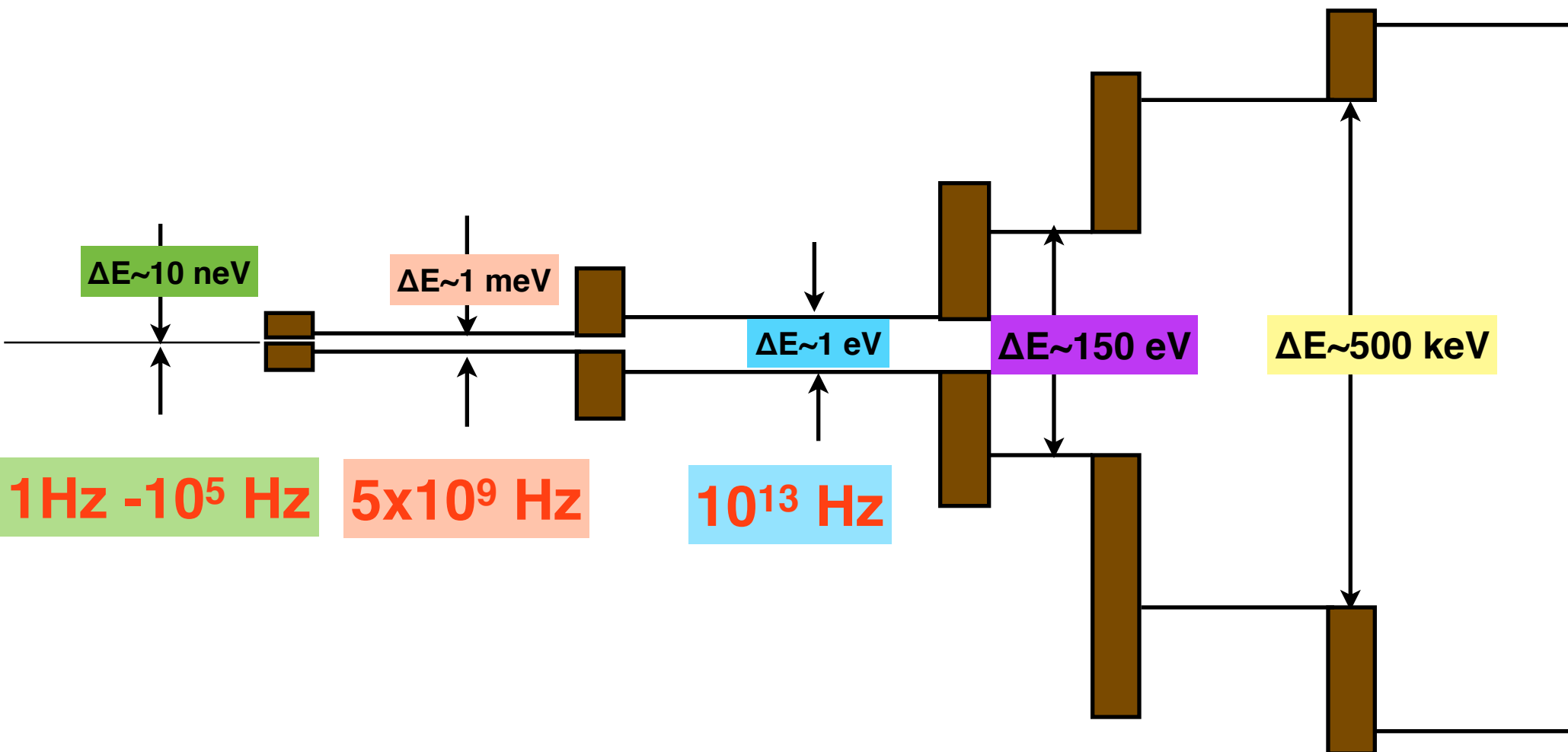
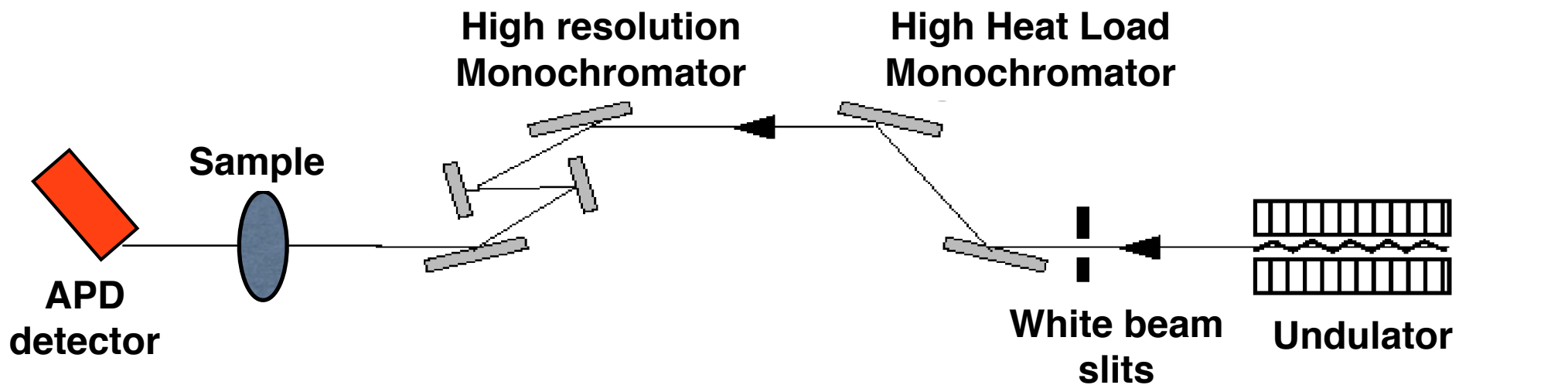
exponential decay

delayed photons

0

time (nsec)

153 nsec

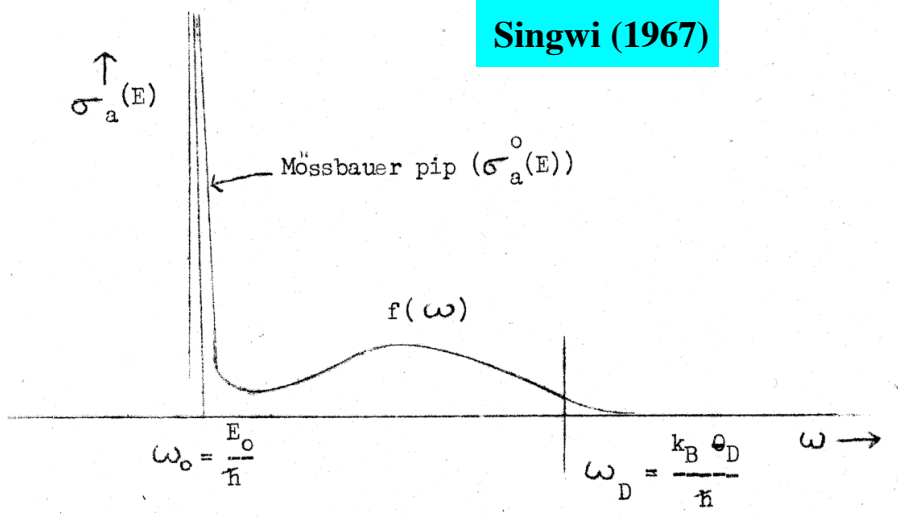


# Early dreamers..

Visualized by W. Vischer at Los Alamos & K. S. Singwi at Argonne (1960), but only properly observed after synchrotron radiation based tunable monochromators are realized.

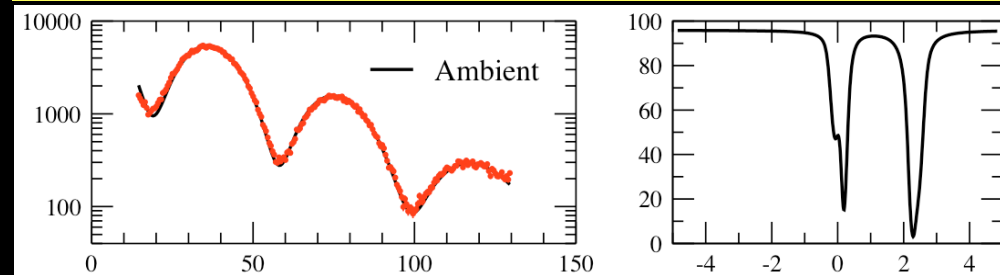
(W. Sturhahn et al, PRL, 74 (1995) p. 3832)

Singwi (1967)



# Zero phonon “Mössbauer pip”

Visualized by Stan Ruby (1974) at Argonne and properly observed by E. Gerdau (Hamburg).  
(S. L Ruby. J. de Physique 35 (1974) C6-209)



5 neV + mono. resolution

Phonon  
annihilation

Phonon  
creation

- 0 +  
Energy (~ meV)



## Phonon Density of States Measured by Inelastic Nuclear Resonant Scattering

W. Sturhahn, T. S. Toellner, and E. E. Alp

*Advanced Photon Source, Argonne National Laboratory, Argonne, Illinois 60439*

X. Zhang and M. Ando

*Photon Factory, National Laboratory for High Energy Physics, Oho 1-1, Tsukuba, Ibaraki 305, Japan*

Y. Yoda and S. Kikuta

*Department of Applied Physics, Faculty of Engineering, The University of Tokyo, Hongo 7-3-1, Bunkyo-ku, Tokyo 113, Japan*

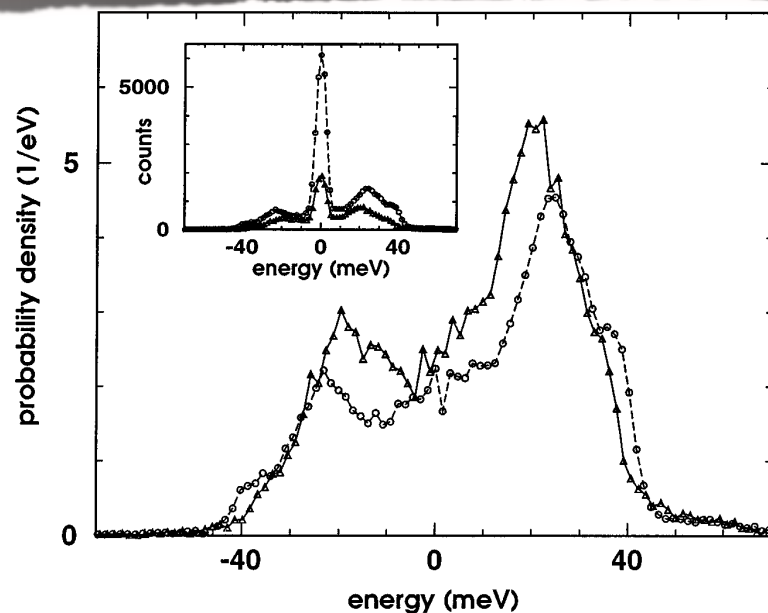
M. Seto

*Research Reactor Institute, Kyoto University, Sennan-gun, Osaka 590-04, Japan*

C. W. Kimball and B. Dabrowski

*Department of Physics, Northern Illinois University, De Kalb, Illinois 60115*

(Received 16 December 1994)



> 400 citations

Phonon Density of States Measured by Inelastic Nuclear Resonant Scattering

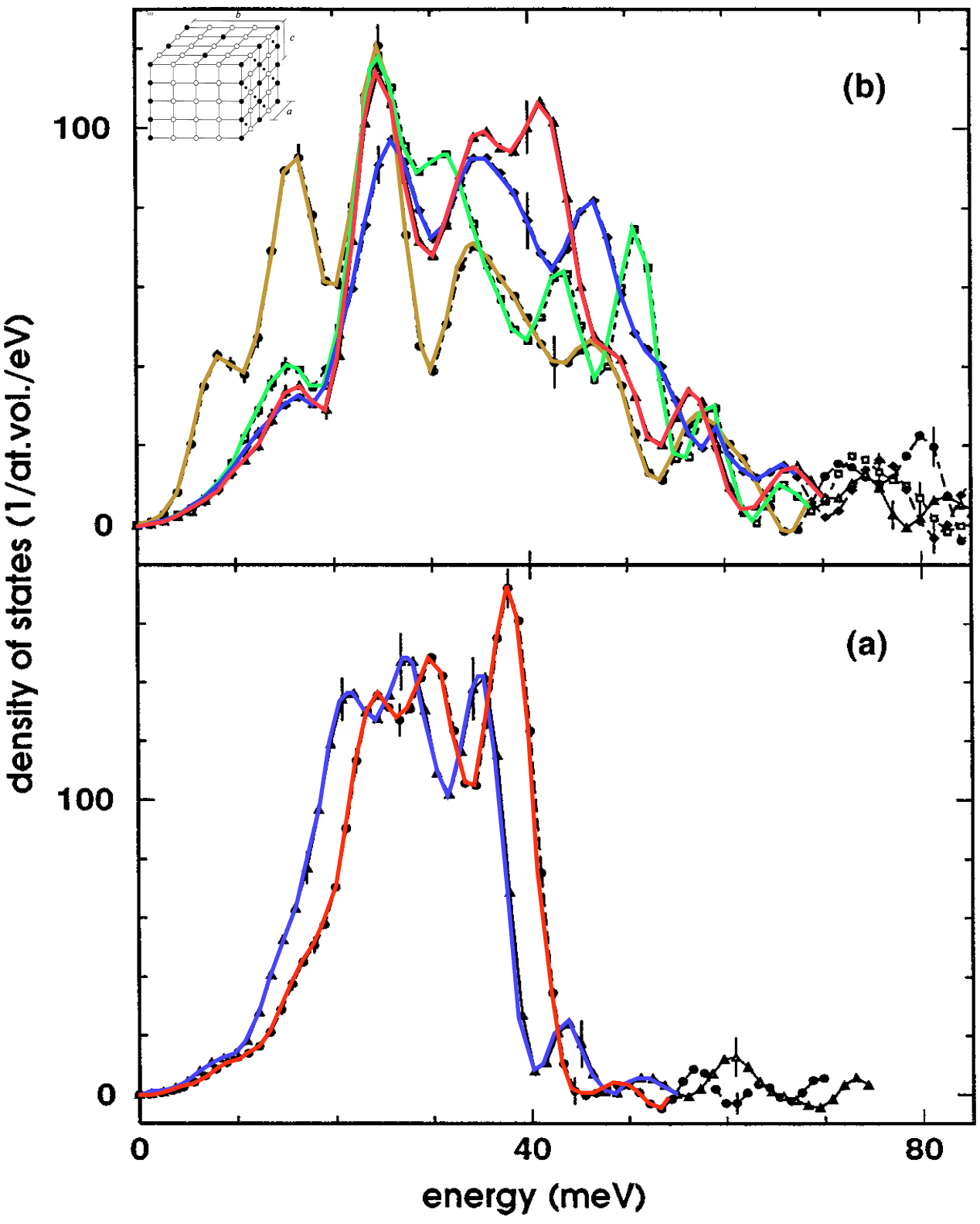
W. Sturhahn, T.S. Toellner, and E.E. Alp  
Advanced Photon Source, Argonne National Laboratory, Argonne, Illinois 60439

X. Zhang and M. Ando  
Photon Factory, National Laboratory for High Energy Physics, Ohno 1-1, Tsukuba, Ibaraki 305, Japan

Y. Yoda and S. Kikuta  
Department of Applied Physics, Faculty of Engineering, The University of Tokyo, Hongo 7-3-1, Bunkyo-ku, Tokyo 113, Japan

M. Seto  
Research Reactor Institute, Kyoto University, Sennan-gun, Osaka 590-04, Japan

C.W. Kimball and B. Dabrowski  
Northern Illinois University, De Kalb, Illinois 60115, USA



- $Sr_2Fe_2O_5$  Brownmillerite
- $Sr_2Fe_2O_{5.5}$  Orthorhombic perovskite
- $Sr_2Fe_2O_{5.75}$  Tetragonal perovskite
- $Sr_2Fe_2O_6$  Cubic perovskite
- bcc-iron
- stainless steel, 304

## Phonons in Nanocrystalline $^{57}\text{Fe}$

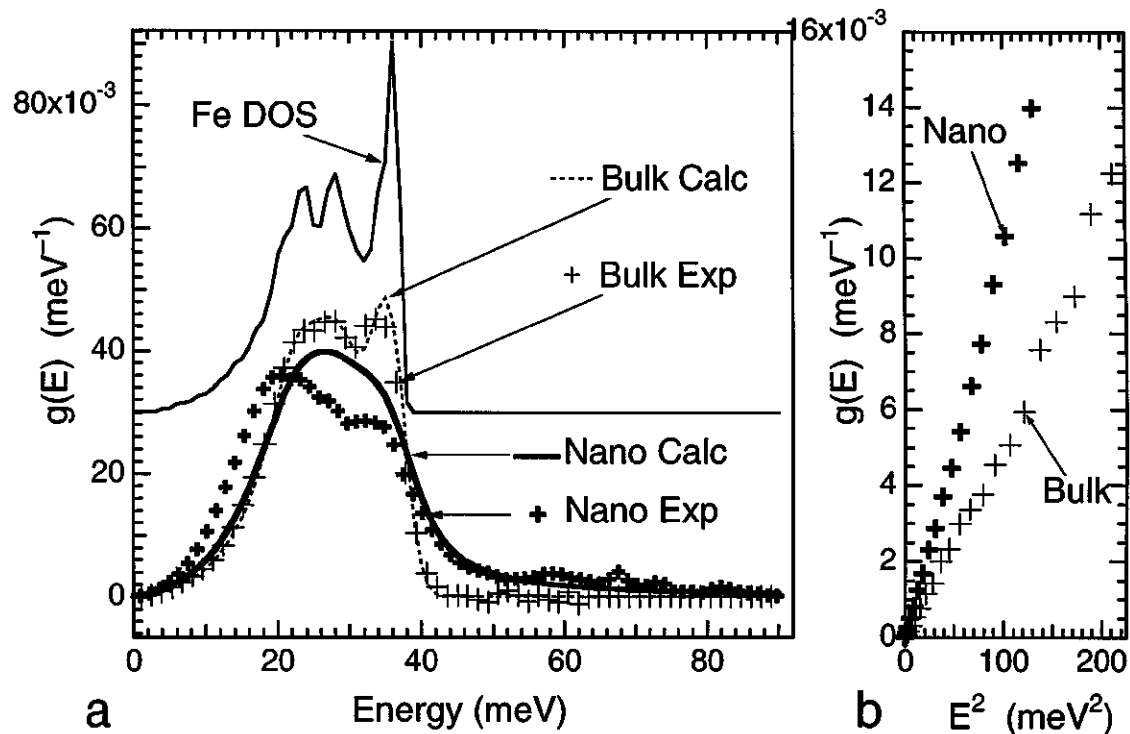
B. Fultz,<sup>1</sup> C.C. Ahn,<sup>1</sup> E.E. Alp,<sup>2</sup> W. Sturhahn,<sup>2</sup> and T.S. Toellner<sup>2</sup>

<sup>1</sup>*Division of Engineering and Applied Science, 138-78, California Institute of Technology, Pasadena, California 91125*

<sup>2</sup>*Advanced Photon Source, Argonne National Laboratory, Argonne, Illinois 60439*

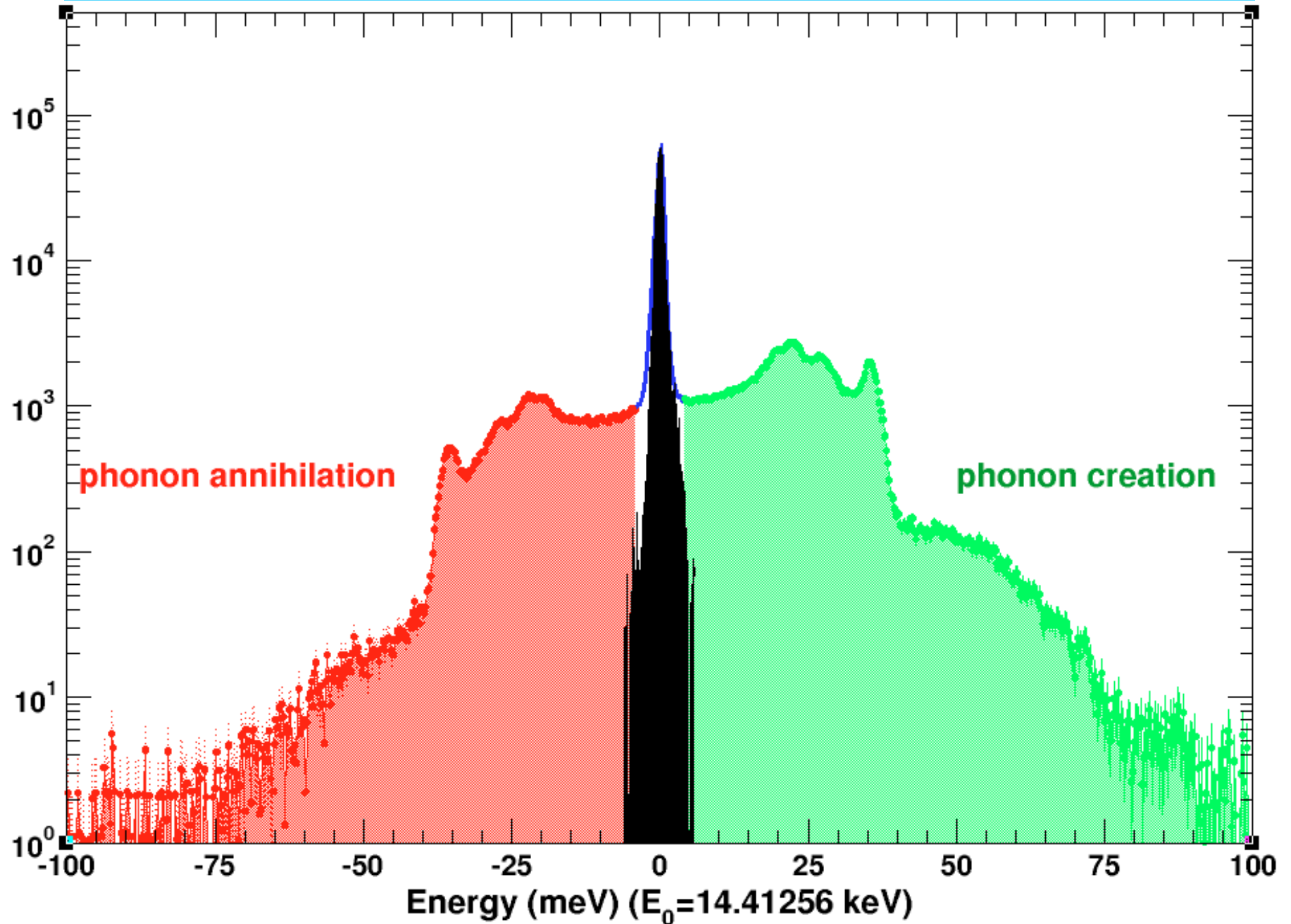
(Received 13 March 1997)

We measured the phonon density of states (DOS) of nanocrystalline Fe by resonant inelastic nuclear  $\gamma$ -ray scattering. The nanophase material shows large distortions in its phonon DOS. We attribute the high energy distortion to lifetime broadening. A damped harmonic oscillator model for the phonons provides a low quality factor,  $Q_u$ , averaging about 5, but the longitudinal modes may have been broadened most. The nanocrystalline Fe also shows an enhancement in its phonon DOS at energies below 15 meV. The difference in vibrational entropy of the bulk and nanocrystalline Fe was small, owing to competing changes in the nanocrystalline phonon DOS at low and high energies.

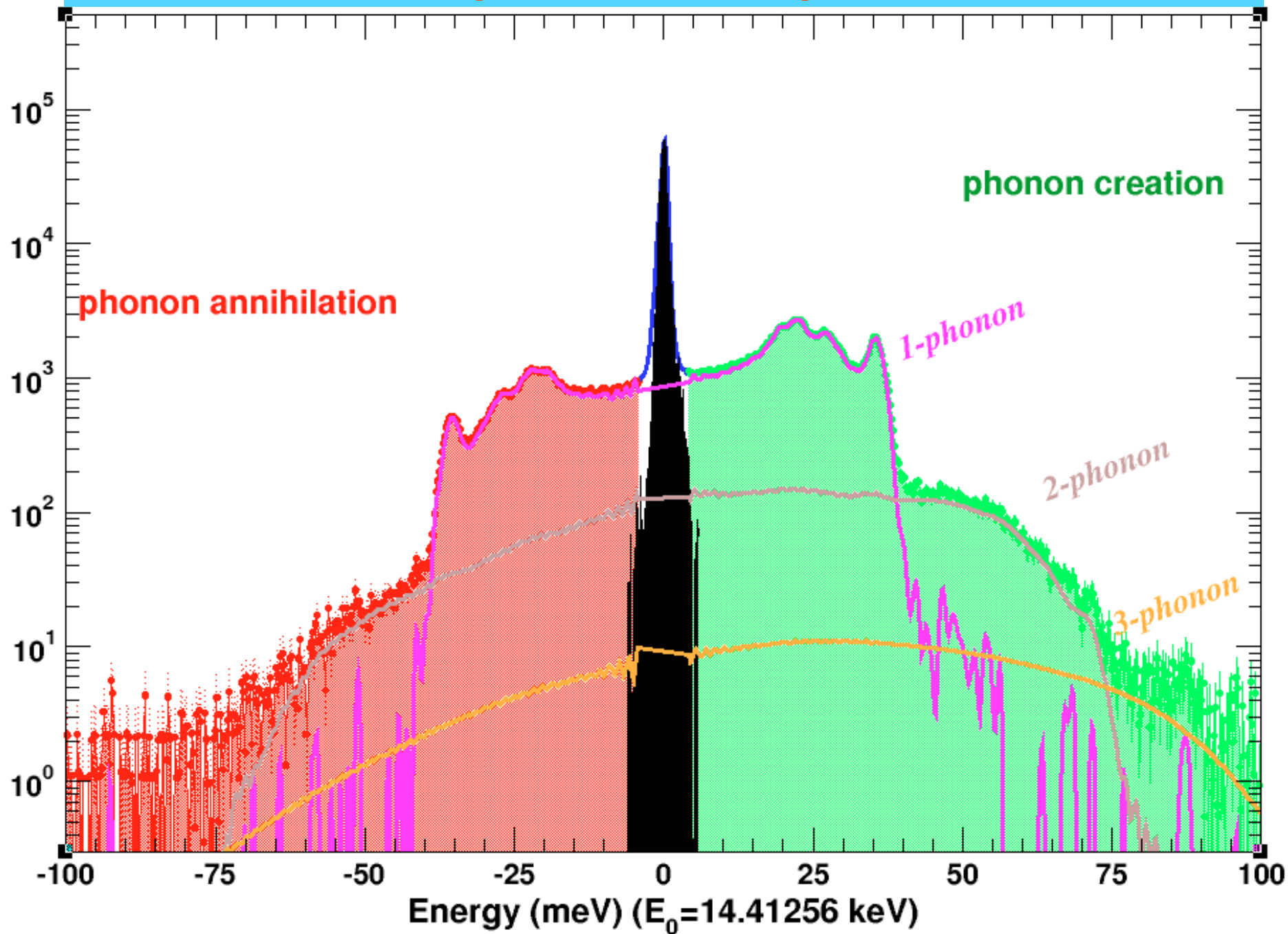


First PRL from APS

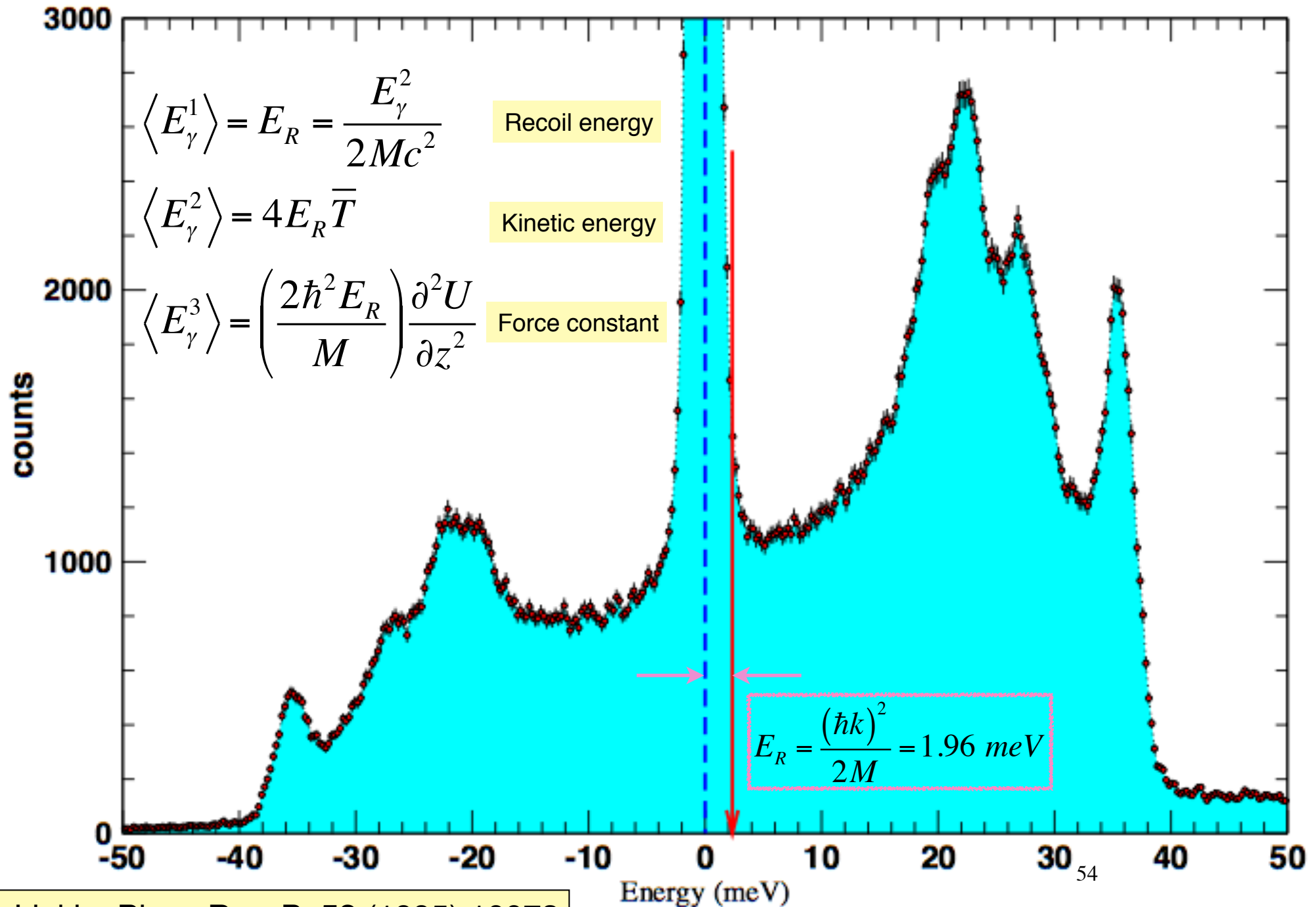
# Phonon excitation probability



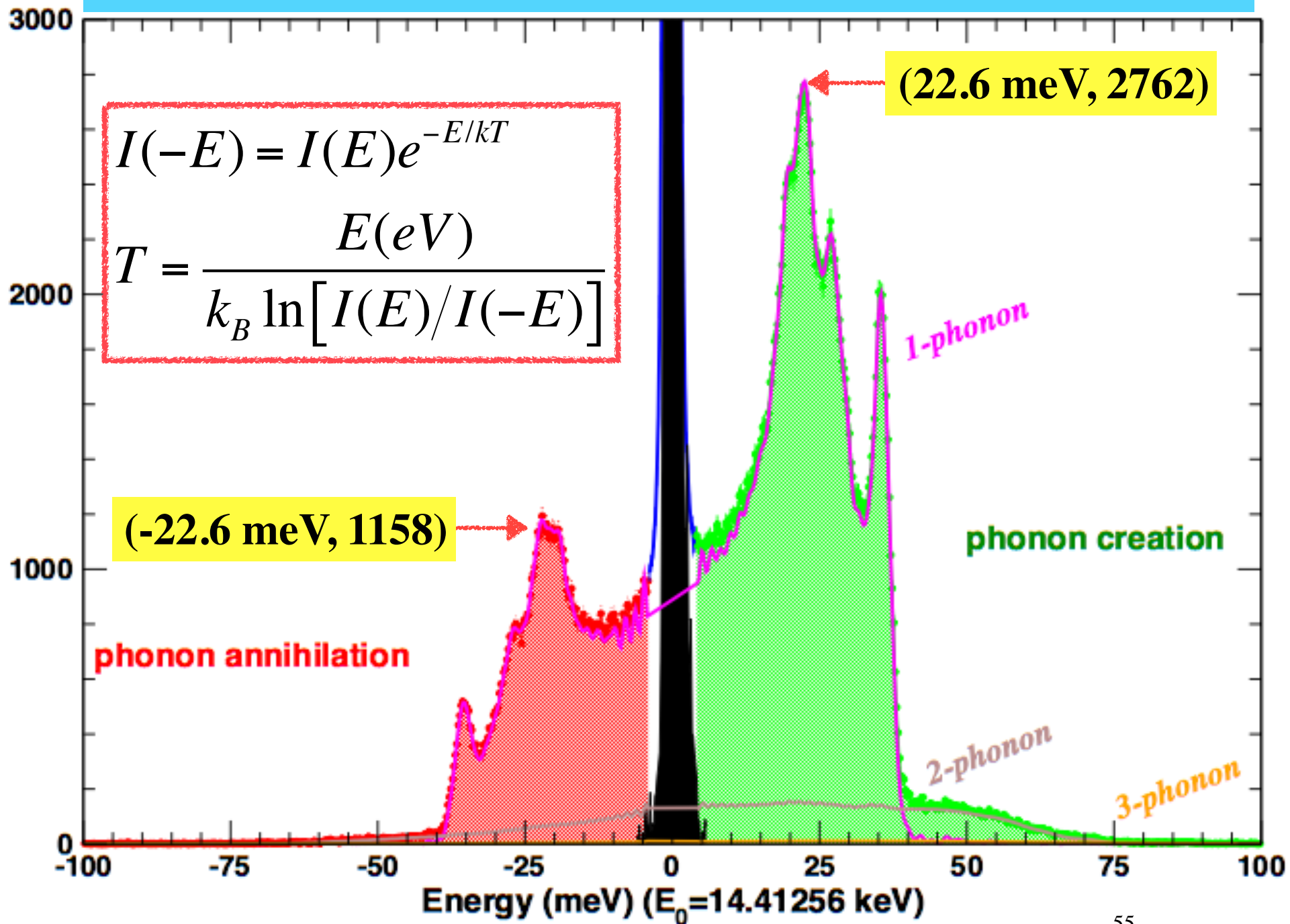
# Multi-phonon decomposition



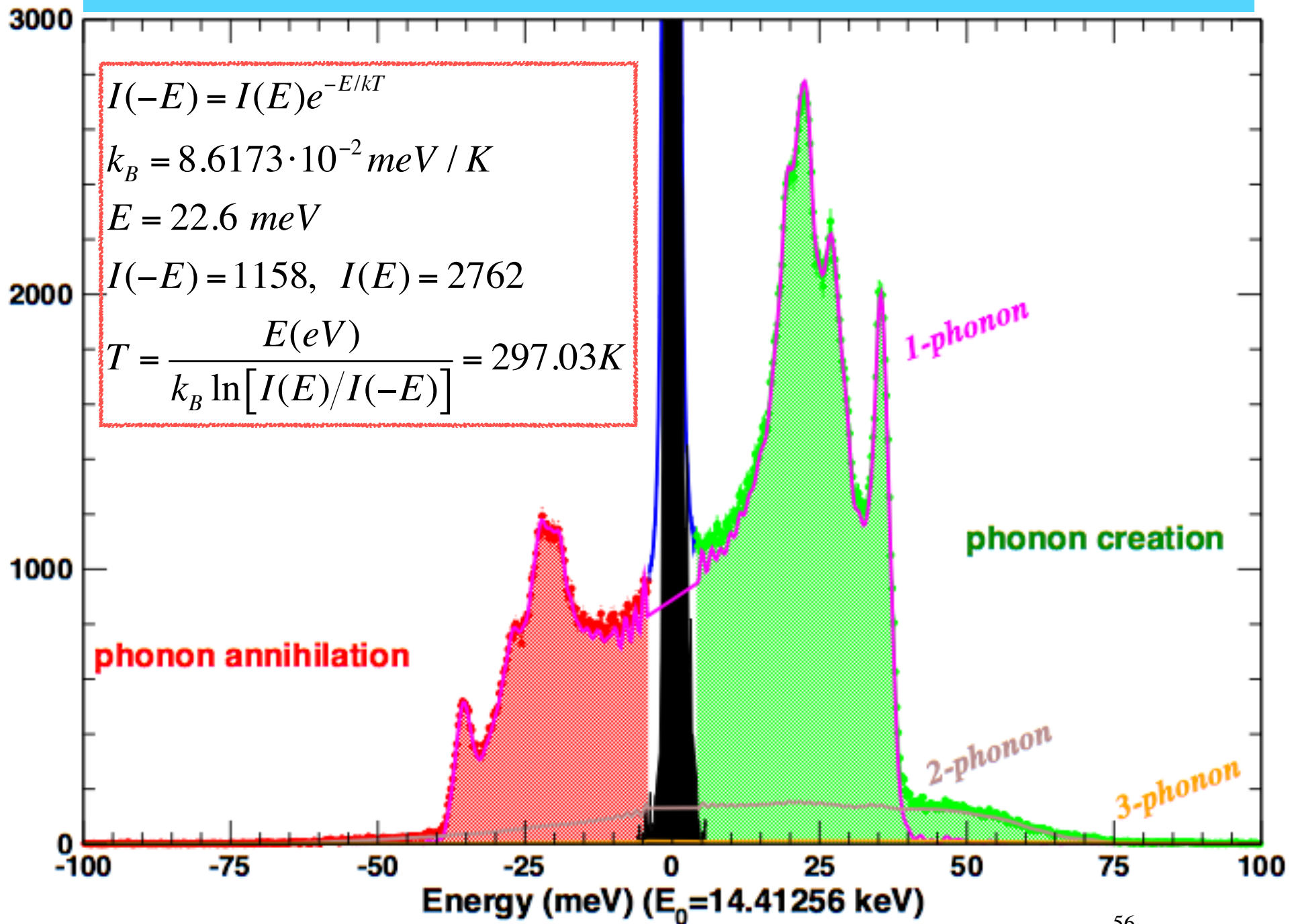
# Lipkin's sum rules related to phonon excitation probability



# Detailed Balance

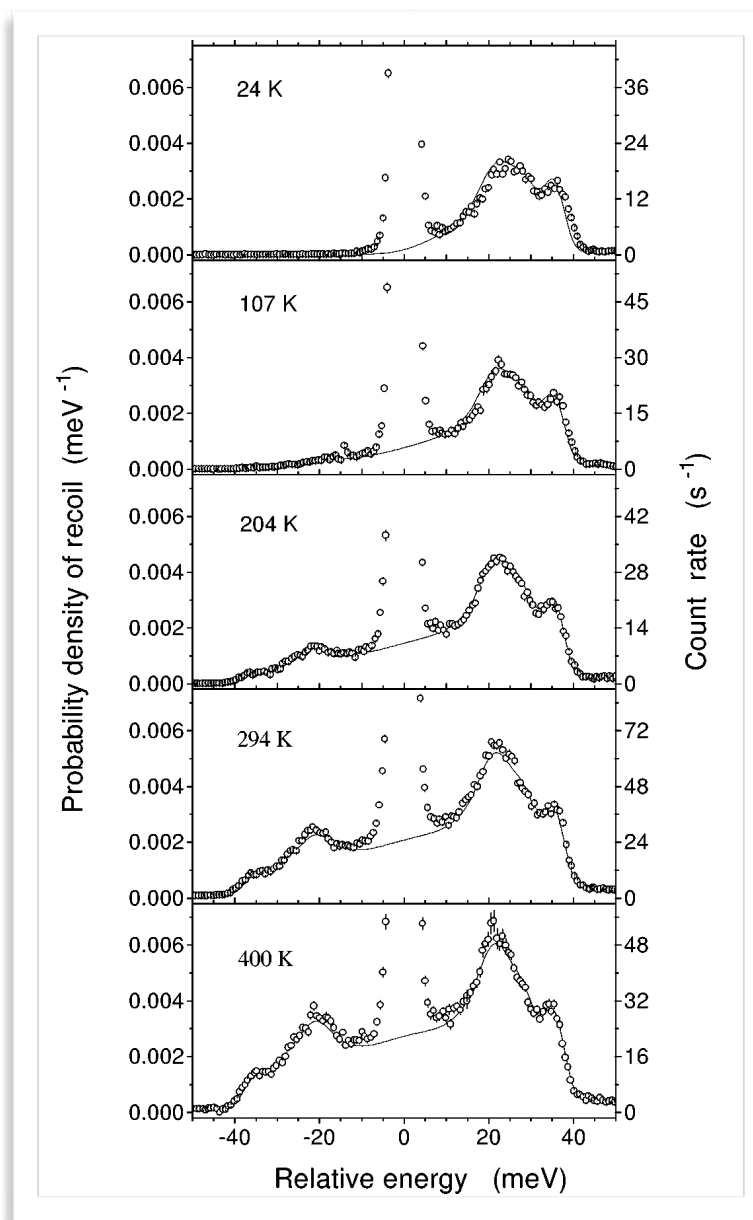
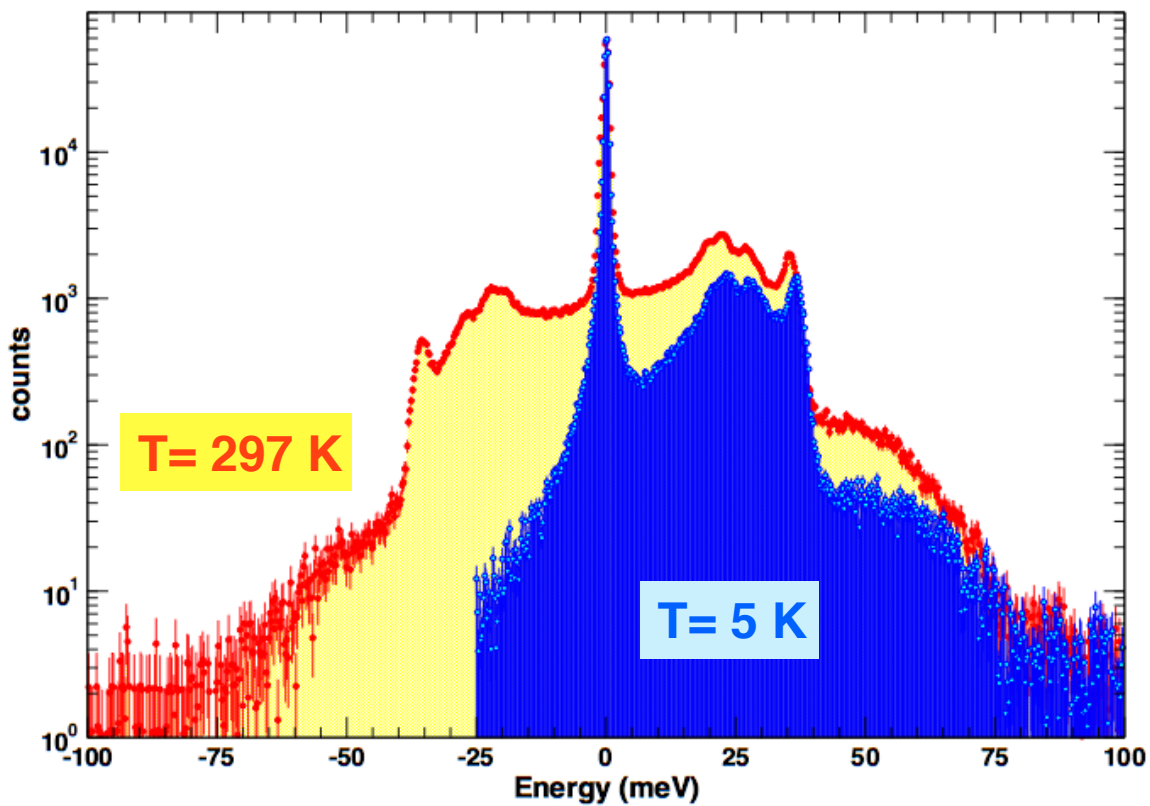


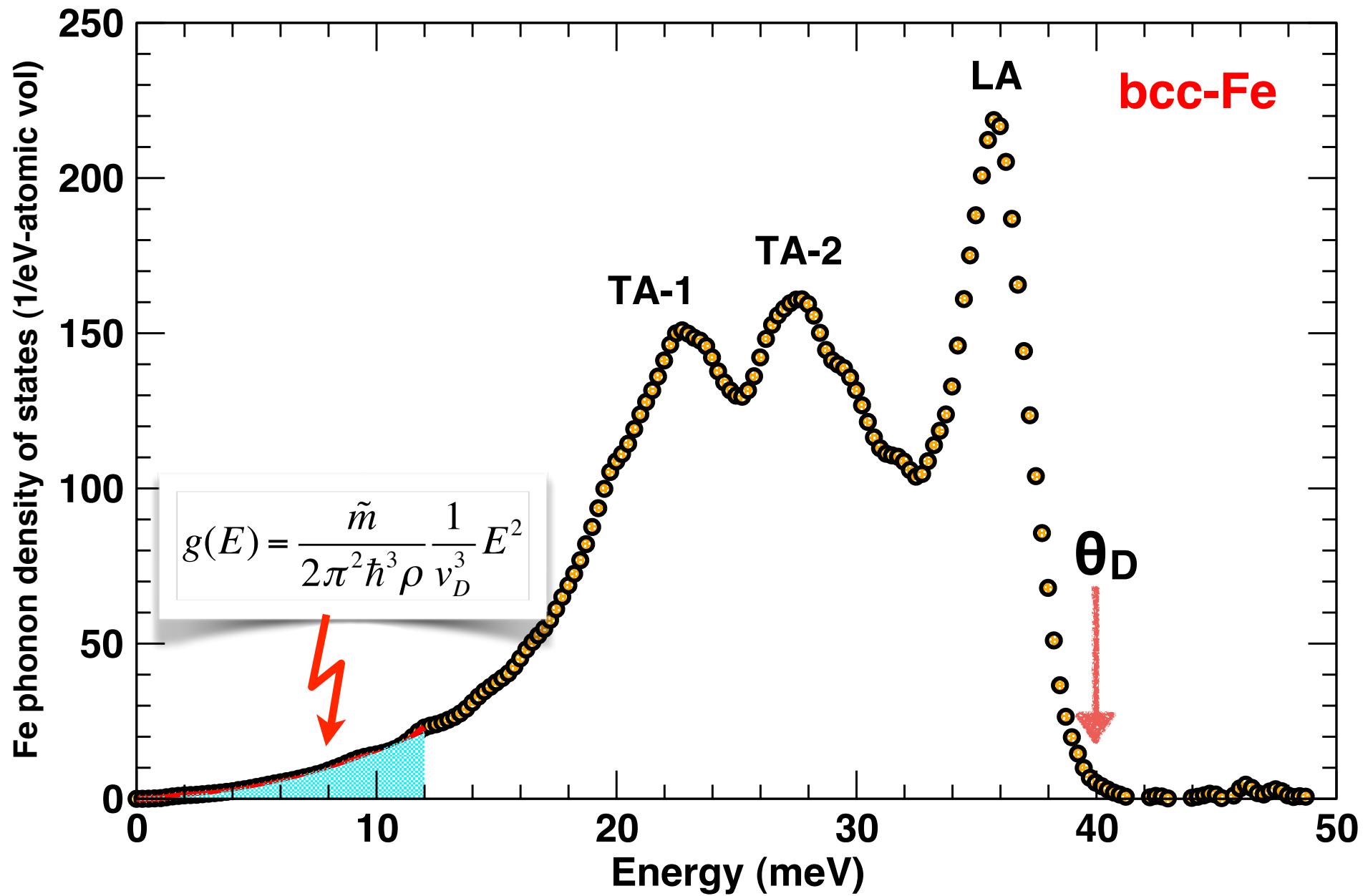
# Detailed Balance



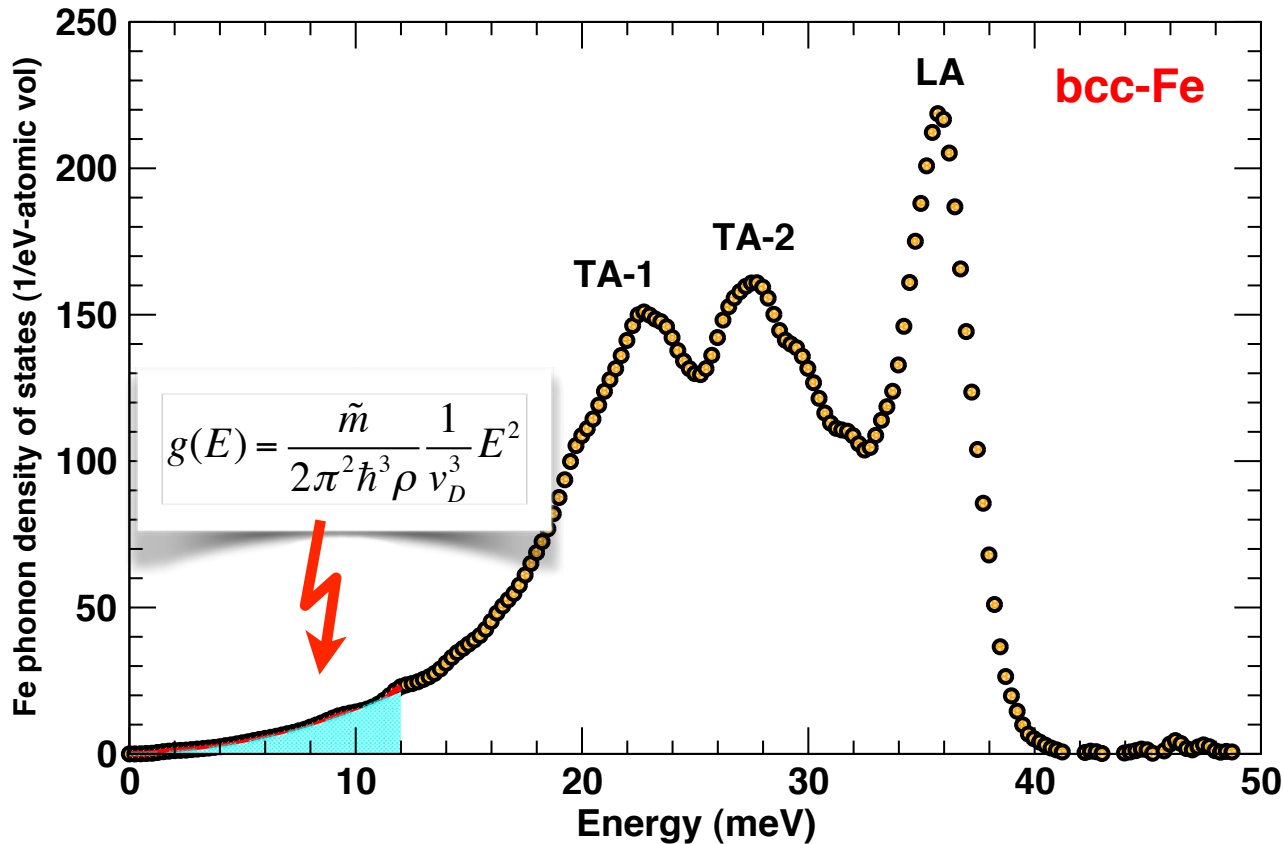


# Temperature dependence of phonon excitation probability





Measurement of  $v_D$ , Debye sound velocity allows to resolve longitudinal and shear sound velocity, provided that bulk modulus and density, is independently and simultaneously measured by x-ray diffraction.



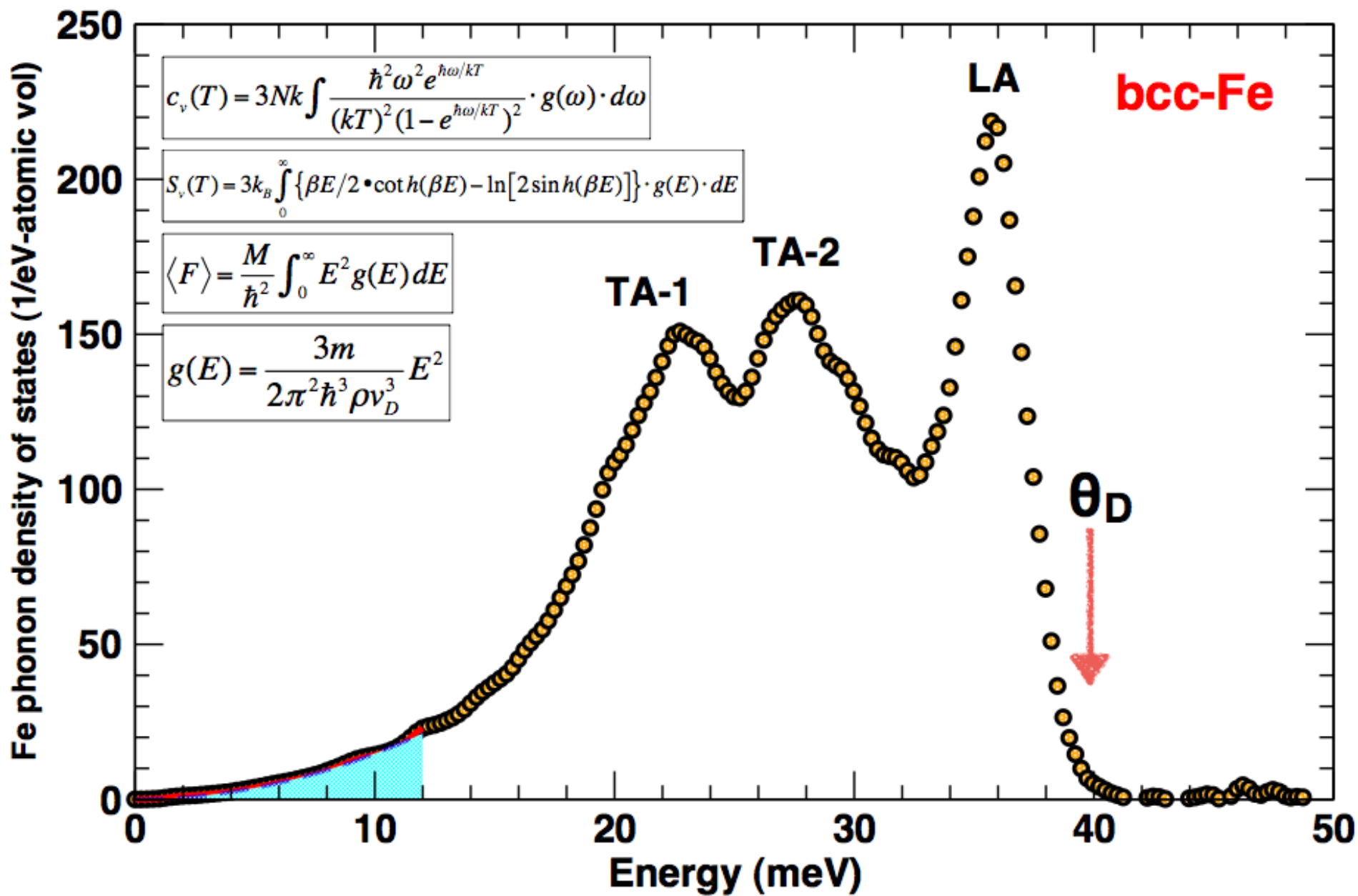
$$\frac{K_S}{\rho} = V_P^2 - \frac{4}{3}V_S^2$$

$$\frac{G}{\rho} = V_S^2$$

$$\frac{3}{V_D^3} = \frac{1}{V_P^3} + \frac{2}{V_S^3}$$

- $K_S$  : adiabatic bulk modulus
- $G$  : shear modulus
- $V_P$  : compression wave velocity
- $V_S$  : shear wave velocity
- $V_D$  : Debye sound velocity
- $\rho$  : density

$K$ (GPa)	$\rho$ (g/cc)	$V_D$ (m/s)	$V_P$ (m/s)	$V_S$ (m/s)	$G$ (GPa)
$165 \pm 1$	$8.01$	$3510 \pm 12$	$5813 \pm 13$	$3146 \pm 11$	$79.3 \pm 0.6$



# Phonon density of states

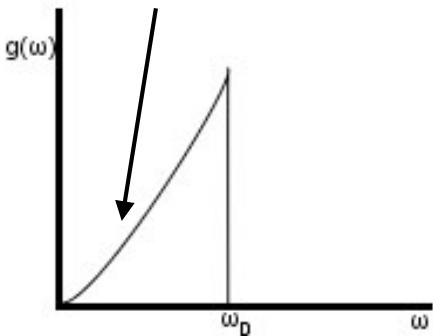
$$g(k) dk = \frac{V}{(2\pi)^3} 4\pi k^2 dk.$$

Number of wave vectors in a spherical shell of radius  $k$  per unit volume of reciprocal space.

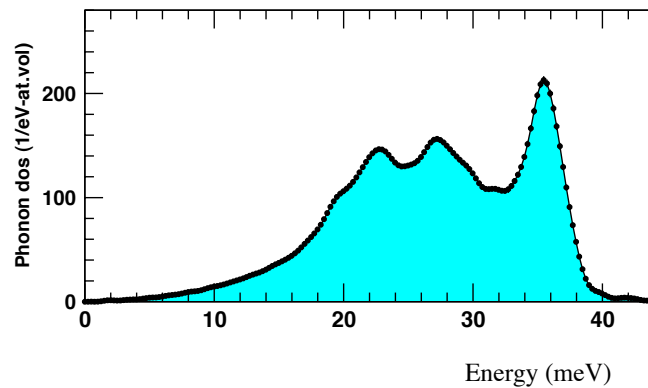
$$g(\omega) = \frac{3V}{2\pi^2 c^3} \omega^2$$

Phonon density of states has a quadratic dependence on frequency, and inversely proportional to the cube of sound velocity.

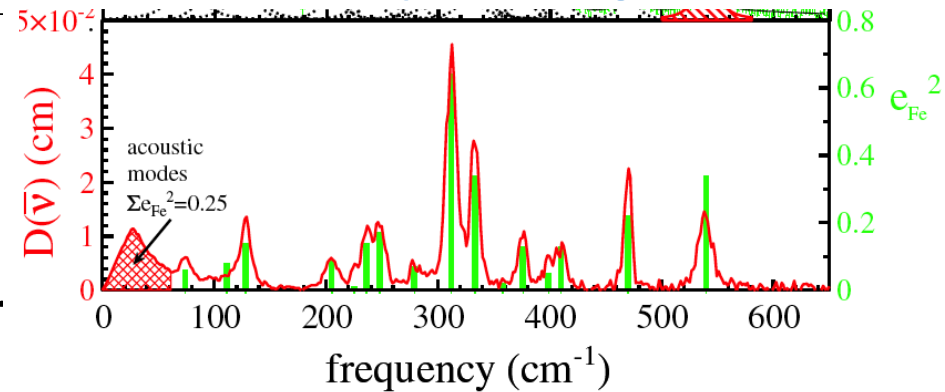
## Debye model



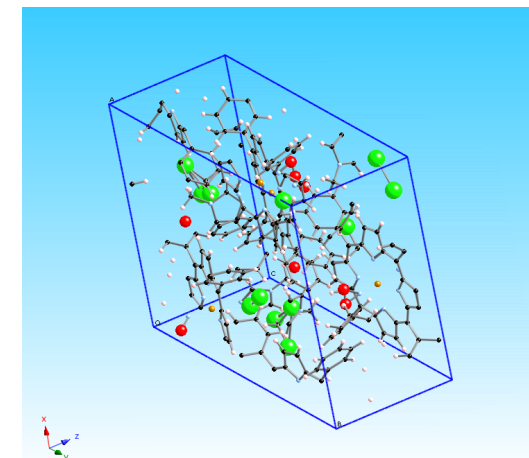
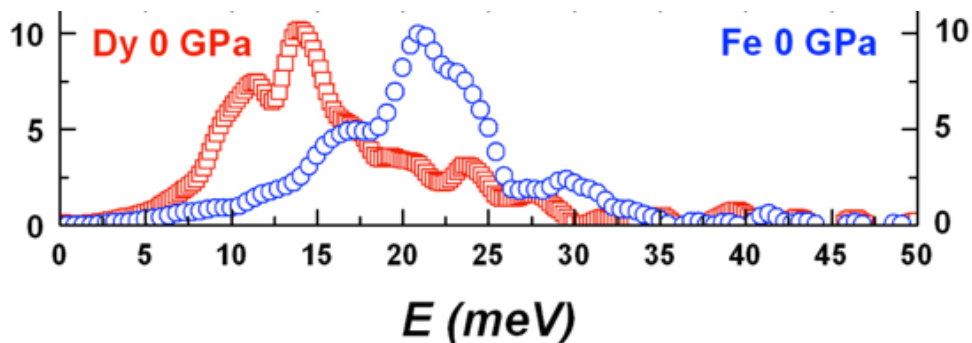
## pure iron

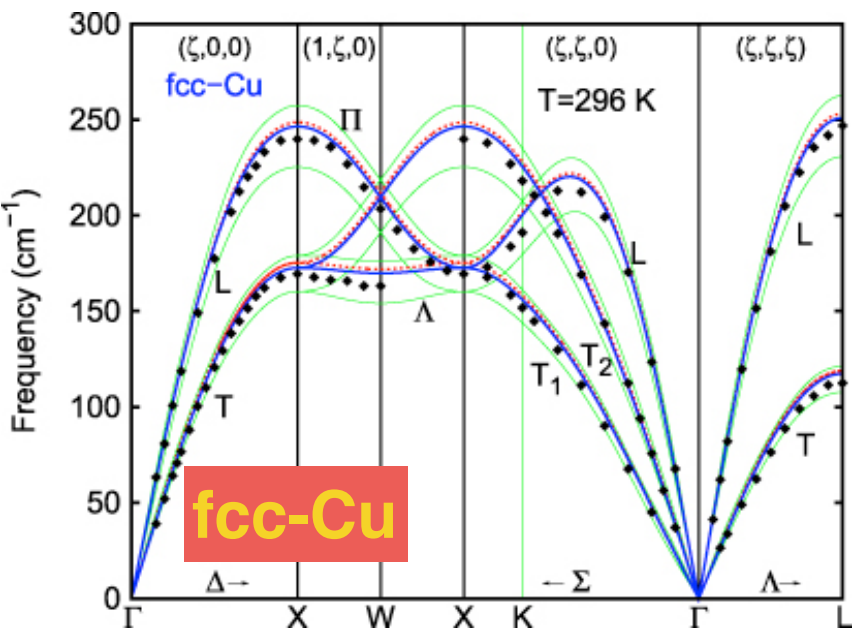
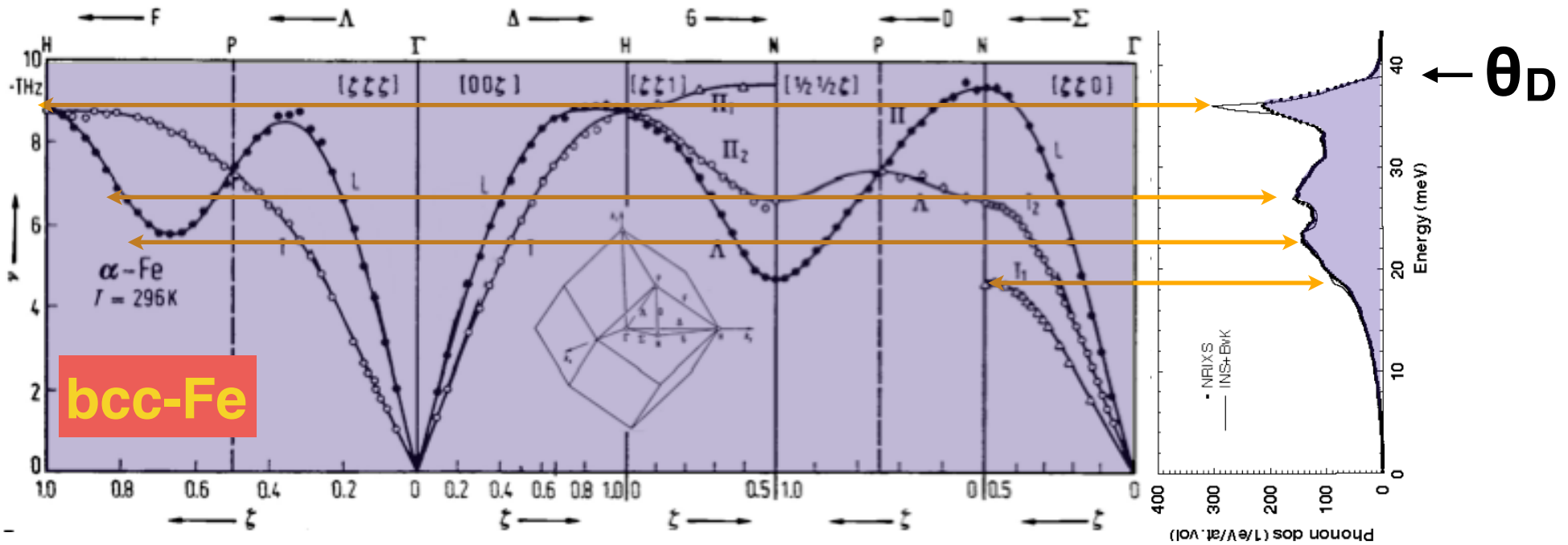


## Fe-TPP-NO



## DyFe<sub>3</sub>

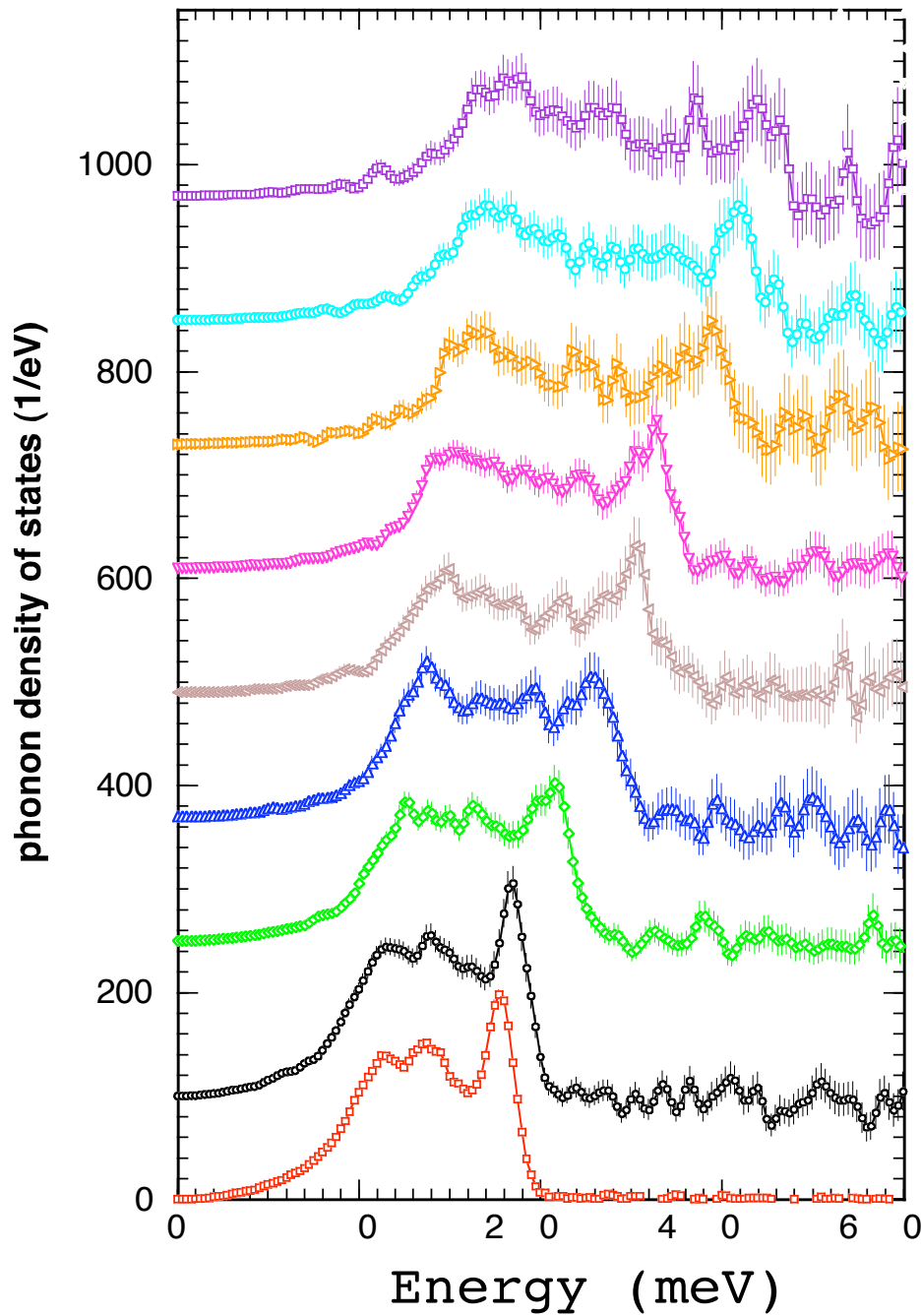




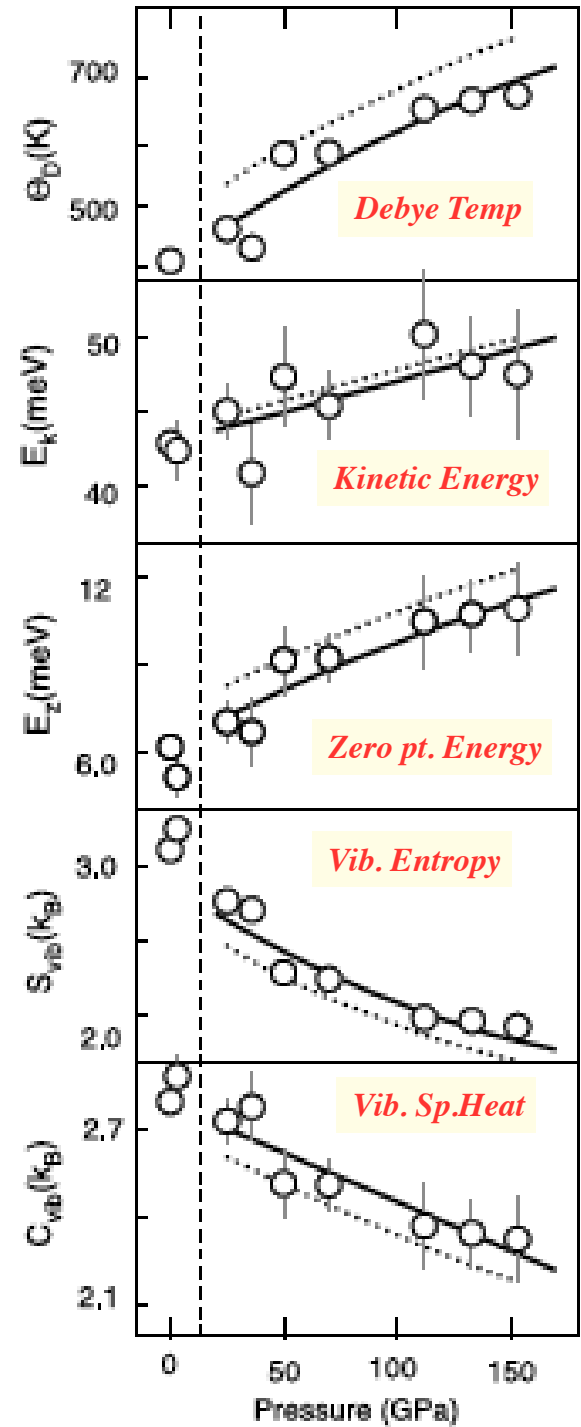
Let's assume that the acoustic modes have a linear relationship between frequency and wave vector:  
 $\omega = ck$  , where  $\mathbf{c}$  is average sound velocity

**Maximum frequency cut off is at Debye energy:**  
*e.g. for Cu, this frequency is  $240 \text{ cm}^{-1}$  ( $\sim 30 \text{ meV}$ ).*  
*Considering  $1 \text{ meV} = 11.605 \text{ K} = 8.065 \text{ cm}^{-1}$ , this corresponds to  $348 \text{ K}$ , which is close to  $344 \text{ K}$ .*  
*For Fe, the measured cut-off value is  $\sim 39.5 \text{ meV}$ , which corresponds to  $458 \text{ K}$ , very close to reported  $460 \text{ K}$ .*

# Phonon density of states of iron under high pressure



153 GPa

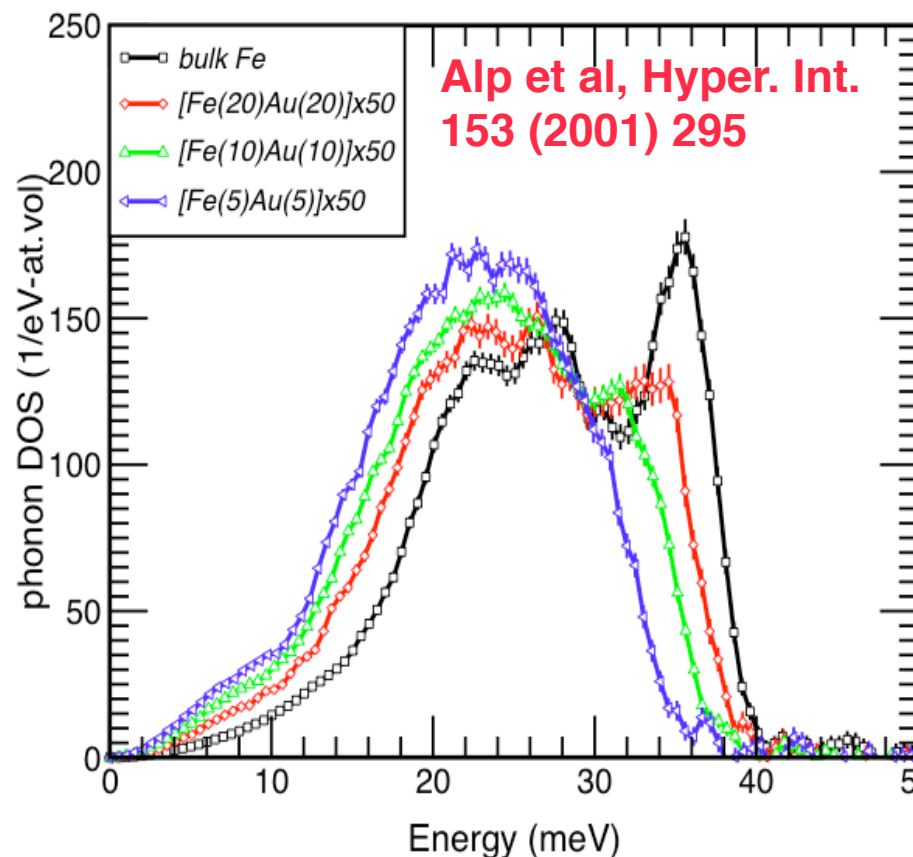
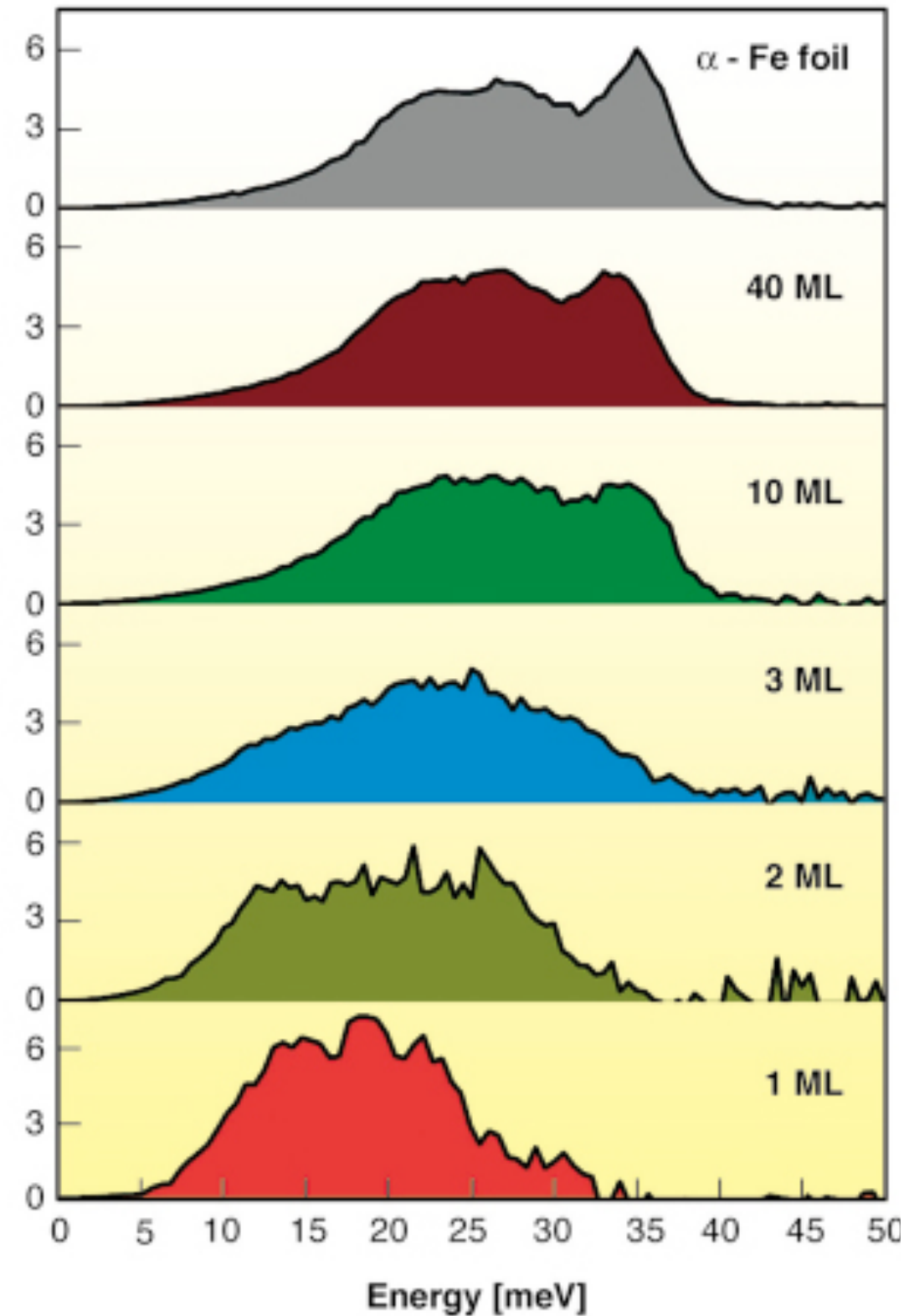


## Fe films deposited on W(110)

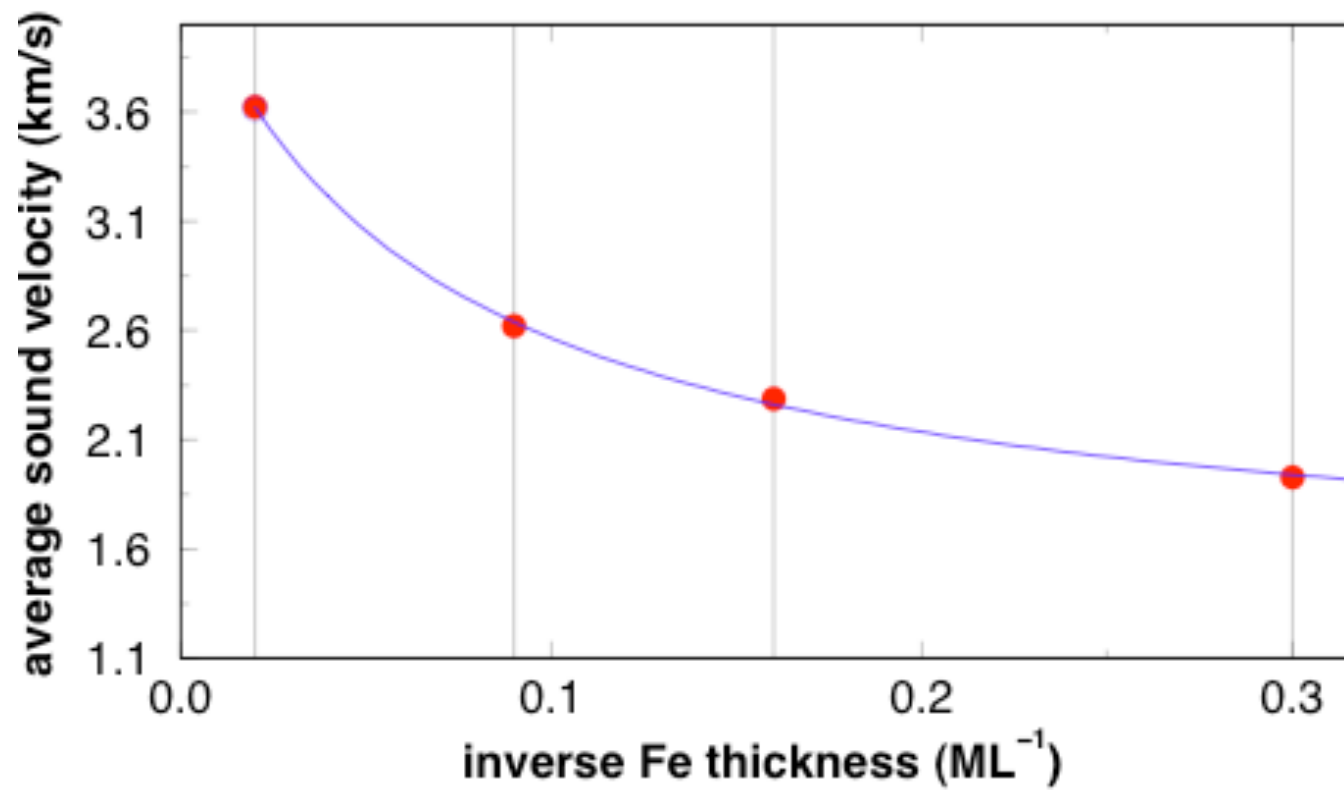
### Transition from the bulk to a single iron monolayer

S. Stankov, R. Röhlberger, T. Slezak, M. Sladeczek, B. Sepiol, G. Vogl, A. I. Chumakov, R. Ruffer, N. Spiridis, J. Lazewski, K. Parlinski, and J. Korecki,

ESRF Highlights 2006

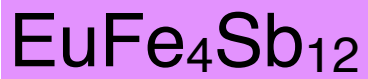
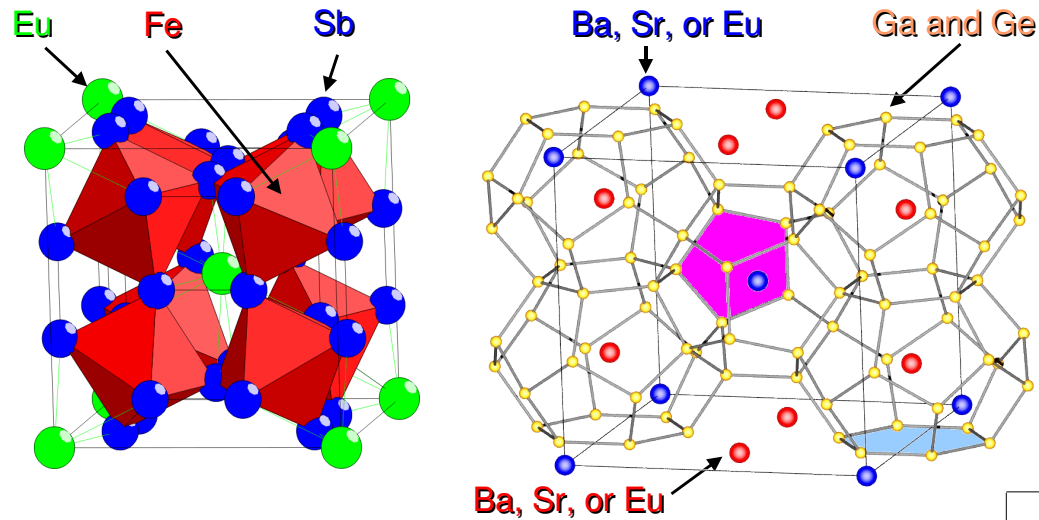






# 1. Thermoelectric materials: always something new !..

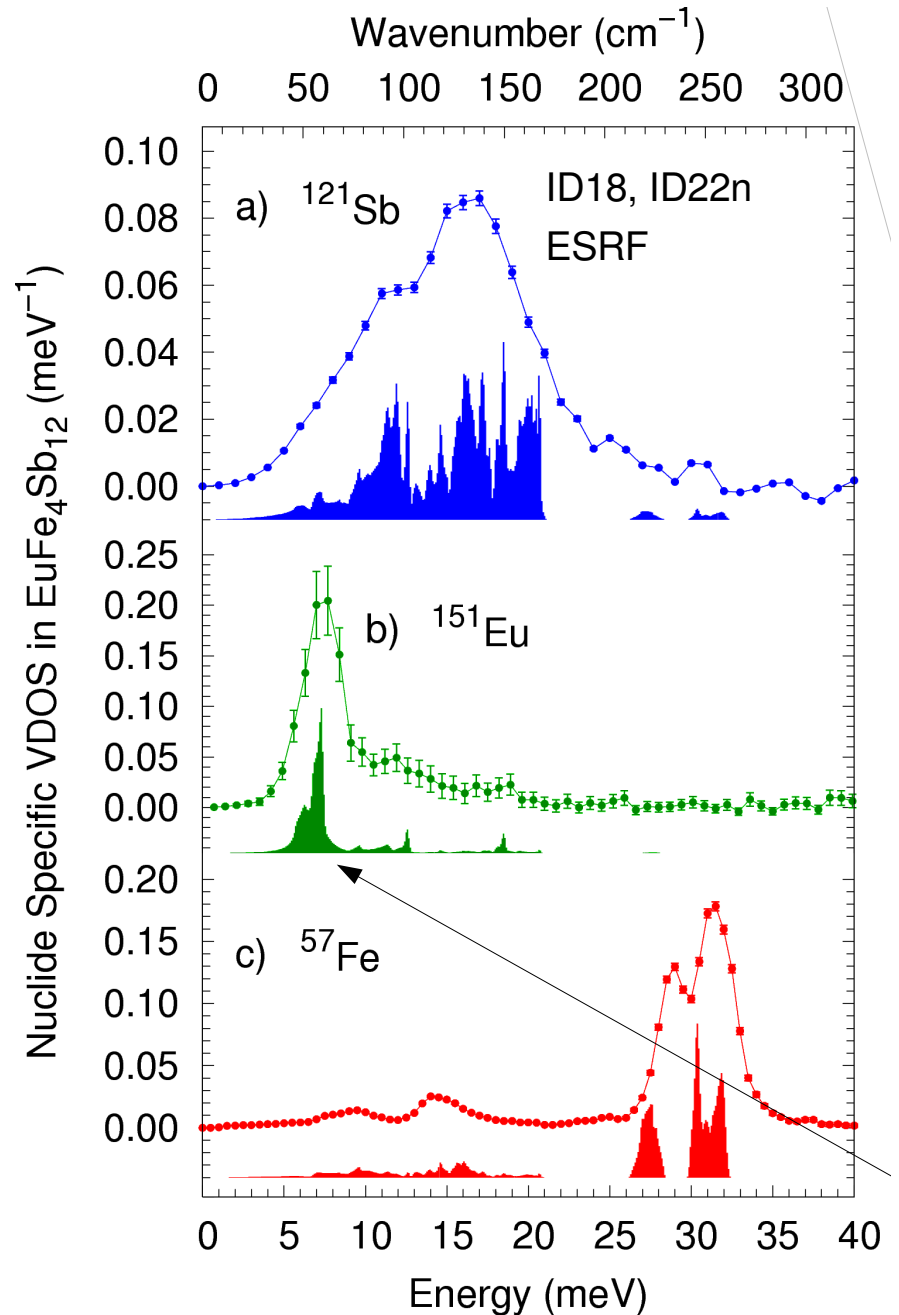
## Skutterudites



The loosely bound guests affect the characteristics of the vibrations, and change the thermal conductivity

Many elements in modern thermoelectric materials include **Fe**, rare-earth atoms like **Eu, Sm, Dy**, as well as **Sb**, and **Te**. These are all proper Mössbauer resonances we can exploit, and we do..

Courtesy: Raphael Hermann, Jülich



## Vibrational dynamics of the host framework in Sn clathrates

Bogdan M. Leu,<sup>1,\*</sup> Mihai Sturza,<sup>2</sup> Michael Y. Hu,<sup>1</sup> David Gosztola,<sup>3</sup> Volodymyr Baran,<sup>4</sup> Thomas F. Fässler,<sup>4</sup> and E. Ercan Alp<sup>1</sup>

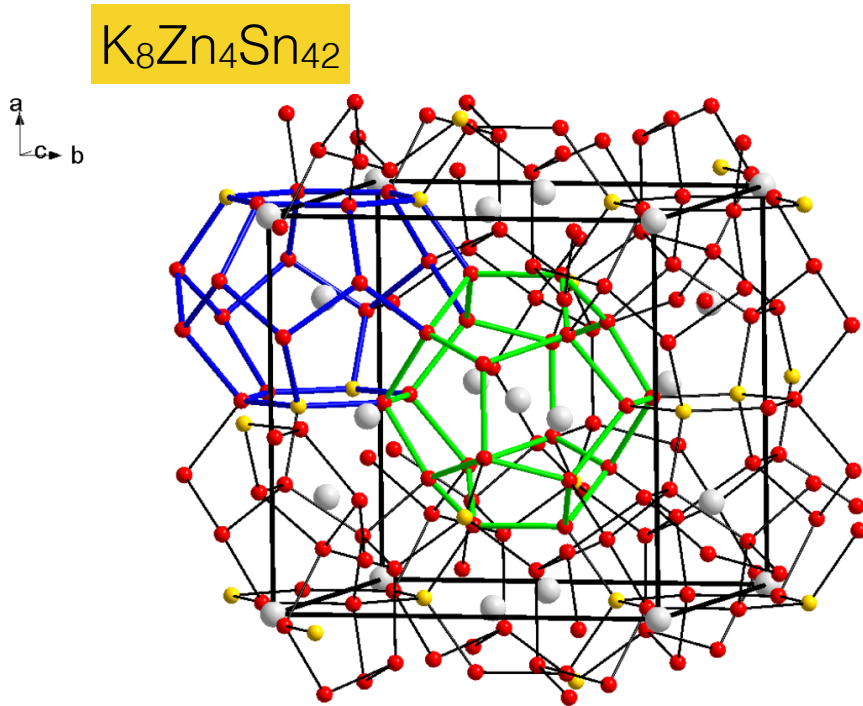


FIG. 1. (Color online) Structure of type-I clathrate  $K_8Zn_4Sn_{42}$ . Color scheme: gray = K, yellow = Zn/Sn, red = Sn. One small (pentagonal dodecahedron) and large (tetrakaidecahedron) host framework cage are highlighted in green and blue, respectively.

type-I clathrate: pentagonal dodecahedra and tetrakaidecahedra alternating in a 1:3 ratio

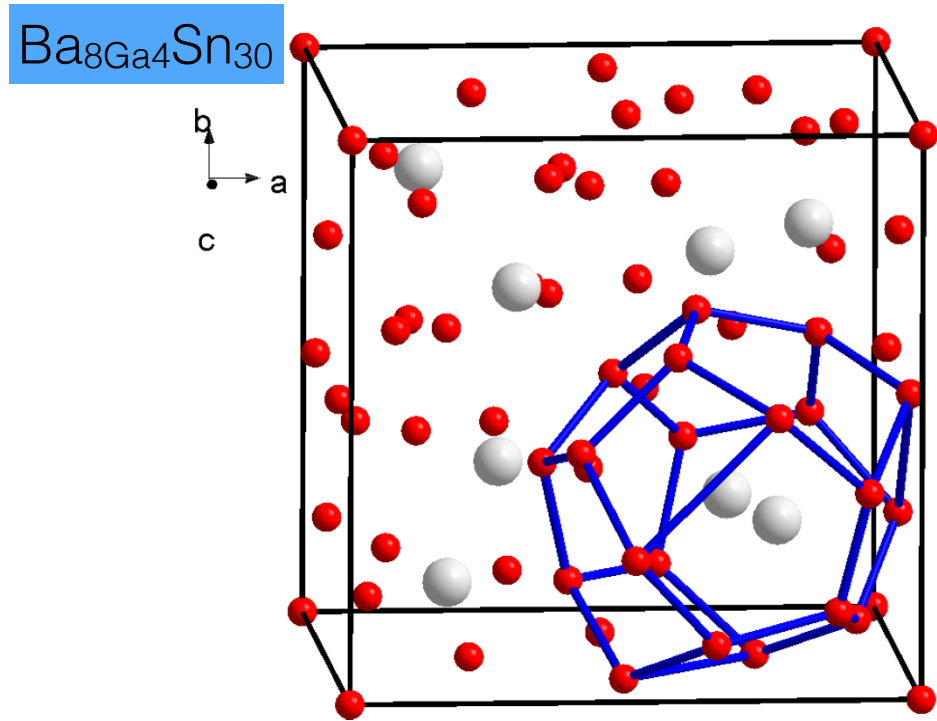
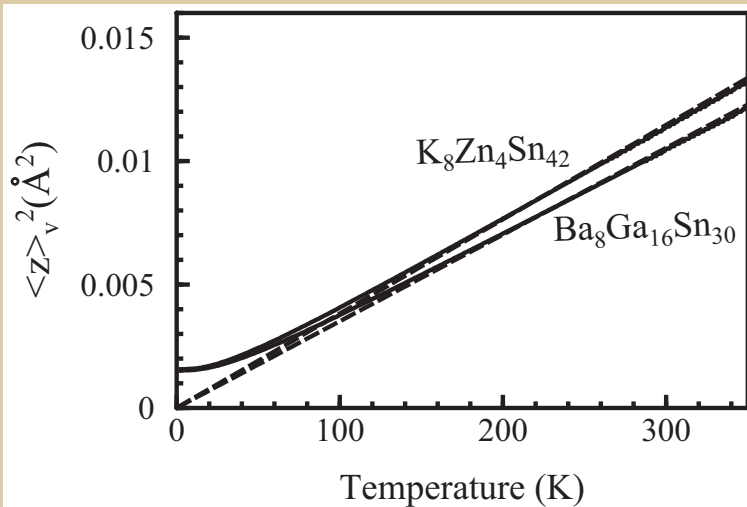
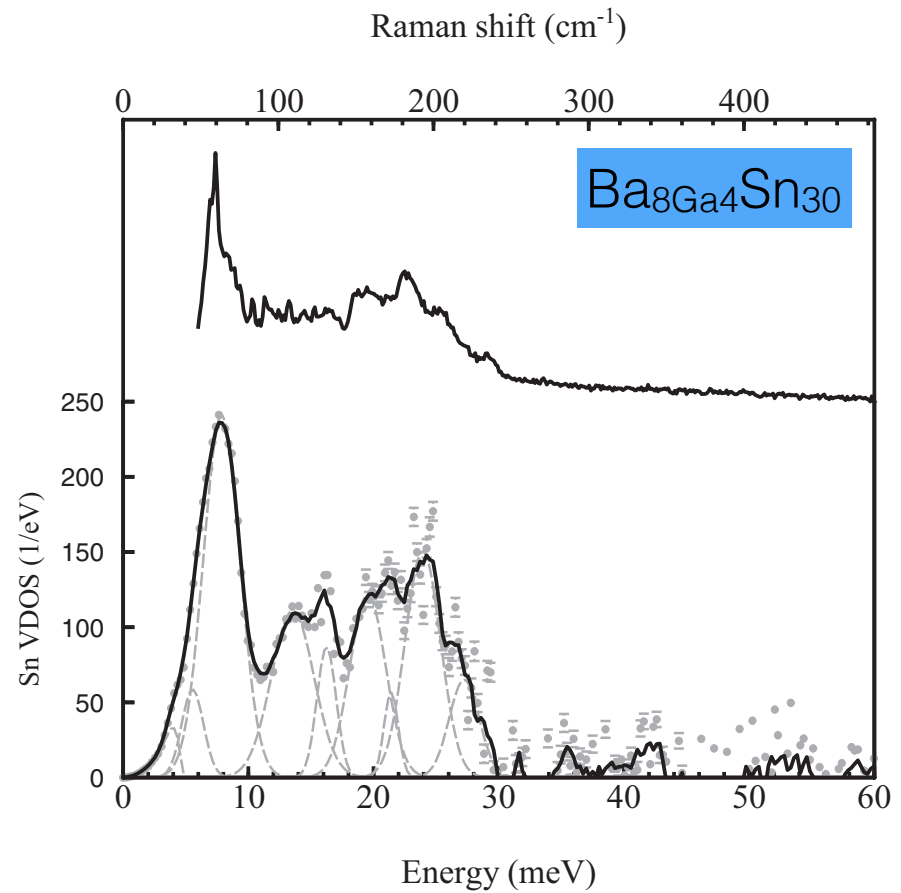
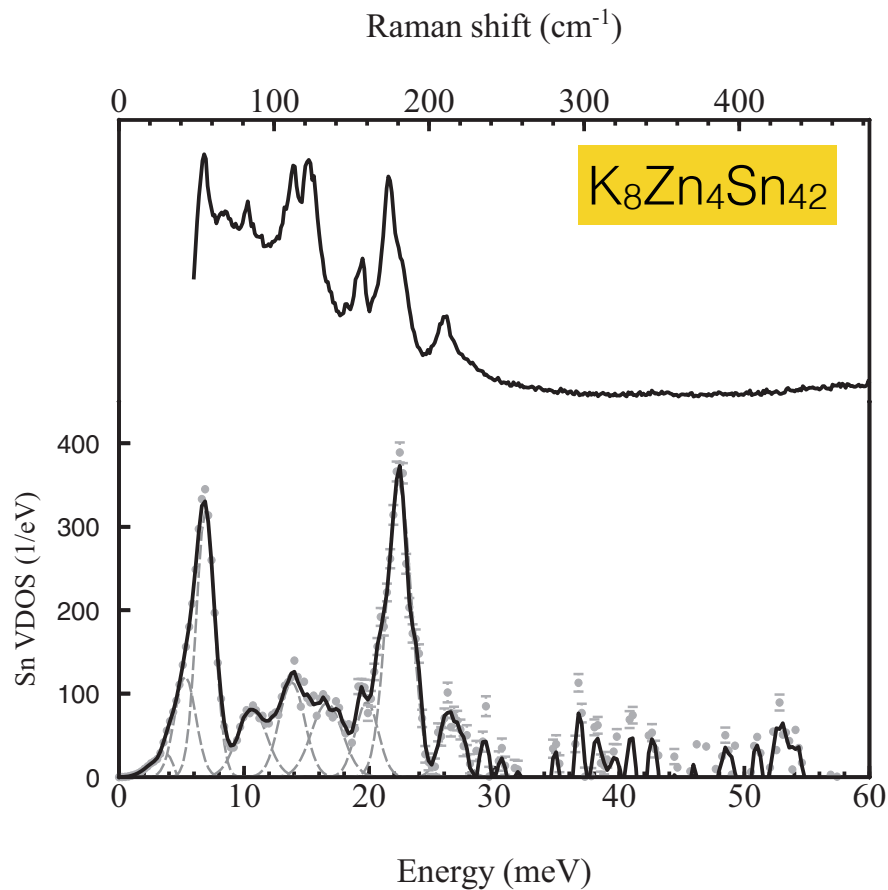


FIG. 2. (Color online) Structure of type-VIII clathrate  $Ba_8Ga_4Sn_{30}$ . Color scheme: gray = Ba, red = Sn/Ga. One host framework cage (pentagonal dodecahedron) is highlighted in blue.

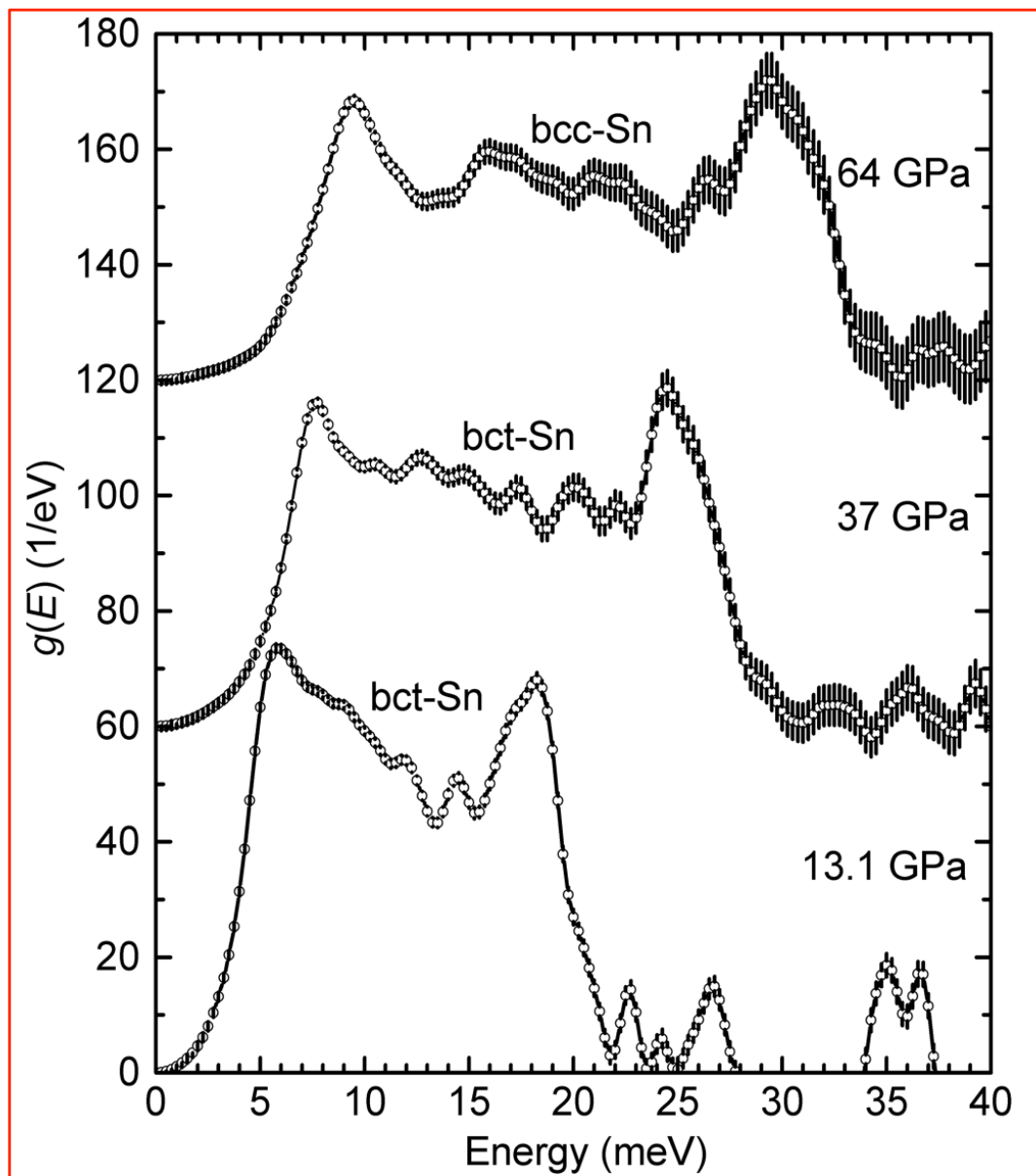
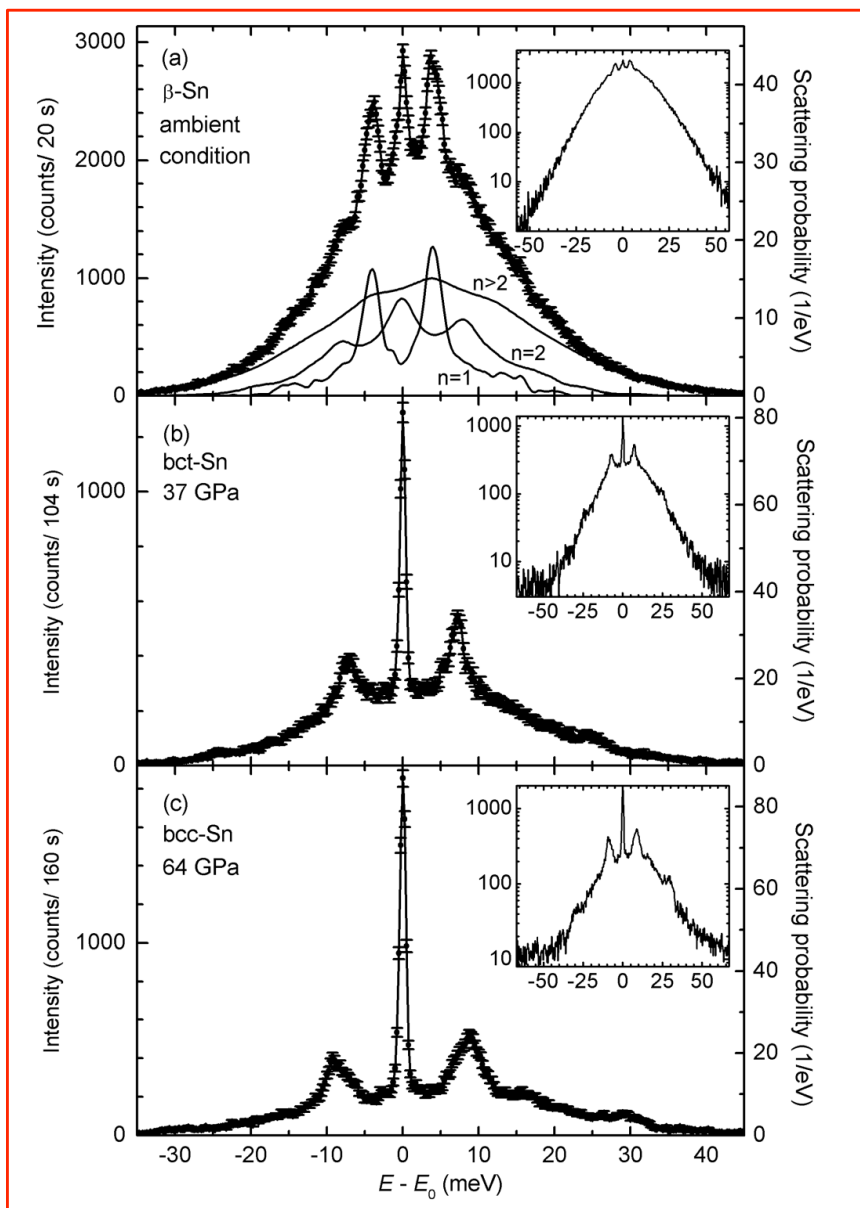
type VIII : pentagonal dodecahedra; however, BGS adopts the type-I clathrate structure at high-temperature



### mean square displacement via phonon dos

$$\langle z^2 \rangle_v = \frac{1}{3k^2} \int [2\bar{n}(\bar{\nu}) + 1] \frac{\bar{\nu}_R}{\bar{\nu}} D(\bar{\nu}) d\bar{\nu},$$

$3.8 \times 10^{-5} \text{\AA}^2/\text{K}$  for KZS and  $3.5 \times 10^{-5} \text{\AA}^2/\text{K}$  for BGS.



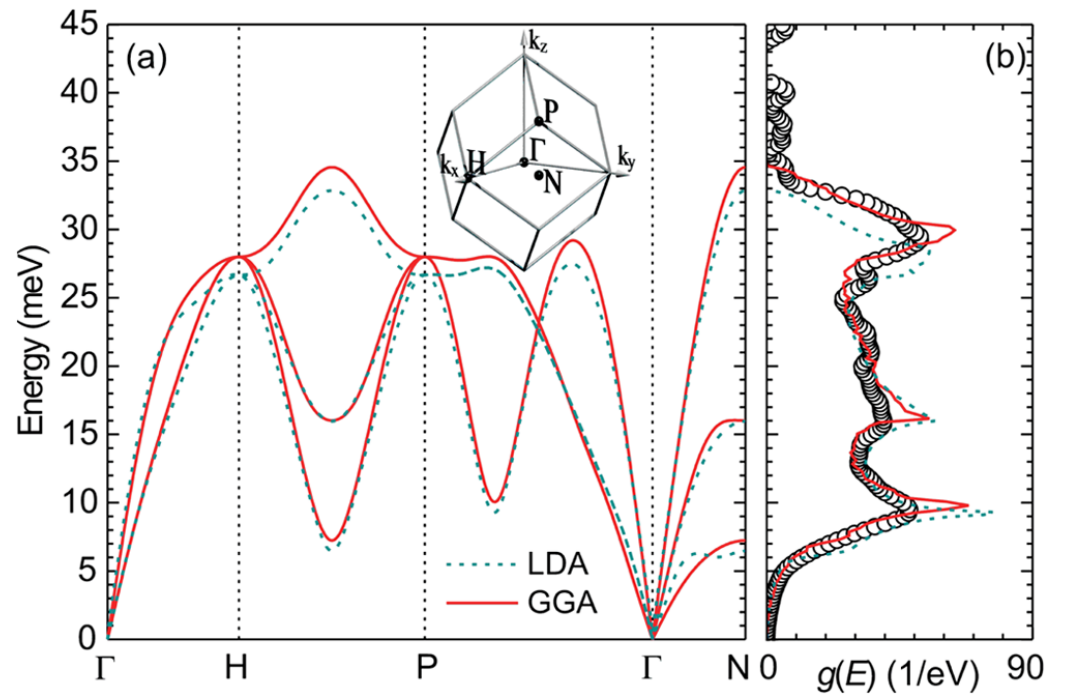
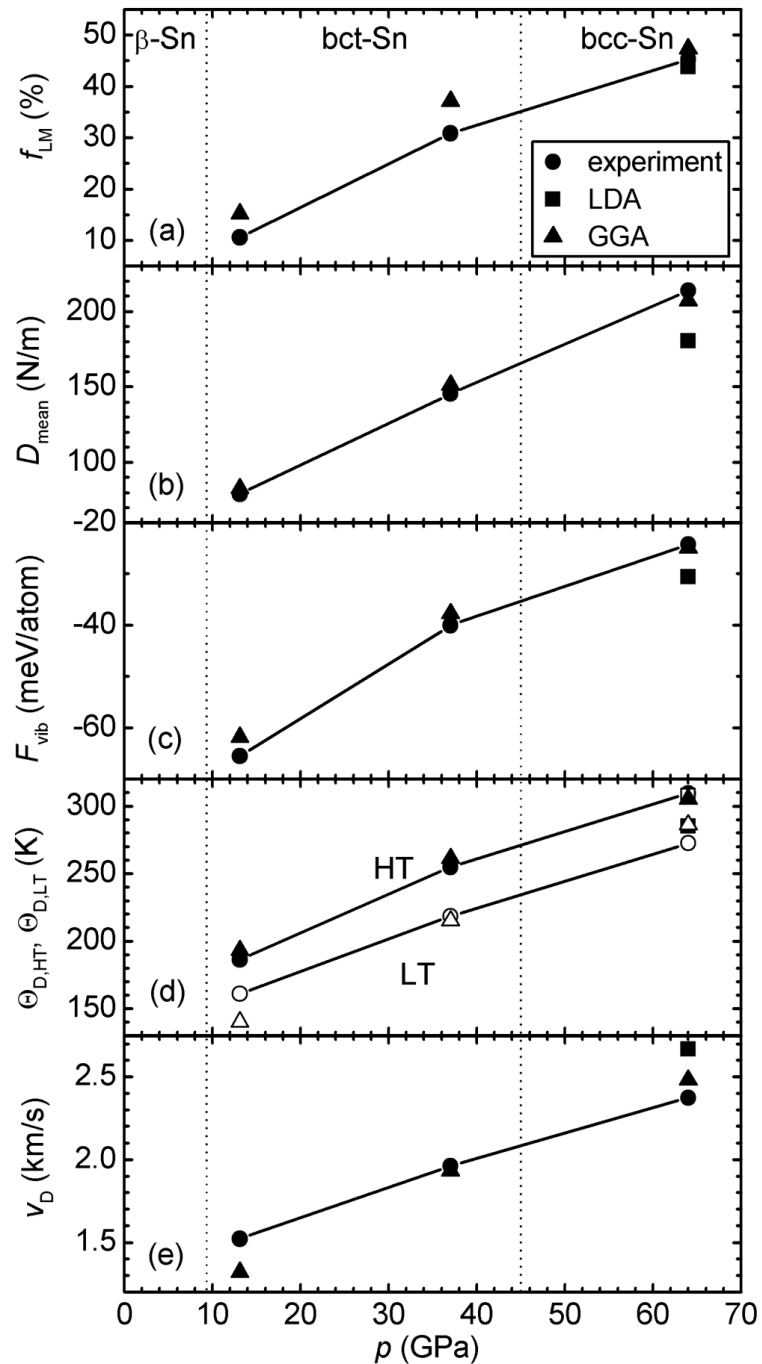
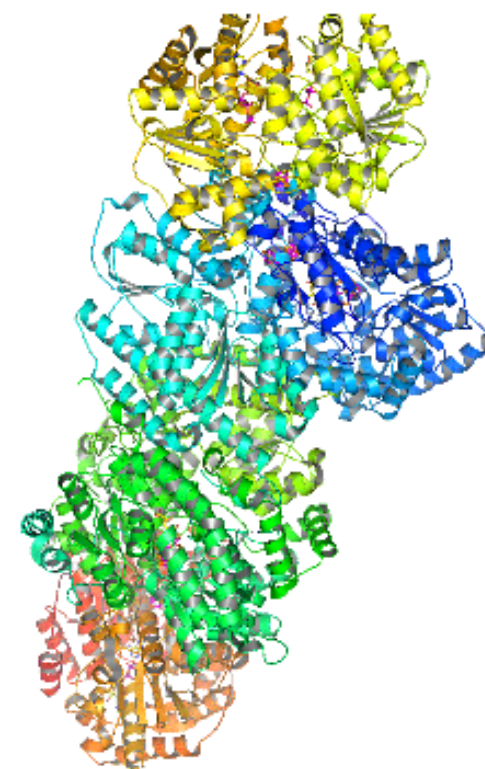
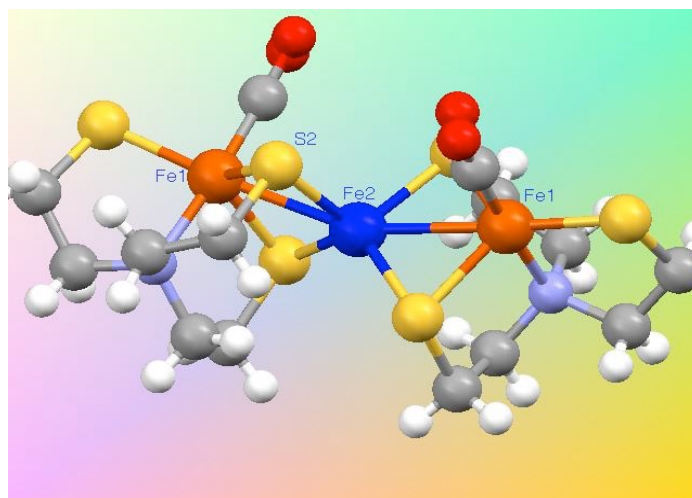
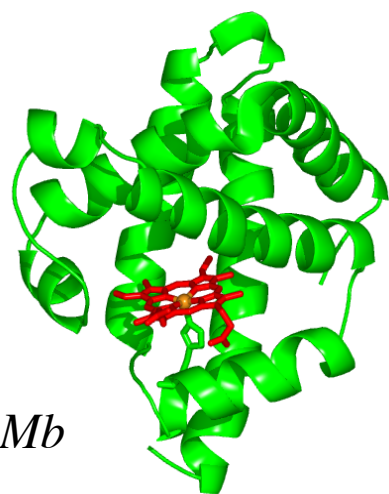


FIG. 3 (color online). (a) Theoretical phonon dispersion relation of bcc-Sn at 64 GPa. The inset shows the Brillouin zone of the bcc-Sn lattice. (b) Comparison between the theoretically calculated phonon DOS (lines) and the experimentally derived phonon DOS at 64 GPa (circles).

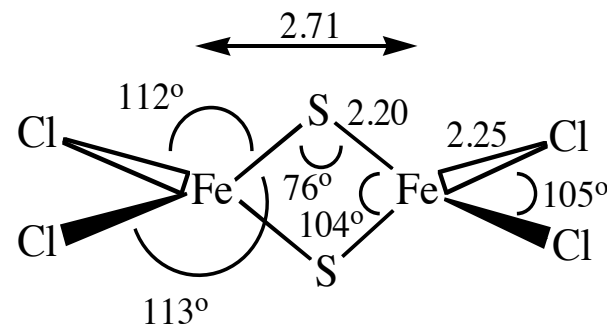
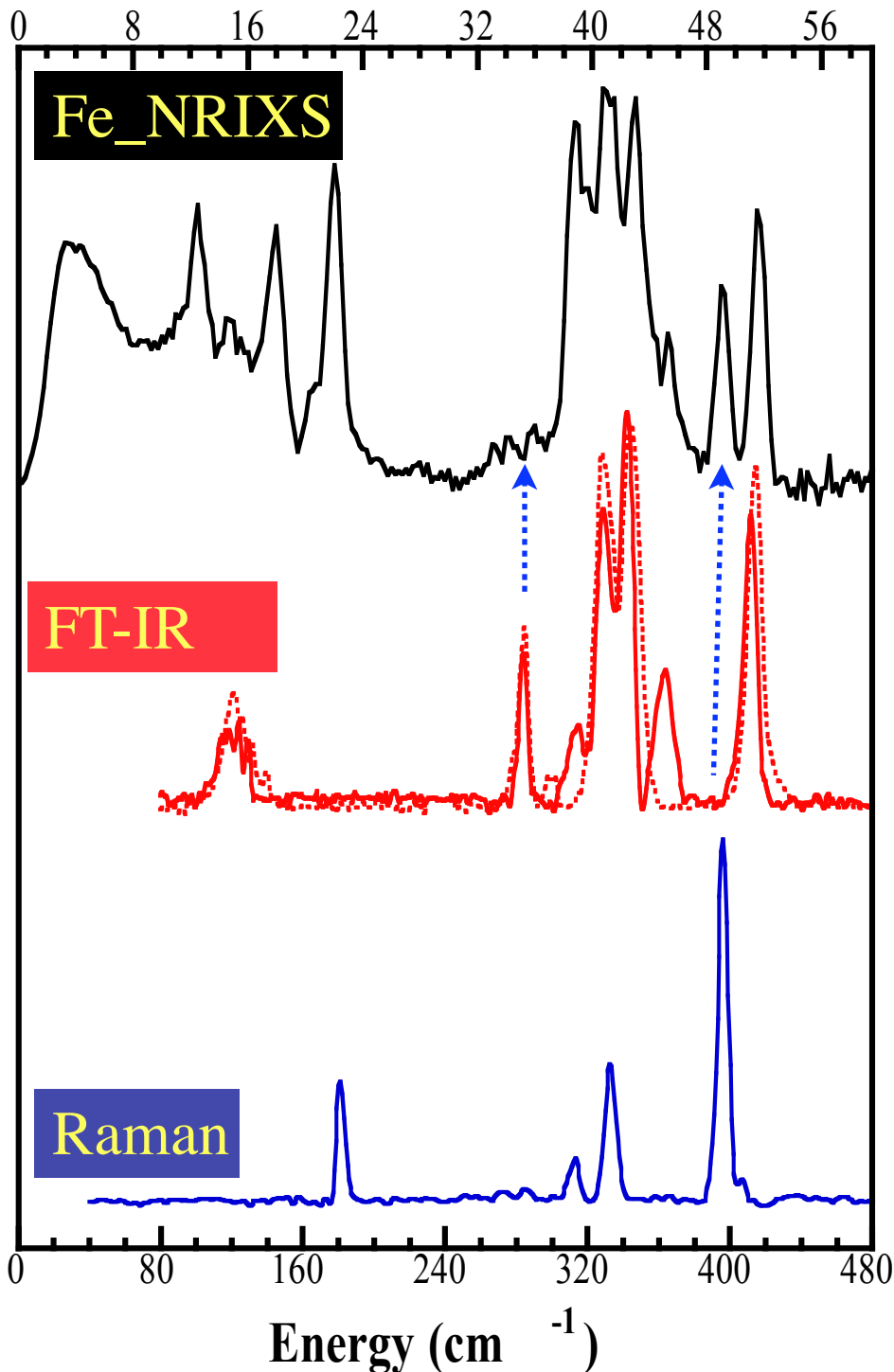
# Biology & bio-inorganic chemistry

S. Cramer	University of California-Davis
E. Solomon	Stanford University
T. Sage	Northeastern University
E. Munck	University of Pittsburg
DeBeer George	Cornell University
Nicolai Lehnert	University of Michigan
R. Scheidt	University of Notre Dame



Vibrational spectroscopy of proteins, enzymes and biomimic model porphyrins and cubanes

Energy (meV)

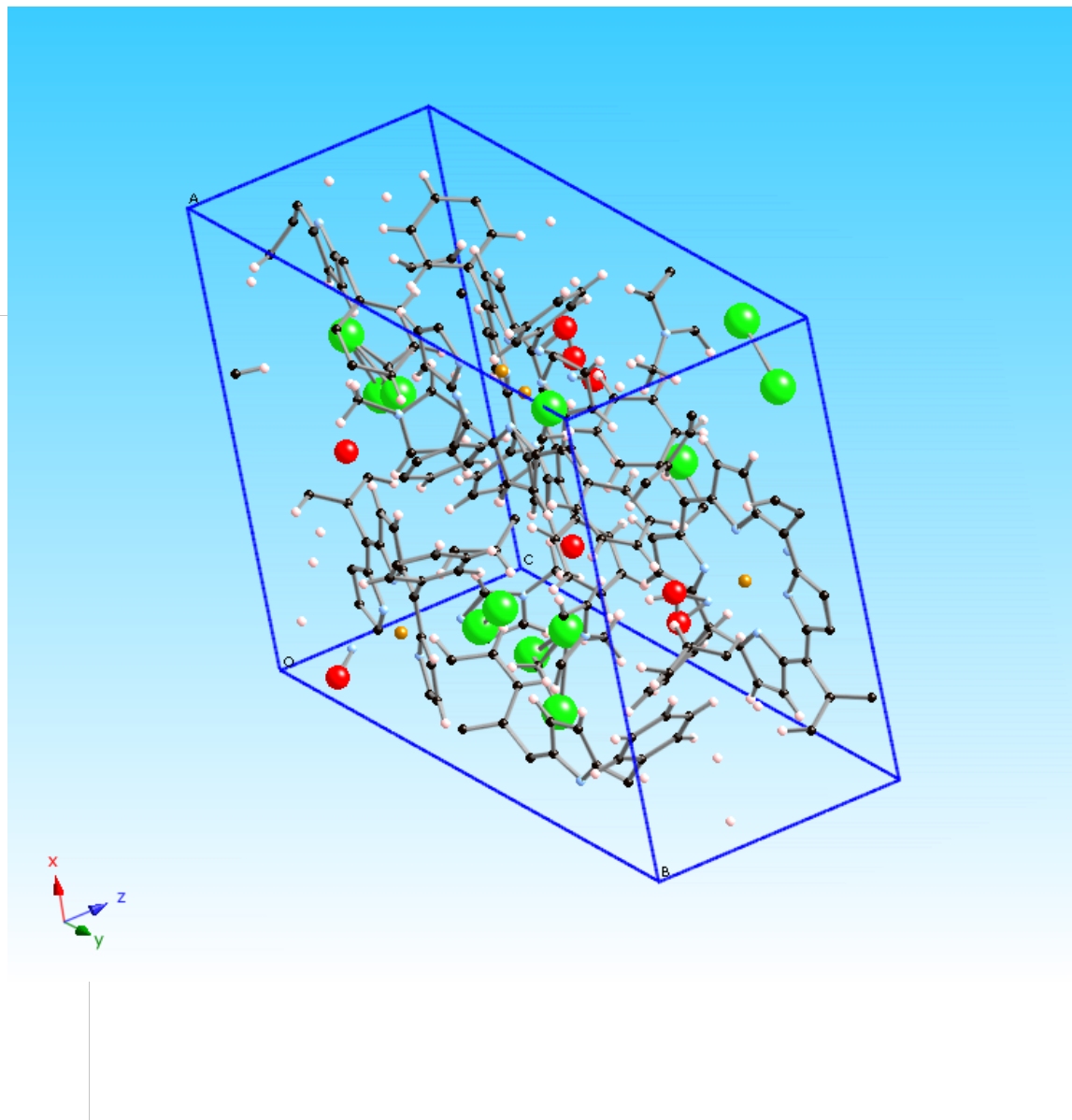
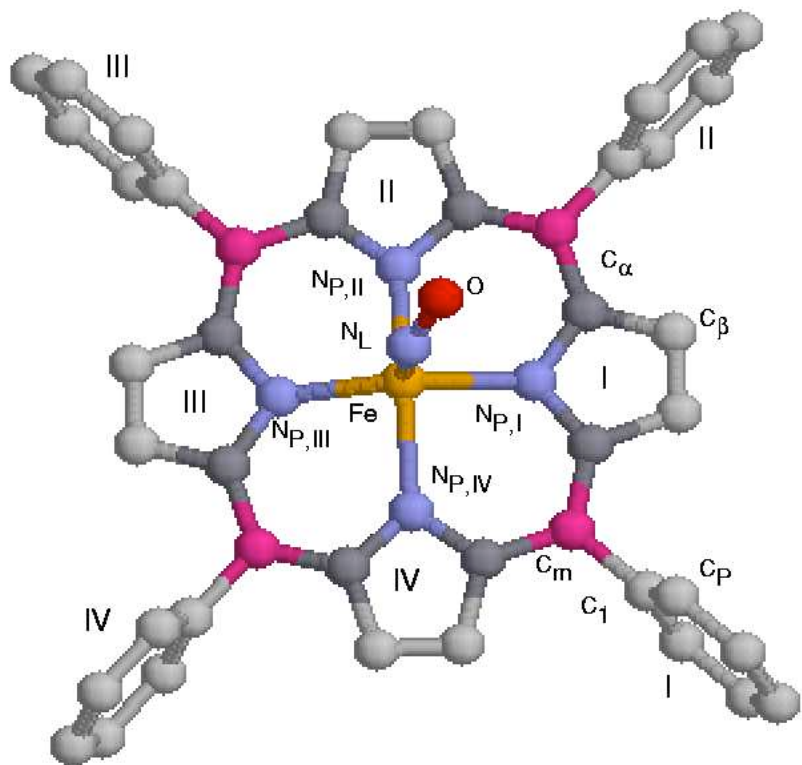


Some unique advantages of NRIXS

1. Low frequency motions: ~ total mass
2. No selection rule except motion of atoms along x-ray propagation
3. Peak intensity ~ mode participation ~ actual displacement
4. No matrix effects or limitations
5. Element and isotope selective
6. No unpredictable cancellations in scattering terms

$$\phi_{\alpha} = \frac{1}{3} \frac{\bar{v}_R}{\bar{v}_{\alpha}} e^{2j_{\alpha}} (\bar{n}_{\alpha} + 1) f$$



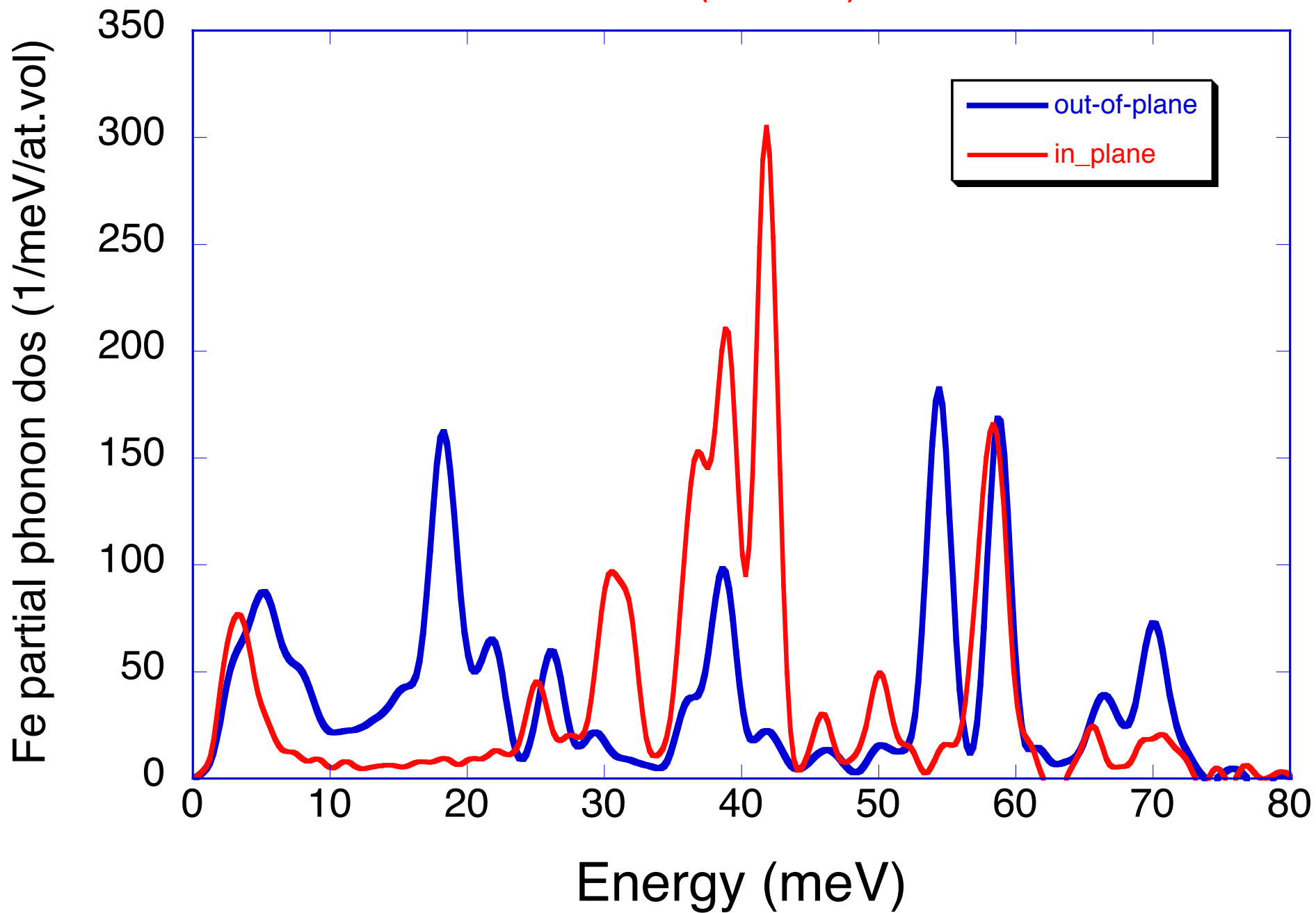


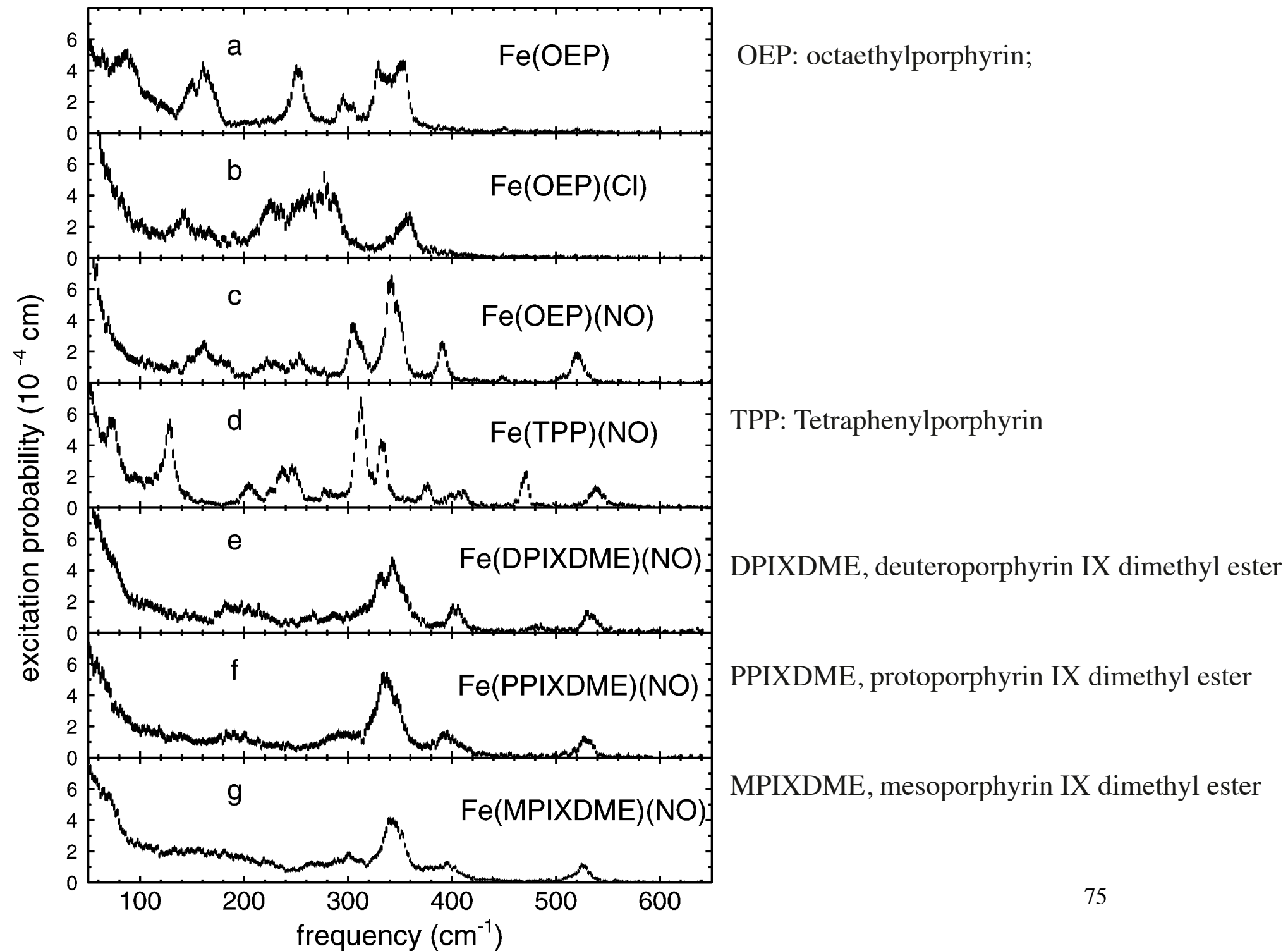
## Porphyrins:

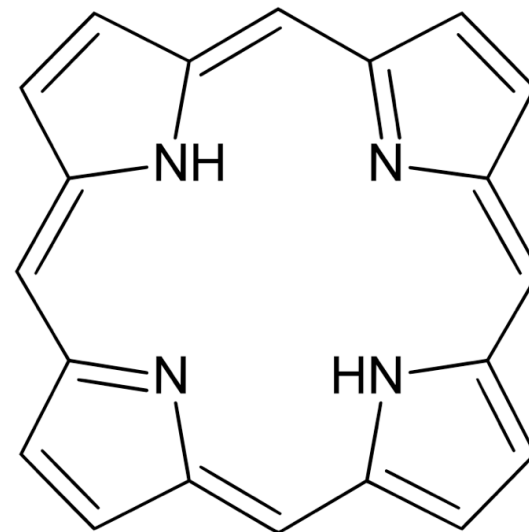
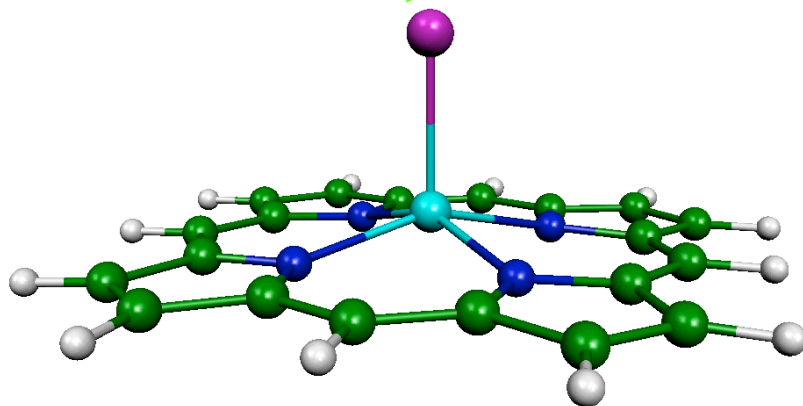
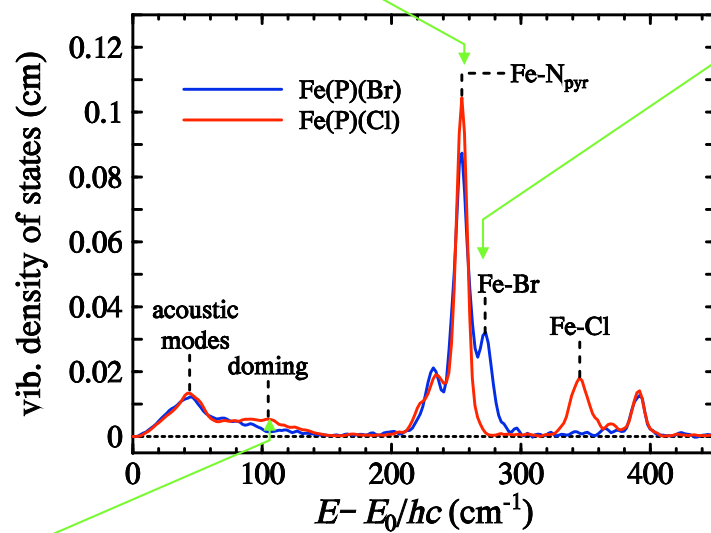
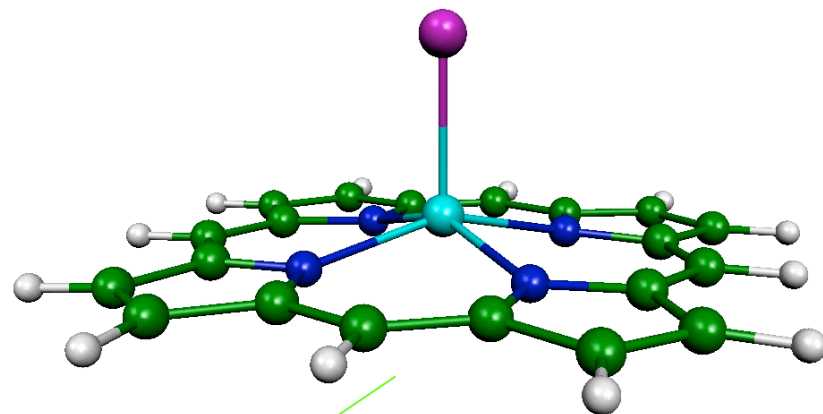
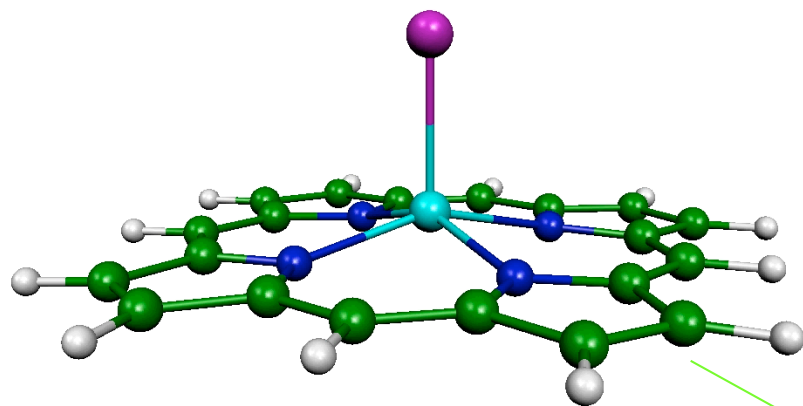
Tetraphenylporphyrin (TPP)  
 Octaethylporphyrin (OEP)

<u>A</u>	<u>B</u>
Phenyl	H
H	Ethyl

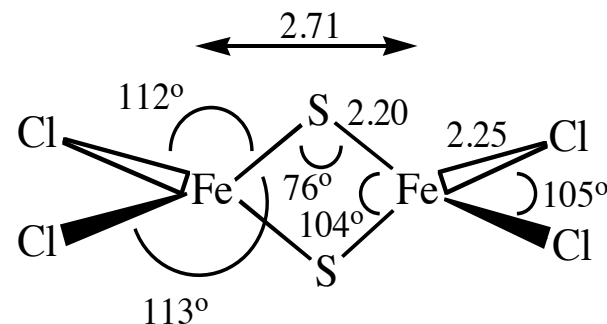
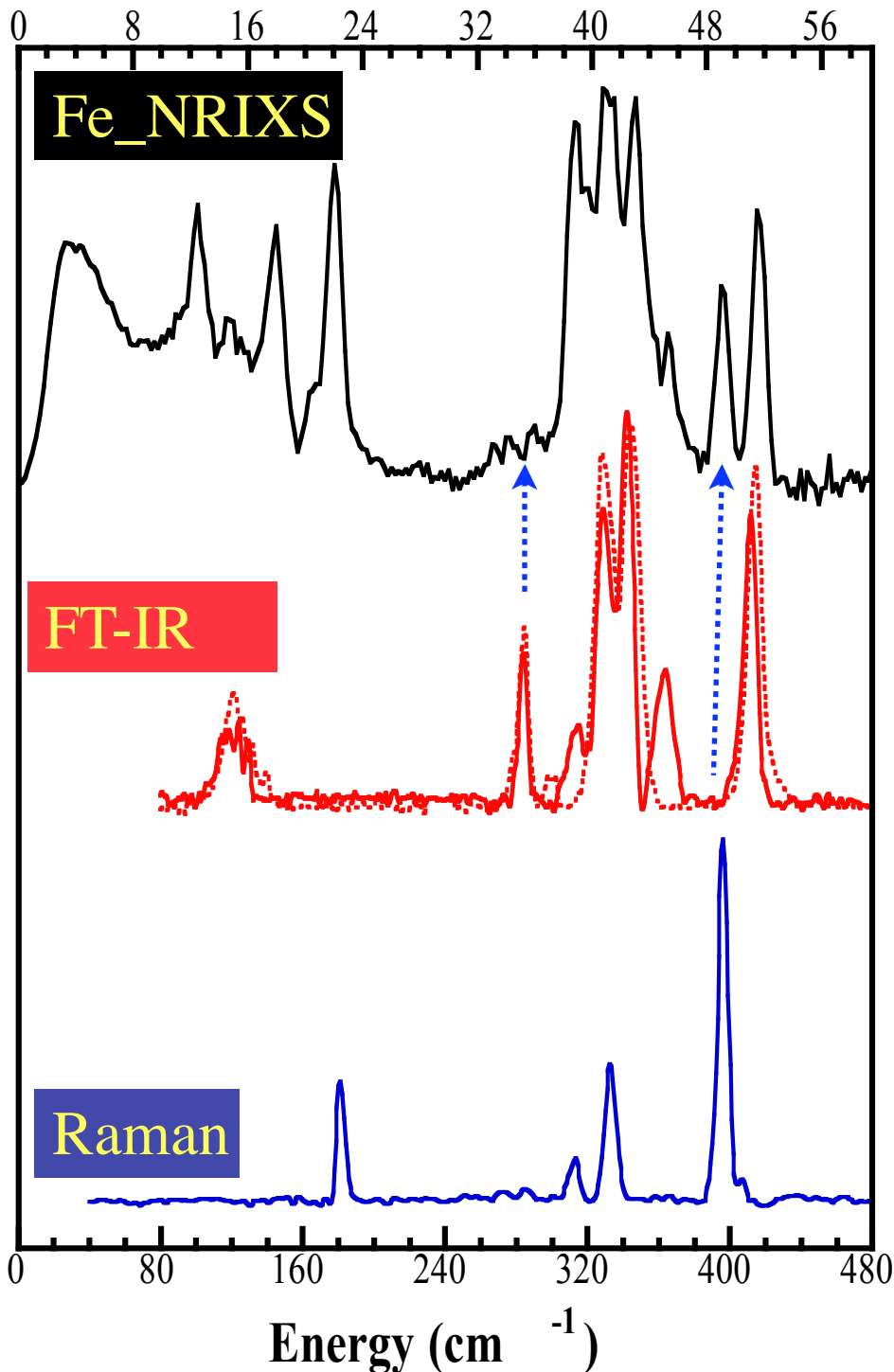
# FeTPP(1MeIm)NO







Energy (meV)

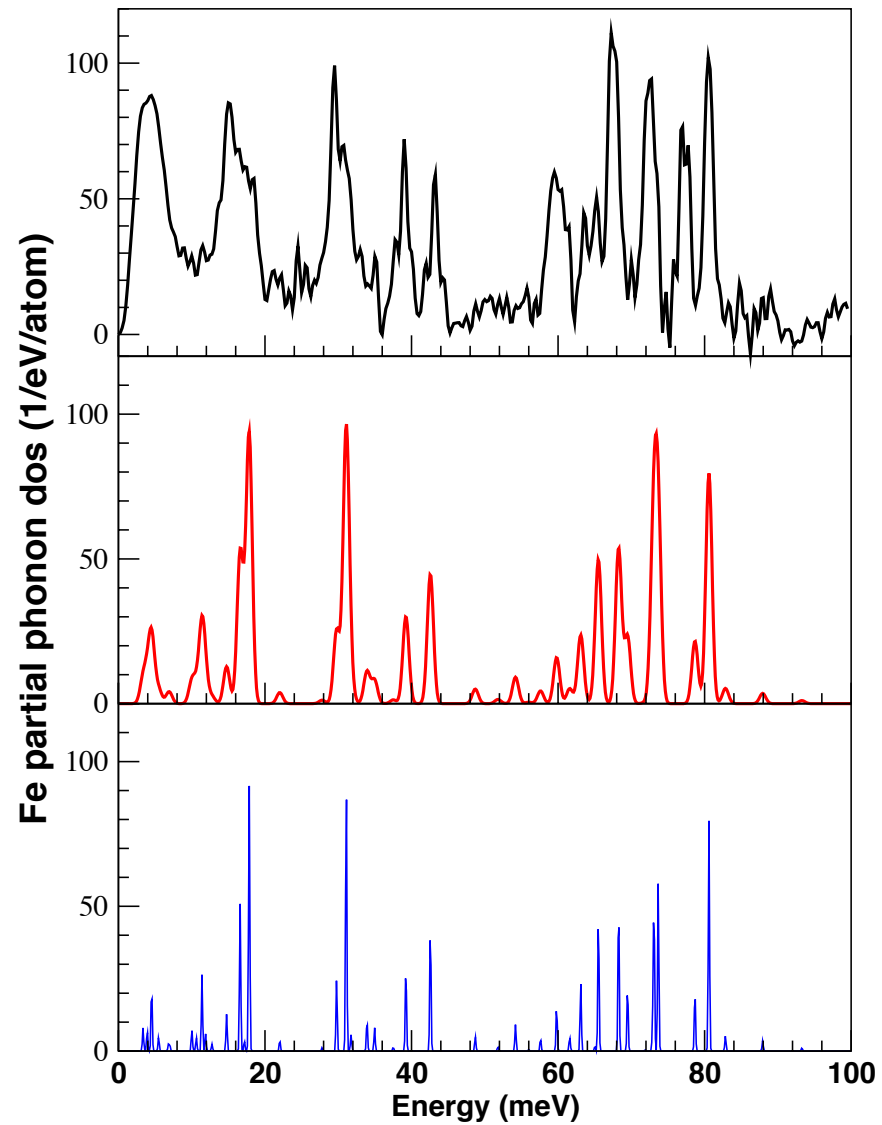
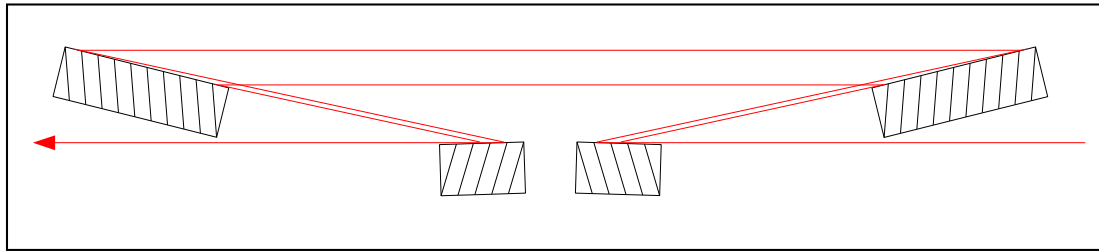


Some unique advantages of NRIXS

1. Low frequency motions: ~ total mass
2. No selection rule except motion of atoms along x-ray propagation
3. Peak intensity ~ mode participation ~ actual displacement
4. No matrix effects or limitations
5. Element and isotope selective
6. No unpredictable cancellations in scattering terms

$$\phi_{\alpha} = \frac{1}{3} \frac{\bar{v}_R}{\bar{v}_{\alpha}} e^{2j_{\alpha}} (\bar{n}_{\alpha} + 1) f$$

~ 0.1 meV, all-vacuum high resolution monochromator



# Protonation state of oxo-ligand in heme protein intermediates:

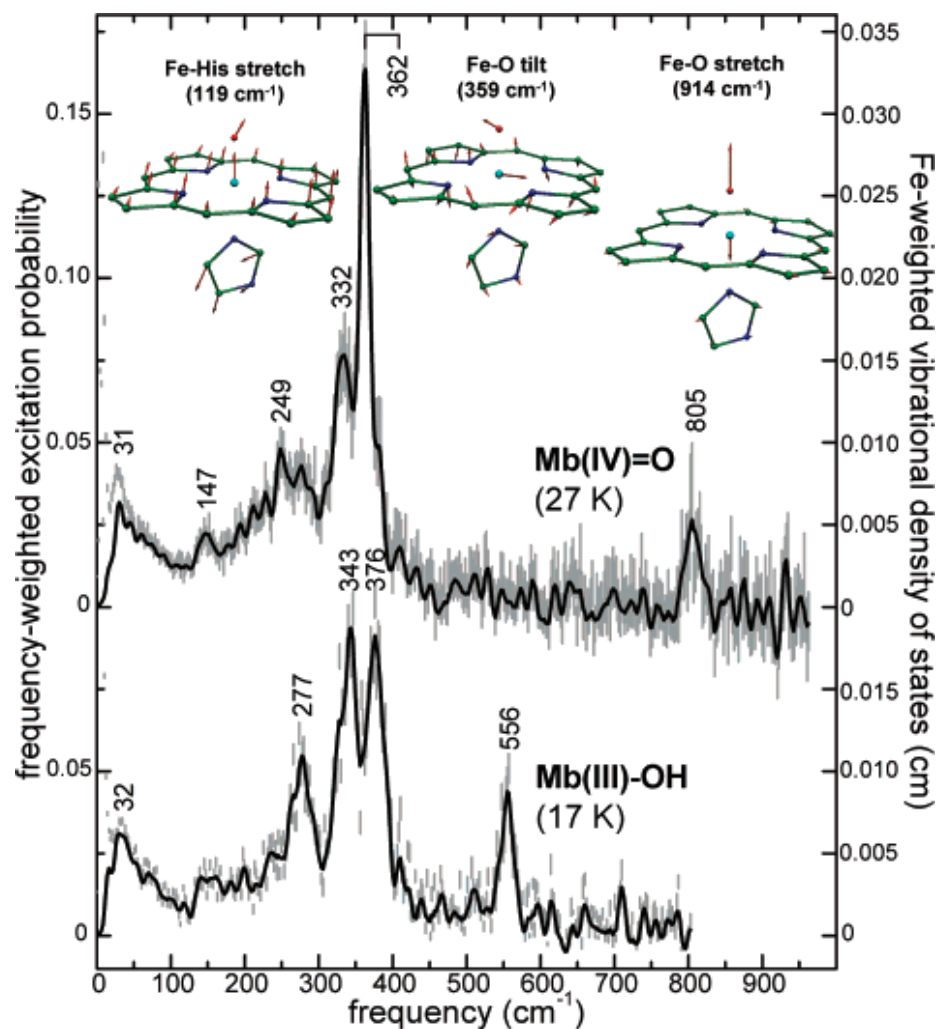
J|A|C|S  
COMMUNICATIONS

Published on Web 01/18/2008

## Synchrotron-Derived Vibrational Data Confirm Unprotonated Oxo Ligand in Myoglobin Compound II

Weiqiao Zeng,<sup>†</sup> Alexander Barabanschikov,<sup>†</sup> Yunbin Zhang,<sup>†</sup> Jiyong Zhao,<sup>‡</sup> Wolfgang Sturhahn,<sup>‡</sup> E. Ercan Alp,<sup>‡</sup> and J. Timothy Sage<sup>\*†</sup>

J. AM. CHEM. SOC. 2008, 130, 1816–1817



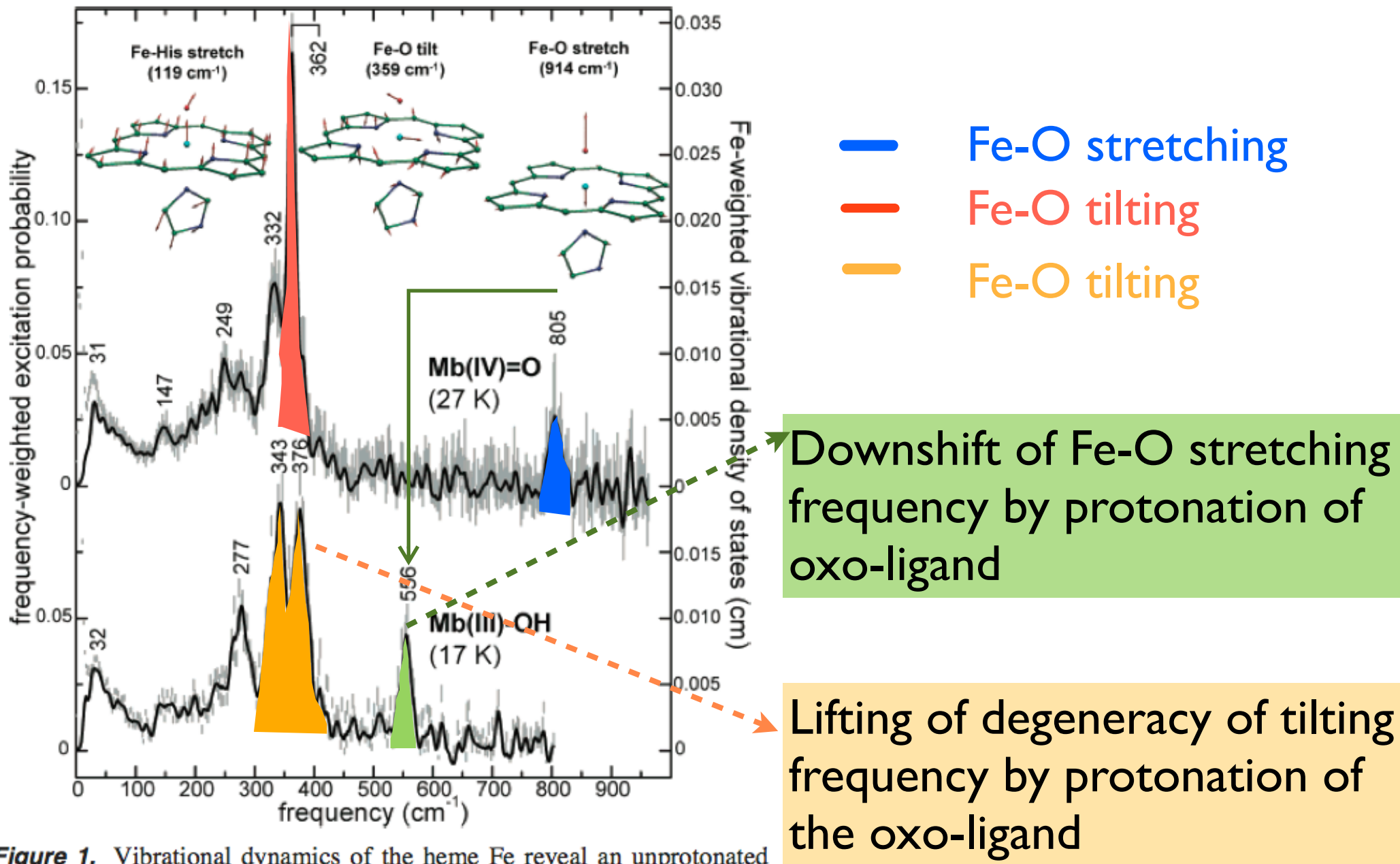


**Figure 1.** Vibrational dynamics of the heme Fe reveal an unprotonated oxo ligand in Mb(IV)=O, in contrast with the bound hydroxyl group in Mb(III)-OH. Protonation of the oxo ligand results in a downshift of the Fe-O stretching frequency from 805  $\text{cm}^{-1}$  to 556  $\text{cm}^{-1}$ , and splits the Fe-O tilting vibrations, which are degenerate near 362  $\text{cm}^{-1}$  in Mb(IV)=O, but are separated by 33  $\text{cm}^{-1}$  in the asymmetrically protonated heme Mb(III)-OH complex. Error bars represent the normalized experimental signal,